

EMERGENCY DROUGHT BARRIER

Impact on Harmful Algal Blooms and Aquatic Weeds in the Delta

Prepared for
California Department of Water
Resources

December 2021



EMERGENCY DROUGHT BARRIER

Impact on Harmful Algal Blooms and Aquatic Weeds in the Delta

Prepared for
California Department of Water
Resources
Contact: Rosemary Hartman
Division of Integrated Science and
Engineering
rosemary.hartman@water.ca.gov
Office: 916-882-2926

December 2021



Authors:

Rosemary Hartman¹, Eli Ateljavich¹, Mine Berg²,
Keith Bouma-Gregson³, David Bosworth¹,
Nicholas Rasmussen¹, Theodore Flynn¹, Toni Pennington²

1. California Department of Water Resources,
Division of Integrated Science and Engineering
2. Environmental Science Associates
3. U.S. Geological Survey, California Water Sciences
Center

Suggested Citation: Hartman, R., E. Ateljavich, M. Berg, K. Bouma-Gregson, D. Bosworth, N. Rasmussen, T. Flynn, and T. Pennington. 2021. *Report on the Impact of the Emergency Drought Barrier on Harmful Algal Blooms and Aquatic Weeds in the Delta*. Sacramento: California Department of Water Resources. 86 pp. + appendix.

EXECUTIVE SUMMARY

Condition 8 of the June 2021 Temporary Urgency Change Order for the Central Valley Project and State Water Project requires a special study of harmful algal blooms (HABs) in the Sacramento–San Joaquin Delta (Delta), particularly HABs caused by cyanobacteria (i.e., cyanoHABs) and the spread of submerged aquatic vegetation (SAV) also referred to as “aquatic weeds” (SWRCB 2021). This report describes the study, presents preliminary results regarding drivers of the occurrence of cyanoHABs and spread of SAV, and identifies possible mitigation strategies. This report will be followed by a more extensive report in spring 2022, which will include data not available at the time of this writing.

ES.1 Harmful Algal Blooms

HABs were monitored using visual assessments from existing surveys, satellite data, continuous water quality cruises, grab samples for taxonomy, and some cyanotoxin data. Major findings were as follows:

- Droughts increase the length, frequency, and severity of cyanobacterial blooms.
- Temperature is an important driver of bloom development. Blooms tend to be the most severe during years in which warm water temperatures (warmer than 19 degrees Celsius [$^{\circ}\text{C}$]) start earlier in the year and last into October, such as 2020.
- Slightly fewer observations of *Microcystis* occurred Delta-wide during summer 2021 than in 2020, but the number of observations was similar to those in other dry years.
- During summer 2021, densities of cyanobacteria in grab samples in the South Delta and San Joaquin River were higher than in 2020, particularly for *Dolichospermum*.
- There was a large cyanobacterial bloom in Franks Tract in July and August 2021, potentially caused by an increase in residence time resulting from the emergency drought barrier, coupled with high water temperatures attributable to local weather patterns.
- Concentrations of cyanobacterial toxins in Franks Tract exceeded the U.S. Environmental Protection Agency’s drinking water standards, although they were below caution levels for recreational use. The potential also exists for these toxins to cause sublethal effects on fish and wildlife. Other periods in the bloom or other locations may have had higher toxicity; however, sampling was not consistent enough to capture these patterns. No toxins were detected at Clifton Court Forebay.

Taken together, these findings suggest that drought and increased water temperatures were major factors leading to the development of HABs across the estuary, and that the 2021 Temporary

Urgency Change Petition (TUCP) and Emergency Drought Barrier are unlikely to have caused Delta-wide increases in *Microcystis* abundance. A local increase in residence time caused by the barrier most likely contributed to the cyanobacterial bloom in Franks Tract during July and August 2021. No major cyanoHABs were detected in Franks Tract during installation of the drought barrier in 2015, but higher temperatures and growth of aquatic weeds may have exacerbated the problem in 2021.

Managing HABs in the Delta is rapidly becoming a priority for State, federal, and local water agencies, and this condition will only increase in a warming climate. Mitigation methods for reducing residence time locally near the barrier are still under development, but ideas include notching the barrier temporarily if blooms develop (if feasible while maintaining water quality protections), using perturbation to increase turbidity and reduce the availability of light, or potentially using algicide. However, most of these control methods may become infeasible at the scale of the entire Franks Tract, may be cost prohibitive, or both. Future research should explore targeted use of these methods, or methods that can be implemented on a larger scale.

ES.2 Aquatic Weeds

Aquatic vegetation was monitored across the Delta using hyperspectral imagery. Imagery has been collected over all or most of the Delta annually since 2014, with additional surveys conducted in 2004 and 2008. Imagery was collected in July 2021, but these data were still being processed at the time of this report. SAV within Franks Tract has also been monitored annually using rake surveys conducted by the California Department of Parks and Recreation, Division of Boating and Waterways (DBW), in collaboration with SePRO Corporation, Carmel, Indiana. Major findings are as follows:

- The total area of aquatic weeds has been increasing over the past 15 years, with marked increases during the 2014–2016 drought.
- Wet years (2017 and 2019) did not produce a significant decrease in the total coverage of aquatic weeds in the Delta.
- The 2015 drought barrier may have caused SAV to fill in the center channel of Franks Tract, and conditions during subsequent years did not restore this channel.
- The relative composition of native and invasive SAV species in Franks Tract has changed over time, but complex interactions between DBW’s herbicide applications, drought, barrier installations, and temperature may all play a role in these dynamics.

Without final imagery for 2021, no statements can be made regarding the Delta-wide impact of the 2021 TUCP or barrier. However, the increasing prevalence of weeds over the past 15 years may be caused in part by the increased frequency of droughts and increases in temperature.

Multiple strategies for controlling aquatic weeds are in development or in use, to varying levels of success. Aquatic herbicides have low efficacy in tidal waters; however, the long residence times caused by the barrier in Franks Tract may provide an opportunity for increased efficacy. Other methods, such as the use of new herbicides, benthic mats, booms, and biocontrol, are also an area of active investigation.

TABLE OF CONTENTS

Impact of the Emergency Drought Barrier on Harmful Algal Blooms and Aquatic Weeds in the Delta

	<u>Page</u>
Acronyms and Other Abbreviations	iv
Acknowledgements	v
Executive Summary	ES-1
ES.1 Harmful Algal Blooms	ES-1
ES.2 Aquatic Weeds	ES-2
Section 1, Overview of the Temporary Urgency Change Petition and Barrier and Need for This Report	1-1
1.1 Introduction	1-1
1.2 Substance of the Temporary Urgency Change Petition	1-2
1.3 Emergency Drought Barrier	1-2
Section 2, Harmful Algal Blooms	2-1
2.1 Introduction	2-1
2.2 Methods.....	2-4
2.3 Results	2-11
2.4 Discussion/Interpretation	2-34
Section 3, Weeds	3-1
3.1 Introduction	3-1
3.2 Methods.....	3-3
3.3 Results	3-8
3.4 Discussion/Interpretation	3-14
Section 4, References	4-1
 Appendix	
A. Additional Statistics Tables	

List of Figures

Figure 1	Emergency Drought Barrier location.....	1-3
Figure 2	Scale for visual <i>Microcystis</i> index used by monitoring programs in the Delta.....	2-5
Figure 3	Stations for long-term monitoring programs contributing <i>Microcystis</i> visual observations (black), phytoplankton grab samples (red), and temperature data (blue).....	2-10
Figure 4	Frequency of visual <i>Microcystis</i> observations in the Delta and Suisun from long-term monitoring programs, 2007–2021.....	2-12
Figure 5	Relative frequency of harmful algal bloom observations by month in different areas of the Delta in 2021.....	2-13
Figure 6	Frequency of occurrence for <i>Microcystis</i> in regions adjacent to the West False River drought barrier in summer and fall (May–October).....	2-13
Figure 7	Percent of visual index values with <i>Microcystis</i> present in the Central and South Delta versus log-transformed Delta Outflow.....	2-14
Figure 8	Potentially toxic cyanobacterial taxa detected via microscopy at Banks Pumping Plant and Clifton Court Forebay.....	2-16
Figure 9	Concentration (organisms/mL) of potentially toxic cyanobacteria collected by the Environmental Monitoring Program in regions adjacent to the emergency drought barrier by month, region, and year.....	2-17
Figure 10	Mean (+/- 1 SE) total concentration of selected potentially toxic cyanobacteria (<i>Aphanizomenon</i> , <i>Dolichospermum</i> , <i>Cylindrospermopsis</i> , <i>Anabaenopsis</i> , <i>Microcystis</i> , <i>Oscillatoria</i> , and <i>Planktothrix</i>) from EMP microscopy samples collected in summer (June–September) in regions adjacent to the barrier by year.....	2-18
Figure 11	Average concentration (+/- 1 SD) of nutrients collected by EMP in the South Delta by season.....	2-19
Figure 12	Monthly maps (May–October 2021) showing concentrations of cyanobacteria in the confluence and interior Delta, as measured using a FluoroProbe (bbe Moldenaek GmbH) during the Environmental Monitoring Program’s water quality cruises.....	2-20
Figure 13	Monthly maps (May, July, and October 2021) showing concentrations of cyanobacteria in the confluence, interior, and southern Delta, as measured using a FluoroProbe (bbe Moldenaek GmbH) on U.S. Geological Survey rapid water quality cruises.....	2-21
Figure 14	Time series of the percent of valid pixels within each Cyanobacteria Index category for summer-fall in 2020 and 2021 within Franks Tract and Mildred Island.....	2-22
Figure 15	Maps of Cyanobacteria Index categories at the beginning (top), peak (middle), and end (bottom) of the cyanobacteria bloom in Franks Tract during summer 2021.....	2-23
Figure 16	Modeled daily averaged age of water in Franks Tract with the barrier (top) and without the barrier (bottom) on August 17, 2021.....	2-24
Figure 17	Modeled flow with and without the emergency drought barrier at False River and at Old River at Franks Tract.....	2-25
Figure 18	Modeled difference in water temperature for scenarios with and without the West False River Barrier.....	2-26
Figure 19	Maximum water temperatures by month at station BET, 2008–2021.....	2-27
Figure 20	Number of days in the calendar year that water temperature reached 19°C or above across 10 stations in Suisun Bay, the Sacramento River, and the Delta.....	2-27

	<u>Page</u>
Figure 21	Number of days in the calendar year that water temperature reached 25°C or above across 10 stations in Suisun Bay, the Sacramento River, and the Delta..... 2-28
Figure 22	Comparison of Delta-wide days above 19°C and 25°C per year with total percent of visual observations with <i>Microcystis</i> present. 2-29
Figure 23	Daily mean pH (2015–2021) at the continuous water quality monitoring station in Franks Tract. 2-30
Figure 24	Daily mean concentration of dissolved oxygen (2015–2021) at the continuous water quality monitoring station in Franks Tract. 2-31
Figure 25	Daily mean concentration chlorophyll a (2015–2021) at the continuous water quality monitoring station in Franks Tract. 2-33
Figure 26	Map of the central and south regions of the Delta for 2019 showing the locations of Franks Tract and the two reference sites, Big Break and Clifton Court Forebay..... 3-4
Figure 27	Locations near the 2021 emergency drought barrier where CSTARS sampled aquatic vegetation to ground-truth the hyperspectral imagery. 3-6
Figure 28	Sampling design for SePRO’s long-term monitoring of submerged aquatic vegetation in Franks Tract, conducted in conjunction with herbicide treatments. 3-7
Figure 29	Time series of hyperspectral imagery for Franks Tract. 3-9
Figure 30	Time series of hyperspectral imagery for Big Break, which serves as a reference site for Franks Tract..... 3-10
Figure 31	Time series of hyperspectral imagery for Clifton Court Forebay, which serves as a reference site for Franks Tract..... 3-11
Figure 32	Coverage of floating aquatic vegetation (FAV) and submerged aquatic vegetation (SAV) in Franks Tract and Clifton Court Forebay..... 3-12
Figure 33	Change in vegetation percent coverage of Delta waterways over time (assuming 55,500 acres of waterways total). 3-12
Figure 34	Changes in composition of submerged aquatic vegetation species during 2014–2021 based on SePRO Corporation rake surveys..... 3-13
Figure 35	Satellite images of Franks Tract in early October 2021 (left) and late October 2021 (right)..... 3-15
Figure 36	Photo provided by SePRO Corporation showing the amount of vegetation and algae present in Franks Tract on October 6, 2021..... 3-16

List of Tables

Table 1	Predicted Ecosystem Impacts of the 2021 Emergency Drought Barrier and TUCP Relevant to Submerged Aquatic Vegetation and Harmful Algal Blooms in the Delta..... 1-4
Table 2	OEHHA and CCHAB Action Levels for Human Recreational Exposure to Cyanotoxins Compared to WHO and EPA Microcystin Guidance Levels for Recreational Exposure and for Drinking Water..... 2-3
Table 3	Results of Ordinal Regression on <i>Microcystis</i> Indices from Visual Surveys in the Area Immediately Surrounding the Emergency Drought Barrier for 2014-2021 2-12
Table 4	Results from Regional Water Quality Control Board Cyanotoxin Monitoring in Franks Tract during Summer 2021 2-15
Table 5	PERMANOVA Results Testing the Difference in Community Composition of Potentially Toxic Cyanobacteria Between Regions and Years for the Regions Surrounding the EDB from 2014-2021 2-16

		<u>Page</u>
Table 6	Coefficients for Zero-Inflated Negative Binomial Mixed Model on Total Potentially Toxic Cyanobacteria Concentration Collected by the Environmental Monitoring Program in the Regions Surrounding the Barrier	2-17
Table 7	Mean Monthly Value of Daily Maximum pH (pH Units)	2-29
Table 8	Mean Monthly Value of Daily Maximum Dissolved Oxygen (% Saturation).....	2-32
Table 9	Mean Monthly Value of Daily Maximum Chlorophyll a (µg/L) at the continuous water quality monitoring station in Franks Tract (FRK)	2-32
Table 10	Area of Franks Tract treated by the Division of Boating and Waterways with the Herbicide Fluridone, by Year	3-5

Acronyms and Other Abbreviations

°C	degrees Celsius
µg/g	micrograms per gram
µg/L	micrograms per liter
µS/cm	microSiemens per centimeter
Banks Pumping Plant	Harvey O. Banks Pumping Plant
barrier	Emergency Drought Barrier
Bay-Delta	San Francisco Bay/Sacramento–San Joaquin Delta
CCHAB	California Cyanobacteria and Harmful Algal Bloom Network
CDEC	California Data Exchange Center
CDFW	California Department of Fish and Wildlife
cfs	cubic feet per second
CI	Cyanobacteria Index
CSTARS	Center for Spatial Technologies and Remote Sensing (University of California, Davis)
cyanoHAB	cyanobacterial harmful algal bloom
D-1641	Water Rights Decision 1641
DBW	California Department of Parks and Recreation, Division of Boating and Waterways
Delta	Sacramento–San Joaquin Delta
DO	dissolved oxygen
DWR	California Department of Water Resources
EAV	emergent aquatic vegetation
EDB	Emergency Drought Barrier
ELISA	Enzyme-Linked Immunosorbent Assay
EMP	Environmental Monitoring Program
EPA	U.S. Environmental Protection Agency
FAV	floating aquatic vegetation
ha	hectare(s)
HAB	harmful algal bloom
LC-MS	liquid chromatography–mass spectroscopy
LD ₅₀	median lethal dose
NTU	nephelometric turbidity units
OEHHA	Office of Environmental Health Hazard Assessment
Reclamation	U.S. Bureau of Reclamation
SAV	submerged aquatic vegetation
SPATT	Solid Phase Adsorption Toxin Tracking
State Water Board	State Water Resources Control Board
TUCP	Temporary Urgency Change Petition
USGS	U.S. Geological Survey
WHO	World Health Organization

Acknowledgements

Thank you to Sarah Perry, Jeff Galef, Tiffany Brown, Jared Frantzich, Tyler Salman, Brianne Sakata, Kristi Arend, Janis Cooke, Shruti Khanna, James White, Tim Malinich, and Ajay Jones for their assistance with data contributions, data analysis, and formatting. Thank you to Peggy Lehman for her review of the manuscript and technical advice. Thank you to Erin Andrews and Chris Fitzer for their assistance with project management and technical editing. Thanks to all of the field staff of the Interagency Ecological Program long-term monitoring surveys and the California Department of Water Resources' North Central Region Office for their tireless work collecting the field data summarized in this report.

SECTION 1

Overview of the Temporary Urgency Change Petition and Barrier and Need for This Report

1.1 Introduction

Water Year 2021 in California was the driest recorded since 1977. Although rainfall was well below average, the snowpack in March 2021 indicated that sufficient reservoir inflow would be available to meet water quality requirements. Conditions changed significantly at the end of April 2021, when it became clear that expected reservoir inflow from snowmelt had failed to materialize. The May forecast for the water year in the Sacramento Valley Four Rivers Index identified a reduction of expected runoff of 685 thousand acre-feet from the forecast generated only a month earlier, in April.

A combination of factors—the May 2021 forecast of inflow that was far less than predicted, parched watershed soils and extremely low rainfall, continued dry and warm conditions, and limited available water supplies in the San Francisco Bay/Sacramento–San Joaquin Delta (Bay-Delta)—created an urgent need to act. As announced by the Governor in his May 10, 2021, Emergency Proclamation on drought conditions for the Bay-Delta and other watersheds, the continuation of extremely dry conditions in the Delta watershed means there is not an adequate water supply to meet water right permit obligations for instream flows and water quality under Water Rights Decision 1641 (D-1641).

The U.S. Bureau of Reclamation (Reclamation) and California Department of Water Resources (DWR) jointly submitted the 2021 Temporary Urgency Change Petition (TUCP), which requested that the State Water Resources Control Board (State Water Board) consider modifying requirements of Reclamation’s and DWR’s water right permits to enable changes in operations of the Central Valley Project and State Water Project that will allow the projects to deliver water with conservation for later instream uses and water quality requirements. On June 1, 2021, the State Water Board issued an order conditionally approving the petition and conditions requiring compliance with Delta water quality objectives in response to drought conditions. The TUCP modification to some D-1641 requirements preserved water quality in the Delta while maintaining some carryover storage in upstream reservoirs, including Shasta and Oroville.

1.2 Substance of the Temporary Urgency Change Petition

The DWR and Reclamation requested the following temporary changes to requirements that were imposed pursuant to D-1641 for the period June 1 through August 15:

- For June 1 through June 30, reduce the required minimum 14-day running-average Delta outflow from 4,000 cubic feet per second (cfs) to 3,000 cfs.
- For July 1 through July 31, reduce the required minimum monthly average Delta outflow from 4,000 cfs to 3,000 cfs, with a seven-day running average of no less than 2,000 cfs.
- For June 1 through July 31, limit the combined maximum export rate to no greater than 1,500 cfs when Delta outflow is below 4,000 cfs; allow the 1,500 cfs limit to be exceeded when the Petitioners are meeting Delta outflow requirements pursuant to D-1641, or for moving transfer water.
- From June 1 through August 15, move the compliance point for the western Delta agricultural salinity requirement from Emmaton on the Sacramento River to Threemile Slough on the Sacramento River.

1.3 Emergency Drought Barrier

Along with the TUCP, DWR requested emergency authorizations in May 2021 for installation of the 2021 West False River Emergency Drought Salinity Barrier (EDB or barrier). The 2021 EDB is a temporary physical rock fill barrier that reduces the intrusion of high-salinity water into the Central and South Delta. **Figure 1** shows the location of the barrier.

Installation of a drought salinity barrier at West False River was shown to be an effective tool for reducing the intrusion of salt water into the Central and South Delta in 2015 (DWR 2019). During drought conditions, water stored in upstream reservoirs may be insufficient to repel salinity moving upstream from San Francisco Bay. Without the protection of the drought salinity barrier, saltwater intrusions could render Delta water unusable for agricultural needs, reduce habitat value for aquatic species, and affect roughly 25 million Californians who rely on the export of this water for personal use. The 2021 EDB is very similar in terms of location, size, and design to the drought salinity barrier that was permitted and installed during the 2015 drought. However, the 2021 EDB was not removed in November of the year it was installed. Instead, a notch will be cut into the top of the barrier to allow fish passage in January of 2022. The notch will be restored in spring of 2022, pending hydrologic conditions.

The biological assessment for the 2021 EDB and the biological review for the TUCP both identified the potential for an increase in cyanoHABs and an increase in SAV, also referred to as “aquatic weeds.” Therefore, the Section 401 certification for the 2021 EDB and Condition 8 of the June 2021 Temporary Urgency Change Order for the Central Valley Project and State Water Project require a special study of cyanoHABs and SAV in the Delta. This report describes the study, presents preliminary results regarding drivers of the occurrence of cyanoHABs and spread of SAV, and identifies possible mitigation strategies. This report will be followed by a more extensive report in spring 2022, which will include data not available in December 2021.



Figure 1
Emergency Drought Barrier location

Predictions developed as part of the Interagency Ecological Program synthesis team’s study of drought impacts on the Delta predicted that the drought would cause increases in the incidence and severity of cyanoHABs and the coverage and density of SAV. The team predicted that the TUCP would not cause detectable changes in either of these parameters above the level of the drought, but that the barrier may cause local increases in cyanoHABs and SAV in the vicinity of Franks Tract or the Central Delta (Table 1).

**TABLE 1
PREDICTED ECOSYSTEM IMPACTS OF THE 2021 EMERGENCY DROUGHT BARRIER AND TUCP RELEVANT TO
SUBMERGED AQUATIC VEGETATION AND HARMFUL ALGAL BLOOMS IN THE DELTA**

Category	Expected Conditions and Impacts	Monitoring
Hydrology/water quality	Higher salinity in the Sacramento River Lower salinity in the Central and South Delta A shift of X2 upstream up by approximately 2 km	DWR/USGS flow and water quality stations Modeling
cyanoHABs	Increase in the Central and South Delta	Visual assessment from monitoring surveys State Water Board cyanotoxin samples DWR/USGS SPATT study DWR pumping plant cyanotoxin samples EMP microscopy samples FluoroProbe data USGS cruises Satellite data
SAV	Increased weeds in Franks Tract	DBW/SePRO Franks Tract survey UC Davis imagery UC Davis grab samples to ground-truth imagery

NOTES: cyanoHABs = cyanobacterial harmful algal blooms; DBW = California Department of Parks and Recreation, Division of Boating and Waterways; Delta = Sacramento–San Joaquin Delta; DWR = California Department of Water Resources; EMP = Environmental Monitoring Program; km = kilometers; SAV = submerged aquatic vegetation; SePRO = SePRO Corporation; SPATT = Solid Phase Adsorption Toxin Tracking; State Water Board = State Water Resources Control Board; TUCP = Temporary Urgency Change Petition; UC Davis = University of California, Davis; USGS = U.S. Geological Survey; X2 = the distance in kilometers from the Golden Gate where the salinity concentration in the Delta is 2 parts per thousand

SECTION 2

Harmful Algal Blooms

2.1 Introduction

A worldwide increase in the incidence of cyanoHABs has prompted a great deal of research into the conditions that favor the growth of these species (Carmichael 2008; Chorus and Welker 2021; Hudnell 2008; Hudnell 2010; O’Neil et al. 2012; Paerl and Paul 2012). Many cyanobacteria genera form cyanoHABs, including the nitrogen-fixing genera *Anabaena/Dolichospermum*, *Aphanizomenon*, *Cylindrospermopsis*, and *Nodularia*; the benthic nitrogen-fixing genera *Lyngbya* and some *Oscillatoria*; and the non-nitrogen-fixing genera *Microcystis* and *Planktothrix*.

Environmental conditions favoring cyanoHAB formation typically include calm and stratified water, warm water temperatures, high light, and an ample supply of nutrients (Berg and Sutula 2015; Huber et al. 2012; Lehman et al. 2013; Lehman et al. 2018; Paerl et al. 2011). The most successful strategies for mitigating cyanoHABs have focused on these environmental factors, including increasing the flow of water, promoting mixing of the water column, and reducing the supply of nutrients (Paerl et al. 2011).

Blooms of the toxin-producing cyanobacteria *Microcystis aeruginosa* have been observed in the Delta by researchers working at DWR and other agencies since the late 1990s. These blooms were first documented visually appearing as little lettuce-like flakes in the water (Lehman and Waller 2003). Studies of these blooms since 2003 have demonstrated that these blooms contain multiple microcystin toxins. In sufficiently high concentrations, these act as liver toxins (Lehman et al. 2005), so the presence of low concentrations in the Delta is cause for concern.

Investigations after 2005 have found that the blooms frequently are composed of a mix of *Aphanizomenon* sp., *Microcystis* sp., *Dolichospermum* (formerly *Anabaena*) sp., *Planktothrix* sp. and *Pseudoanabaena* sp. (Lehman et al. 2010; Mioni et al. 2012).

Although they frequently co-occur, these genera are distinguished by different physiological capabilities and environmental optima. *Microcystis* has the highest temperature optimum (28 degrees Celsius [°C]), and increases its growth rate fastest with every 10°C increase in temperature (i.e., Q_{10}), but requires high light availability because of its low photosynthetic efficiency (Reynolds 2006; Wu et al. 2009). Other taxa, such as *Aphanizomenon*, *Pseudoanabaena*, and *Dolichospermum*, have lower temperature and light requirements, and can fix nitrogen gas, but they have lower growth rates (Li et al. 2016; Reynolds 2006; Stal et al. 2003). Therefore, *Microcystis* is predicted to dominate later in the summer when temperatures are warmest and the water is clearest, with other taxa in higher turbidity or cooler temperature conditions earlier in the year.

Overall, the Central and South Delta have the highest surface concentrations of *Microcystis* and *Aphanizomenon* (Berg and Sutula 2015; Lehman et al. 2013; Lehman et al. 2008; Lehman et al. 2018; Mioni et al. 2012). Starting in 2012, very high abundances of *Microcystis* colonies were observed in the South-East Delta region in the Turning Basin of the Stockton Shipping Channel, in Discovery Bay, and at Rough and Ready Island (Lehman et al. 2018; Spier et al. 2013). *Microcystis* abundance is typically much lower in Suisun Bay west of Antioch and north of Collinsville on the Sacramento River (Lehman et al. 2013; Lehman et al. 2005; Lehman et al. 2008; Lehman et al. 2018; Mioni et al. 2012).

Blooms of *Microcystis* in the Delta are associated with the release of cyanotoxins such as microcystins in the water and potential impacts on aquatic health. For example, embryonic and larval stages of fish appear to be very sensitive to the toxin microcystin, with chronic exposures as low as 0.25 micrograms per liter ($\mu\text{g/L}$) leading to oxidative stress, reduced growth, developmental defects, and lethality (OEHHA Ecotoxicology et al. 2009).

Consumption of prey items with body burdens of cyanotoxins can also be a potential pathway of impact (Banerjee et al. 2021). Lehman et al. (2010) traced increasing concentrations of microcystins from the water ($0.05\mu\text{g/L}$) to zooplankton (0.4 to 1.5 micrograms per gram [$\mu\text{g/g}$] dry weight) to striped bass muscle tissue (1 to $3.5\mu\text{g/g}$ dry weight). These values are similar to sublethal microcystin doses to fish ($2.5\mu\text{g/g}$ dry weight) as determined by the Office of Environmental Health Hazards (OEHHA) (OEHHA Ecotoxicology et al. 2009). Tumor lesions in liver tissue of juvenile Striped Bass and Mississippi Silversides caught in the San Joaquin and Sacramento Rivers where the total microcystin concentration was high are consistent with sublethal effects caused by the microcystin toxin (Lehman et al. 2010; OEHHA Ecotoxicology et al. 2009). This finding is consistent with fish feeding studies demonstrating that diets containing microcystin result in lesions of the liver (Acuna et al. 2012a; Acuna et al. 2012b; Deng et al. 2010). Recent research indicated that wild fish are continually exposed to dietary toxins through the accumulation of microcystins in the gut and liver tissue (Acuña et al. 2020).

Microcystin concentrations around $3.5\mu\text{g/g}$ fish tissue found in striped bass in the Delta are one-third of the OEHHA Action Level for human consumption of fish (**Table 2**) and therefore also poses a risk to human health. Microcystin concentrations of 0.05 to $2\mu\text{g/L}$ measured in the Central Delta before 2020 (i.e., Lehman et al. 2008; Lehman et al. 2018; Spier et al. 2013) were usually lower than exposure guidelines given by the World Health Organization (WHO) and U.S. Environmental Protection Agency (EPA) for human health in recreational waters, but are within the caution tier of the California Cyanobacteria and Harmful Algal Bloom Network (CCHAB) three-tiered warning system, identified in Table 2. Microcystin concentrations greater than 0.3 to $1.0\mu\text{g/L}$ exceed drinking water guidelines, however, for both EPA and the WHO (Table 2) (World Health 2021).

TABLE 2
OEHHA AND CCHAB ACTION LEVELS FOR HUMAN RECREATIONAL EXPOSURE TO CYANOTOXINS COMPARED TO WHO AND EPA MICROCYSTIN GUIDANCE LEVELS FOR RECREATIONAL EXPOSURE AND FOR DRINKING WATER

Toxin	Fish Consumption (ng/g fish wet weight)	Recreational Exposure (µg/L water)			Drinking Water Level (µg/L water)	
	OEHHA	OEHHA/CCHAB	WHO	EPA	WHO	EPA
Microcystins	10	0.8=Caution 6.0=Warning 20.0=Danger	24	8	1	0.3
Cylindro-spermopsin	70	4				
Anatoxin-a	5,000	90				

NOTES: µg/L = micrograms per liter; CCHAB = California Cyanobacteria and Harmful Algal Bloom Network; EPA = U.S. Environmental Protection Agency; ng/g = nanograms per gram; OEHHA = Office of Environmental Health Hazard Assessment; WHO = World Health Organization

SOURCES: OEHHA and CCHAB 2021; WHO 2021

Critically, not all cyanobacteria capable of producing toxins will be producing those toxins at any given time. Furthermore, many strains of cyanobacteria from genera known to produce cyanotoxins, including *Microcystis*, may or may not carry the gene to produce toxins, nor are they necessarily producing the toxin in the environment (Chorus and Welker 2021), including those found in the Delta (Moisander et al. 2009; Moisander et al. 2020). Toxicity for animals in the ecosystem depends on whether they are exposed to toxins bound within the cyanobacterial cells or free in the environment. Toxin concentrations in the water may be relatively low during a bloom, but increase as cells lyse and release stored toxins into the water column (Zastepa et al. 2014).

As with cyanoHABs worldwide, the primary factors associated with increases in biomass in the Central Delta are water temperature, residence time, and water clarity (Lehman et al. 2013; Lehman et al. 2018). Water temperatures in this region increased substantially starting in 1999 (Brooks et al. 2011). Both water temperature and clarity increase with increased residence time of water resulting from decreases in the flow of the San Joaquin River (Lehman et al. 2013; Spier et al. 2013). Increased residence time of the water allows the water column to stratify, which warms the surface layer of the water and allows suspended particulate matter to sink. In a recent analysis, Lehman et al. (2013) predicted that water temperature and water clarity would have the greatest impact on accelerating the growth of *Microcystis* and increase the frequency and duration of blooms in the Delta. Decreased flow typically occurs during July–September, which coincides with the occurrence of *Microcystis* blooms (Lehman et al. 2013, 2018, 2020; Spier et al. 2013).

Given that increased residence time and stratification increases the risk of the occurrence of blooms of *Microcystis* and other cyanoHABs, the drought is expected to result in an increase in both the duration and the severity of blooms of *Microcystis* and other potentially toxic cyanobacteria, with the potential for localized increases in other phytoplankton. An important concern is whether the TUCP will increase the effect of the drought on cyanoHABs, and whether placing a drought barrier in West False River will promote cyanoHABs in the Central Delta by restricting flows and increasing residence times.

Both times that the emergency drought barrier was in place, it was during the time of year (June–October) when cyanoHABs are most common in the Central Delta. Two previous analyses focused on ecosystem differences during successive drought years (2014 versus 2015) without and with the drought barrier in place. The analyses found that no impact on overall phytoplankton biomass, or on *Microcystis* biomass specifically, resulted from the barrier being in place (Kimmerer et al. 2019; Lehman et al. 2018). Biomass of *Microcystis* and concentrations of total microcystin toxins at Central Delta stations were greater in 2014 when the barrier was not in place than in 2015 when the barrier was in place, despite warmer median water temperatures (Lehman et al. 2018) and lower water flow rates east of the barrier in 2015 (Kimmerer et al. 2019). Although impacts on phytoplankton biomass associated with the barrier could not be detected, the growth and extent of SAV increased in Franks Tract directly east of the barrier, potentially aided by a reduction in jet flow through the middle of the water body (Kimmerer et al. 2019).

This report presents the results of an analysis of the variability in *Microcystis* biomass in drought years with and without drought barriers in place. Two drought years with barriers in place (2015 and 2021) have been compared with drought years without barriers in place (2014, 2016, and 2020).

The analysis is divided into three parts:

1. A comparison of harmful cyanobacteria levels in the Central Delta in 2020 and 2021 versus 2014, 2015, and 2016, using visual assessments and phytoplankton community composition as enumerated in grab samples. The visual assessments are also compared to potential covariates, including temperature, turbidity, and flow.
2. A comparison of cyanobacteria in different regions of the Central Delta in 2020 and 2021, with particular focus on Franks Tract and Mildred Island (the latter a reference site), using satellite data and rapid mapping using a FluoroProbe.
3. Hydrodynamic modeling of residence time and water temperature in the Franks Tract area.

2.2 Methods

2.2.1 Visual Assessments

Most monitoring surveys that collect data on water quality and fisheries in the Delta also collect visual observations of *Microcystis* and other visually detectable algal blooms. Because *Microcystis* colonies are relatively easy to identify visually in the field, this visual ranking gives a general idea of when and where the most common harmful cyanobacteria in the Delta occurs. A surface water sample is brought on board in a bucket and *Microcystis* is ranked on a scale of 1–5, 1 meaning “absent” and 5 meaning “very high” (**Figure 2**). Although this method is imprecise, it is generally reliable on the “presence/absence” level.

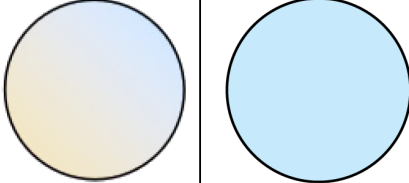
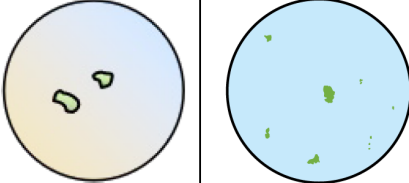
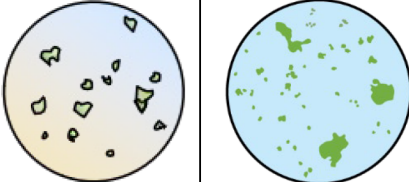
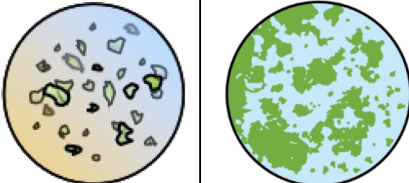
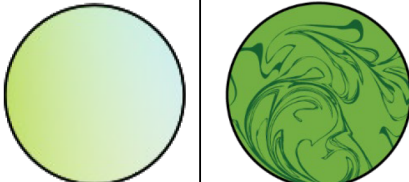
	1 – Absent No visible <i>Microcystis</i> colonies
	2 – Low Visible but widely scattered <i>Microcystis</i> colonies.
	3 - Medium Adjacent colonies of <i>Microcystis</i> .
	4 - High Contiguous colonies of <i>Microcystis</i> .
	5. Very High Concentrated contiguous colonies of <i>Microcystis</i> forming mats or scum.

Figure 2

Scale for visual *Microcystis* index used by monitoring programs in the Delta.

Visual assessment data for this report come from five surveys:

- The Environmental Monitoring Program (EMP) is conducted jointly by DWR, the California Department of Fish and Wildlife (CDFW), and Reclamation and collects water quality, phytoplankton, zooplankton, and benthic invertebrate data throughout the Delta, Suisun Bay, and San Pablo Bay. The EMP has recorded *Microcystis* observations at each of its discrete stations using the scale shown in Figure 2 since fall 2015. EMP also collects data on phytoplankton community composition via microscopic enumeration of grab samples, allowing an evaluation of which species are contributing to phytoplankton blooms. These data are collected at 24 fixed stations and up to four floating stations each month throughout the year (IEP 2020). These data are published annually on the Environmental Data Initiative repository.
- The CDFW Summer Townet Survey samples fixed locations from eastern San Pablo Bay to Rio Vista on the Sacramento River, and to Stockton on the San Joaquin River and a single station in the lower Napa River. The survey runs twice per month during June, July, and

August and samples at 40 stations. The survey primarily monitors young-of-the-year fishes, but also measures environmental variables including water temperature (°C), water clarity (Secchi Depth and nephelometric turbidity units [NTU]), and specific conductance (microSiemens per centimeter [$\mu\text{S}/\text{cm}$]). Visual observations of *Microcystis* have been collected since 2007. Data are available via the CDFW website.

- The CDFW Fall Midwater Trawl survey samples at fixed locations from eastern San Pablo Bay to the Cache Slough complex and Sacramento Deep Water Ship Channel, on the Sacramento River, and to Stockton on the San Joaquin River. This survey runs once per month during September, October, and November at 122 stations. The survey primarily monitors young-of-the-year fishes, but also measures environmental variables including water temperature (°C), water clarity (Secchi Depth and NTU), and specific conductance ($\mu\text{S}/\text{cm}$). Visual observations of *Microcystis* have been collected since 2007. Data are available via the CDFW website.
- DWR’s North Central Region Office conducts water quality and cyanoHAB sampling at stations throughout the South Delta. These samples include chlorophyll, nutrients, bromide, and organic carbon. When collecting water samples, the study also measures environmental variables including water temperature (°C), water clarity (Secchi Depth and NTU), specific conductance ($\mu\text{S}/\text{cm}$), and visual *Microcystis* index. Data are available from DWR’s Water Data Library platform.
- Reclamation’s Directed Outflow Project samples at randomly selected stations throughout Suisun Bay, Suisun Marsh, and the Delta in coordination with the U.S. Fish and Wildlife Service Enhanced Delta Smelt Monitoring Program. This program primarily collects zooplankton and water quality samples, as well as environmental variables including water temperature (°C), water clarity (Secchi Depth and NTU), specific conductance ($\mu\text{S}/\text{cm}$), and visual *Microcystis* index.

2.2.2 Analysis

The visual *Microcystis* scale goes from 1 (absent) to 5 (very high). However, because the scale is somewhat subjective and varies between observers, these data were categorized for this analysis using a three-point scale. Values of 1 were recoded as “absent,” values of 2 or 3 as “low,” and values of 4 or 5 as “high.” First, the difference between incidence of cyanoHABs across the entire Delta was assessed, to determine impacts of the TUCP; then the data were subset to include only those stations in the three regions near the emergency drought barrier (Lower Sacramento, Lower San Joaquin, and Southern Delta) (Figure 3).

An ordered logistic regression (the ‘polr’ function from the MASS package in R (Ripley et al. 2021)) was then used to test for differences between regions and between years. This regression was followed by a pairwise post-hoc test using the function ‘emmeans’ in the emmeans package (Lenth et al. 2021) to evaluate whether drought years had an increased probability of cyanoHAB presence or increased probability of high cyanoHAB presence compared to wet years, and whether there were significant differences between years with a drought barrier (2015, 2021) and drought years without a barrier (2014, 2016, 2020).

To assess the impact of change in Delta Outflow on probability of detection of *Microcystis* in visual index surveys, the data were subset to the Lower Sacramento, Lower San Joaquin, and

South Delta, because these regions regularly have the highest incidence of cyanoHABs. These data were summarized by month to calculate the monthly percentage of observations with *Microcystis* present. Daily Delta Outflow data were queried from CDEC (station DTO) from 2014–2021 and summarized to calculate the monthly average outflow. A binomial mixed model was performed on the likelihood of detected *Microcystis* in visual observations versus the log-transformed Delta Outflow with year as a random effect using the function ‘glmer’ from the package ‘lme4’ (Bates et al. 2020).

2.2.3 Community Composition

The EMP also provides data on phytoplankton community composition via microscopy from subsurface grab samples, allowing a determination of which species are contributing to phytoplankton blooms. These data are collected at 24 fixed stations and two stations that track the location of the salinity field each month throughout the year. Phytoplankton samples are collected with a submersible pump from a water depth of 1 meter below the water surface. Samples are stored in 50-milliliter (mL) glass bottles with 2 mL of Lugol’s solution to act as a stain and preservative. Samples are analyzed by BSA Environmental Services, Inc. (Beachwood, Ohio). Phytoplankton are identified to the lowest taxonomic level possible using the Utermöhl method and American Public Health Association standard methods (APHA 2017; Utermöhl 1958). A subset of samples from 2021 in regions near the barrier were prioritized for analysis and are reported here; data from other regions of the Delta will be available in spring 2022.

To assess the impacts of the barrier on phytoplankton abundance and community composition, the EMP samples were subset to include data from June through September for 2014–2021 in regions near the barrier. Only cyanoHAB species were subset. (These are defined as species in the genera *Anabaenopsis*, *Aphanizomenon*, *Cylindrospermopsis*, *Dolichospermum*, *Microcystis*, *Oscillatoria*, and *Planktothrix*.) The total concentration of cyanoHAB species in each sample was calculated and a zero-inflated negative binomial mixed model was applied, using the glmmTMB package (Magnusson et al. 2019) with the formula:

$$\text{Count} \sim \text{Region} + \text{Year} + \text{Error}(\text{Station}) + \text{offset}(\text{Volume})$$

The package ‘emmeans’ was used to conduct post-hoc pairwise comparisons between years and between regions (Lenth et al. 2021).

The authors of this report also conducted a permutational multivariate analysis of variance on the relative abundance of each taxon in the samples to assess whether there were significant differences in species present between regions and years, using the ‘adonis’ function in the ‘vegan’ package (Oksanen et al. 2020).

2.2.4 Nutrients

Discrete water quality grab samples were collected at all stations where phytoplankton community composition were collected. Water is collected using a flow-through system whereby it is pumped into the ship-board laboratory from a fixed intake located one meter below the water’s surface or from a Van Dorn water sampler or via a submersible pump as per (IEP 2020).

Analyses were performed for dissolved ammonia, dissolved nitrate + nitrite, total kjedahl nitrogen, total phosphorus, and dissolved orthophosphate by CDWR’s Bryte Laboratory using EPA methods or Department-approved modifications of these methods (IEP 2020). Data were subset to include stations in the Lower Sacramento, Lower San Joaquin, and South Delta (where cyanoHABs are most frequent) and summarized by month. Values below the reporting limit were replaced with 0 for purposes of visualization.

2.2.5 Cyanotoxin Data

The State Water Board’s freshwater HAB program collects samples for cyanotoxins when large blooms are reported (https://www.waterboards.ca.gov/water_issues/programs/swamp/freshwater_cyanobacteria.html). The Central Valley Regional Water Quality Control Board collected cyanotoxin samples from Franks Tract on July 2 and August 6, 2021. Samples were lysed and analyzed for total microcystins/nodularians using the enzyme-linked immunosorbent assay (ELISA) method, and using a quantitative polymerase chain reaction (i.e., qPCR) to detect the number of microcystin-producing cells present.

DWR collects cyanotoxin samples at Clifton Court Forebay and the Harvey O. Banks Pumping Plant (Banks Pumping Plant) to ensure that the water exported from the Delta is safe for use. Samples are collected every two weeks in April–October and analyzed by GreenWater Laboratories (Palatka, Florida), using a tiered approach. Samples are first assessed via microscopy to identify whether potentially toxic algae or cyanobacteria are present. If potentially toxic algae are detected, cells are lysed and samples are then tested for probable toxins using either ELISA or liquid chromatography–mass spectrometry (LC-MS), as appropriate (Foss and Aubel 2015).

A more comprehensive study of cyanotoxins is also underway at several stations throughout the Delta: Jersey Point (JPT), Decker (DEC), Middle River (MDM), Liberty Island (LIB), Rough and Ready Island (P8, DWR-EMP), and Vernalis (C10; DWR-EMP). For these efforts, cyanotoxins are being measured in whole water discrete samples as well as using Solid Phase Adsorption Toxin Tracking (SPATT) samplers every two to four weeks. All (100 percent) of these cyanotoxin samples will be analyzed using LC-MS, and—upon review of LC-MS data—a subset (approximately 20 percent) will be selected for analysis using ELISA. Data from this comprehensive U.S. Geological Survey (USGS)/DWR cyanotoxin project will not be available until spring 2022.

2.2.6 FluoroProbe Data

The EMP and USGS both employ vessels equipped with high-resolution sensors that collect data continuously on both water quality and phytoplankton community composition while underway. During these surveys, the EMP monitors water quality using a YSI EXO2 water quality sonde (Xylem, Inc.) to measure pH, turbidity, specific conductance, chlorophyll a (with the Total Algae™ sensor), dissolved oxygen (DO), and water temperature. Both surveys monitor the phytoplankton community’s composition using a FluoroProbe instrument (bbe moldaenke GmbH, Schwentinental, Germany) that differentiates cyanobacteria, diatoms, green algae, and chlorophytes based on the wavelength of the fluorescence given off by each taxonomic group’s

characteristic photopigments. USGS conducted mapping surveys in May, July, and October 2021, while EMP surveys are collected monthly throughout the year. Each month, these agencies covered approximately 350 miles of channels in the Delta over three to four consecutive days. USGS boat-based survey data can be visualized on [USGS's online data portal](#).

FluoroProbe data collected by both the EMP and USGS were processed following the methodology described in the Methods PDF of the USGS data release at www.doi.org/10.5066/P9FQEUAL (Bergamaschi et al. 2020). Briefly, data were spatially aligned to equally spaced polygons spaced at approximately 150 meters. Interpolated values were calculated in ArcGIS using the Spline with Barriers tool (Terzopoulos and Witkin 1988) and used to create a continuous map of values (e.g., the concentration of chlorophyll a from blue-green algae) across the mapped domain.

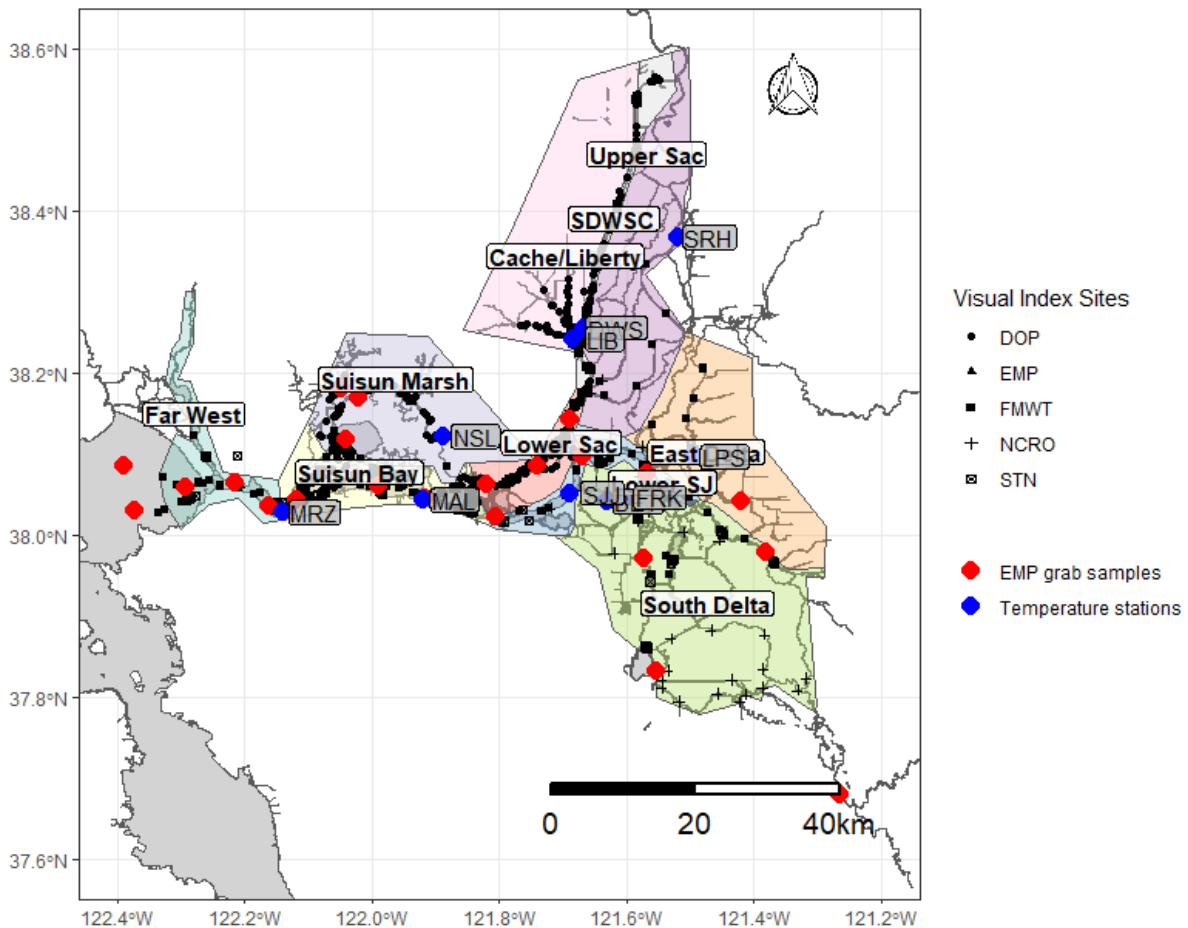
2.2.7 Satellite Data

To contribute higher spatial and temporal resolution data, the analysis used satellite data collected by the Copernicus Sentinel-3 mission provided by EUMETSAT. Imagery collected by Sentinel 3a estimates the abundance of cyanobacteria by measuring the absorption of light by chlorophyll and phycocyanin, an accessory pigment in photosynthesis specific to cyanobacteria. Satellites can separately estimate the average cyanobacteria abundance in the upper 1 meter of the water column for pixels that are 300 meters by 300 meters, an area of roughly 22 acres. Values for each pixel are reported in an exponential, satellite-specific, unitless metric called the Cyanobacteria Index (CI) derived from post-processing methods established by the National Oceanic and Atmospheric Administration's National Ocean Service (Wynne et al. 2018). Because of the limitations of the satellite-based sensor in distinguishing subtle differences in light absorbance from cyanobacteria at levels that are very low (CI of 6.310×10^{-05} is near natural background levels of cyanobacteria) or very high (CI of 6.327×10^{-02} in extremely dense scums), minimum and maximum detectable levels have a smaller range than are possible using traditional water grab samples.

The report authors downloaded raster files of CI data across the Central Delta for June–October in 2020 and 2021 as reported by the San Francisco Estuary Institute's HAB Satellite Analysis Tool (SFEI 2021). Raster pixels for the Franks Tract and Mildred Island geographical areas were extracted from each file using the 'exact_extract' function in the 'exactextractr' R package version 0.7.1 (Baston 2021). Franks Tract and Mildred Island were defined using polygons from CDFW expanded by 200 meters around their perimeters to account for the large raster pixels. Pixels were categorized into four CI categories (Low, Moderate, High, and Very High) based on WHO recreational guidance level thresholds (WHO 2021). Additionally, pixels that were below the detection limit for the imagery processing method ($CI \leq 6.310 \times 10^{-05}$) were categorized as "Non Detect," and pixels that were either invalid or missing were categorized as such. Including only pixels that were completely within either of the polygons for the two regions, the numbers of pixels within the "Non Detect," "Invalid," and four CI categories were counted for each polygon and raster image. Using only days when there were greater than 25 percent valid pixels within a region, the time series of pixel counts within the "Non Detect" and four CI categories were visualized using area plots for each region and year.

2.2.8 Continuous Water Quality Data

Water temperature data collected continuously (i.e., every 15 minutes) with sondes were downloaded from the DWR California Data Exchange Center (CDEC) portal, cdec.water.ca.gov, for 10 stations located between Suisun Bay to the west and the eastern Delta to the east. These stations included Martinez (MRZ) and Mallard Island (MAL) in Suisun Bay, the National Steel station in Suisun Marsh (NSL), the Sacramento Deep Water Shipping Channel (DWS) and Liberty Island (LIB) in the Cache Slough Complex, the Sacramento River at Hood (SRH) in the Upper Sacramento region, the San Joaquin River at Jersey Point (SJJ), Bethel Island (BET), Franks Tract (FRK) in the Central Delta, and Little Potato Slough (LPS) in the eastern Delta (Figure 3).



NOTE: Analysis to assess the impact of the 2021 Emergency Drought Barrier will focus on the Lower Sacramento, Lower San Joaquin, and Southern Delta. Analysis to assess the impact of the TUCP will encompass the entire area.

Figure 3
Stations for long-term monitoring programs contributing *Microcystis* visual observations (black), phytoplankton grab samples (red), and temperature data (blue).

For this analysis, water temperature data were parsed according to two thresholds: 19°C and 25°C. These thresholds were chosen based on literature indicating they are associated with increased risk of occurrence of *Microcystis* in the Central Delta (Lehman et al. 2013; Lehman et

al. 2018). Water temperature data were examined from January 2014 through October 2021 for all stations except station FRK. Water temperature data from station FRK were only available from 2015 onward. The number of days in each calendar year when water temperatures reached 19°C or above, and 25°C and above, were tabulated for each of the 10 stations. In addition, the maximum water temperature attained in each month of the calendar year, across the years 2008–2021, was tabulated for station BET (Bethel Island) near Franks Tract. This station had a longer record than the other stations, providing a point of reference for changes in water temperature over time in the Central Delta.

The number of days above 19°C and the number of days above 25°C for each station in each region, as outlined in Figure 3, were then used as predictor variables in a generalized linear mixed model with a binomial distribution predicting the presence of *Microcystis* in visual surveys. Region was used as a random effect. This model was conducted using the `lmer` function from the R package `lme4` (Bates et al. 2020).

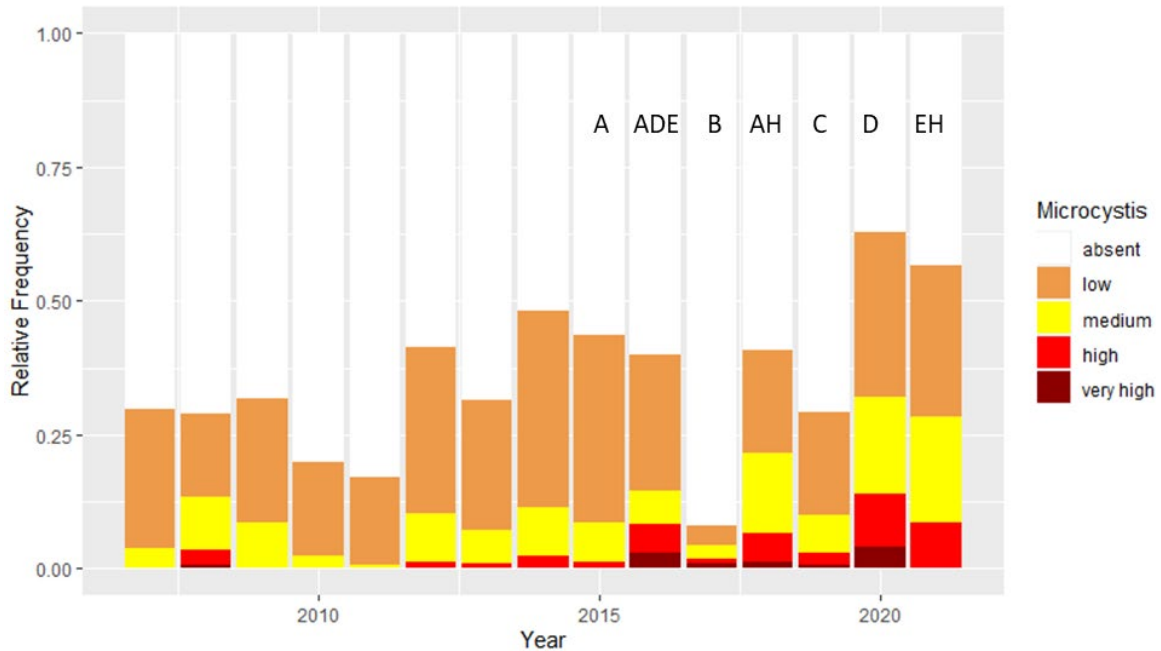
2.2.9 Hydrodynamic Modeling and Flow

To assess changes in residence time and temperature, three-dimensional simulations were carried out using the Bay-Delta SCHISM three-dimensional circulation model (Ateljevich et al. 2014), which is an application of the Semi-implicit Cross-scale Hydroscience Integrated System Model (Zhang et al. 2016). Mean water age was used as a surrogate for residence time, evaluated using the Constituent oriented Age and Residence Time theory or CART (Deleersnijder et al. 2001) and the formulation described by Delhez et al. (2014). This method uses pairs of supplementary tracer transport equations to evolve the mean age of water at each point in the domain; the method naturally incorporates multiple pathways of travel and dispersion and is an economical tool for evaluating spatial patterns. “Age” in this case is defined as the time of last contact with the San Joaquin River. Quantitative results within Franks Tract are sensitive to assumptions concerning the vegetation field. Vegetation was included using the method of Zhang et al. (2020b), which was originally tested in Franks Tract using spatial patterns of vegetation inferred from hyperspectral imagery from 2015 (Ustin et al. 2016).

2.3 Results

2.3.1 Visual Index Data

The *Microcystis* visual index data provided a broad-scale but low-accuracy picture of harmful cyanobacteria across the Delta since 2007 (Figure 4). An ordinal regression of *Microcystis* across the entire Delta/Suisun found that 2021 had a slightly lower incidence of *Microcystis* observations than 2020, but a similar incidence to 2016. When focusing just on the area surrounding the emergency drought barrier, 2020 and 2021 were not different (**Table 3**), most likely because of the high concentration of *Microcystis* in the South Delta and San Joaquin River in all years (Figure 5, Figure 6).



NOTE: Letters indicate groups of years that were not significantly different at the $p = 0.05$ level (results of an ordinal regression, Appendix A, Table A-2). The ordinal regression was only run on 2014–2021, but earlier years are shown for comparison.

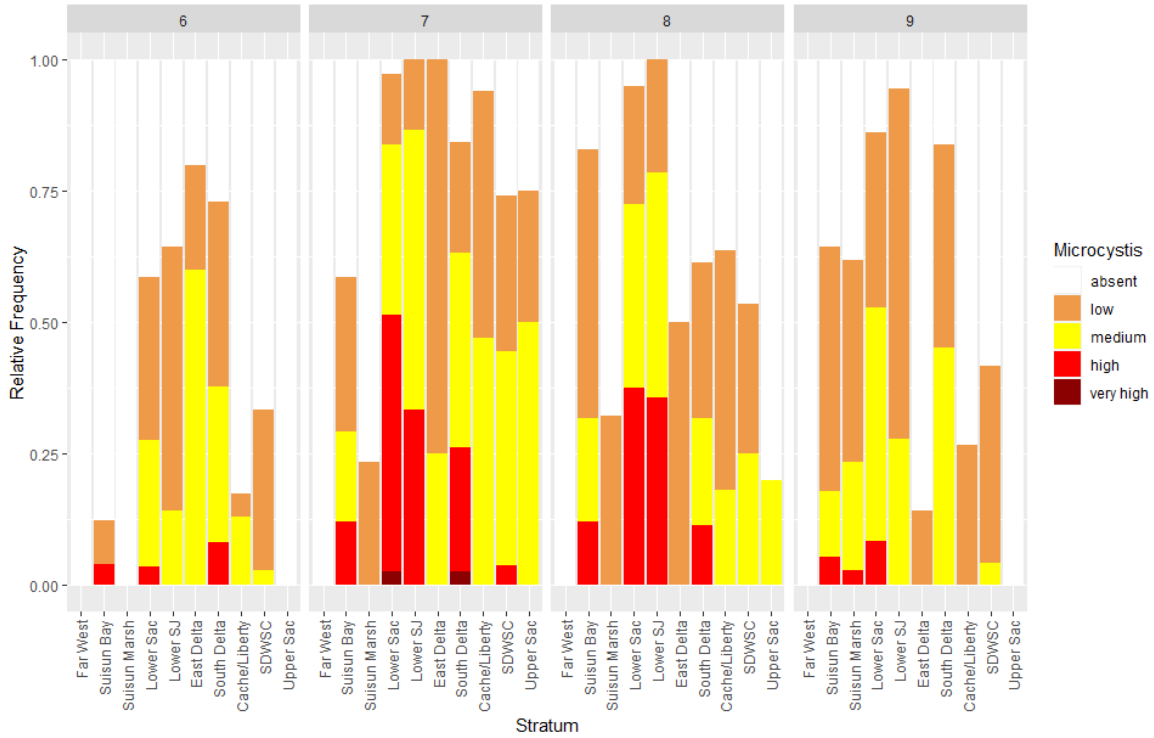
Figure 4

Frequency of visual *Microcystis* observations in the Delta and Suisun from long-term monitoring programs, 2007–2021.

TABLE 3
RESULTS OF ORDINAL REGRESSION ON *MICROCYSTIS* INDICES FROM VISUAL SURVEYS IN THE AREA IMMEDIATELY SURROUNDING THE EMERGENCY DROUGHT BARRIER FOR 2014-2021

Predictor	Likelihood Ratio (X^2)	Degrees of Freedom	P-value (X^2)
Year	371.5	7	< 0.0001
Region	165.86	2	< 0.0001
Temperature	133.81	1	< 0.0001

NOTE: Visual surveys were conducted in the Lower Sacramento, Lower San Joaquin, and Southern Delta Regions.



NOTE: Data were integrated across the CDFW Summer Townet Survey, the Environmental Monitoring Program survey conducted jointly by DWR, CDFW, and Reclamation, the CDFW Fall Midwater Trawl, Reclamation’s Directed Outflow Project, and sampling by DWR’s North Central Region Office.

Figure 5
Relative frequency of harmful algal bloom observations by month in different areas of the Delta in 2021.

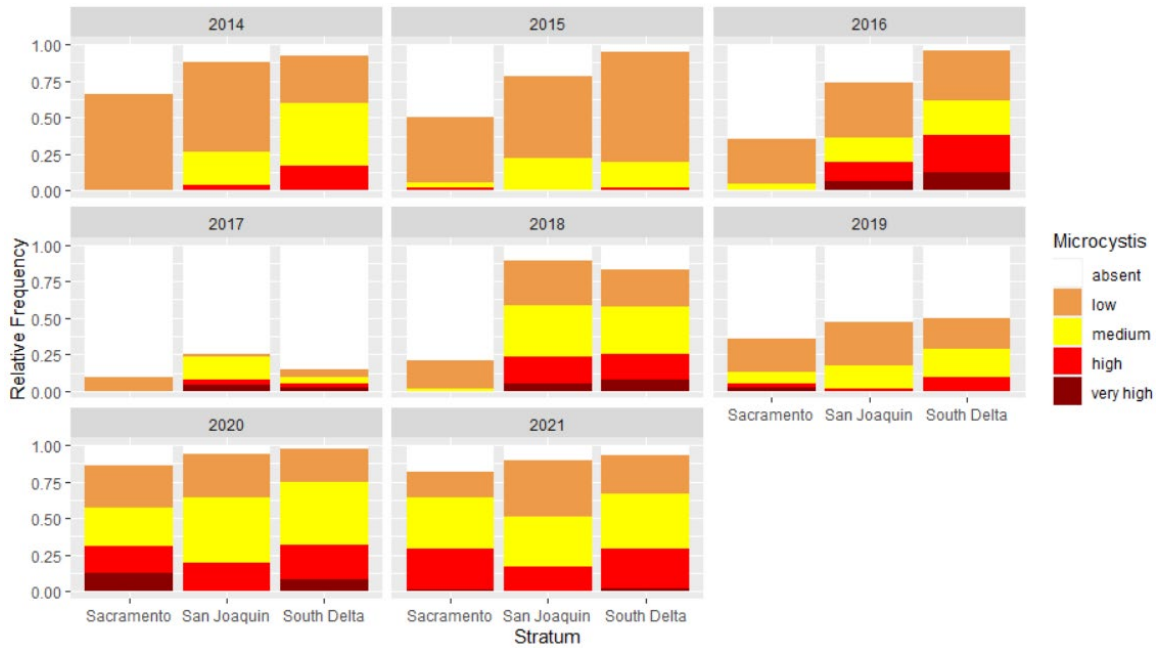


Figure 6
Frequency of occurrence for *Microcystis* in regions adjacent to the West False River drought barrier in summer and fall (May–October).

The binomial regression of the monthly probability of *Microcystis* presence versus monthly average Delta Outflow found a significant negative relationship between log-transformed flow and *Microcystis* (estimate = -0.959, St. Error = 0.08, z-value = -11.3, $p < 0.0001$, r-squared 0.068). Higher outflow was associated with lower probability of observing *Microcystis*, and there may be a threshold of flow above which *Microcystis* is not observed (Figure 7). The TUCP reduced the monthly average Delta Outflow by approximately 750 CFS, from 4000 to 3236 in June and 3328 in July (CDEC station DTO). Applying the regression, this equated to a change in probability of detecting *Microcystis* from 56.6% without the TUCP to 69.9% in June and 67.6% in July with the TUCP. Actual values for percent of observations with *Microcystis* present were 53% in June and 86% in July.

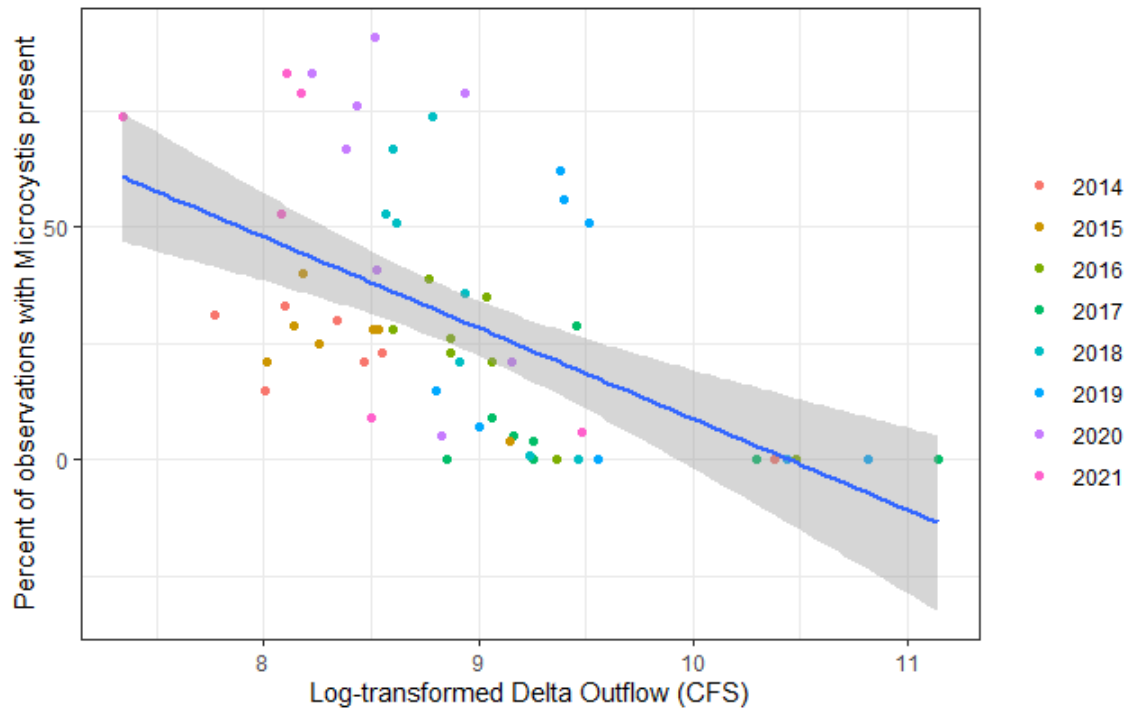


Figure 7
Percent of visual index values with *Microcystis* present in the Central and South Delta versus log-transformed Delta Outflow.

2.3.2 Cyanotoxin Data

Sampling for cyanotoxins within Franks Tract during summer 2021 was limited to two sampling events conducted during the bloom event by the freshwater harmful algal bloom program of the Regional Water Quality Control Board. The first sampling event, on July 2, did not detect any cyanotoxins (Table 4). The second sampling event, at the beginning of August, found high levels of microcystin-producing DNA in the water, indicating that *Microcystis* was present in high abundance and capable of producing toxins. Microcystin-Nodularian toxin concentration was 0.63 $\mu\text{g/L}$, above the EPA cutoff for safe drinking water (0.3 $\mu\text{g/L}$), though approximately 40 percent below the WHO cutoff for safe drinking water levels (1 $\mu\text{g/L}$). This concentration is well below the median lethal dose (LD_{50}) reported for most fish taxa (20–1,500 $\mu\text{g/L}$), although

sublethal effects cannot be ruled out (OEHHA Ecotoxicology et al. 2009). Toxin sampling also occurred every two weeks at Clifton Court Forebay and Banks Pumping Plant. Although some harmful cyanobacteria were detected via microscopy, all toxin analysis was below the detection level (**Figure 8**; Appendix A, Table A-1).

TABLE 4
RESULTS FROM REGIONAL WATER QUALITY CONTROL BOARD CYANOTOXIN MONITORING IN FRANKS TRACT
DURING SUMMER 2021

Location	Date	Latitude	Longitude	Constituent	Result
Franks Tract	7/2/2021	38.0511	-121.583	Microcystins/Nodularins	ND
				Chlorophyll	2 µg/L
				Phycocyanins	3 µg/L
Franks Tract	8/6/2021	38.03793	-121.586	Microcystins/Nodularins	0.63 µg/L
				Chlorophyll	9 µg/L
				Phycocyanins	>199 µg/L
				Microcystins qPCR	24,685*
				Anatoxin qPCR	ND
				Cylindrospermopsin qPCR	ND

NOTES:

µg/L = micrograms per liter; ND = Non Detect; qPCR = quantitative polymerase chain reaction

* Refers to the number of repeats.

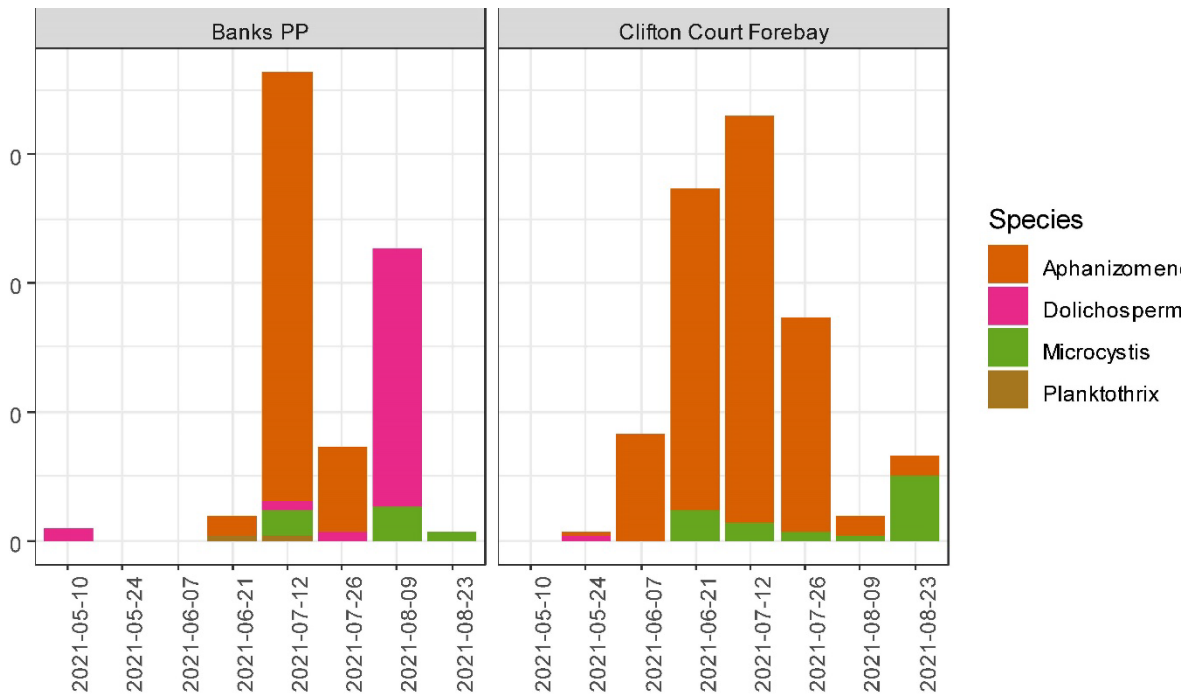


Figure 8
Potentially toxic cyanobacterial taxa detected via microscopy at Banks Pumping Plant and Clifton Court Forebay.

2.3.3 Community Composition Data

The results from phytoplankton samples collected by the EMP throughout the Central Delta showed that community composition of potentially toxic cyanobacteria varied between years but did not vary between regions (Table 5). In particular, *Aphanizomenon* was the most abundant potentially toxic cyanobacteria in 2015 and 2020, while *Microcystis* was the most abundant potentially toxic cyanobacteria in 2014, 2016, 2017, 2018, and 2021 (**Figure 9**). *Dolichospermum* was more abundant in 2021 than in any previous year.

TABLE 5
PERMANOVA RESULTS TESTING THE DIFFERENCE IN COMMUNITY COMPOSITION OF POTENTIALLY TOXIC CYANOBACTERIA BETWEEN REGIONS AND YEARS FOR THE REGIONS SURROUNDING THE EDB FROM 2014-2021

	Df	SS	MS	F	R2	Pr(>F)
Year	7	11.358	1.623	7.205	0.349	0.001
Region	2	0.917	0.458	2.035	0.028	0.087
Residuals	90	20.269	0.225		0.623	
Total	99	32.544			1.000	

NOTES: Df = degrees of freedom; MS = mean sum of squares; SS = sum of squares

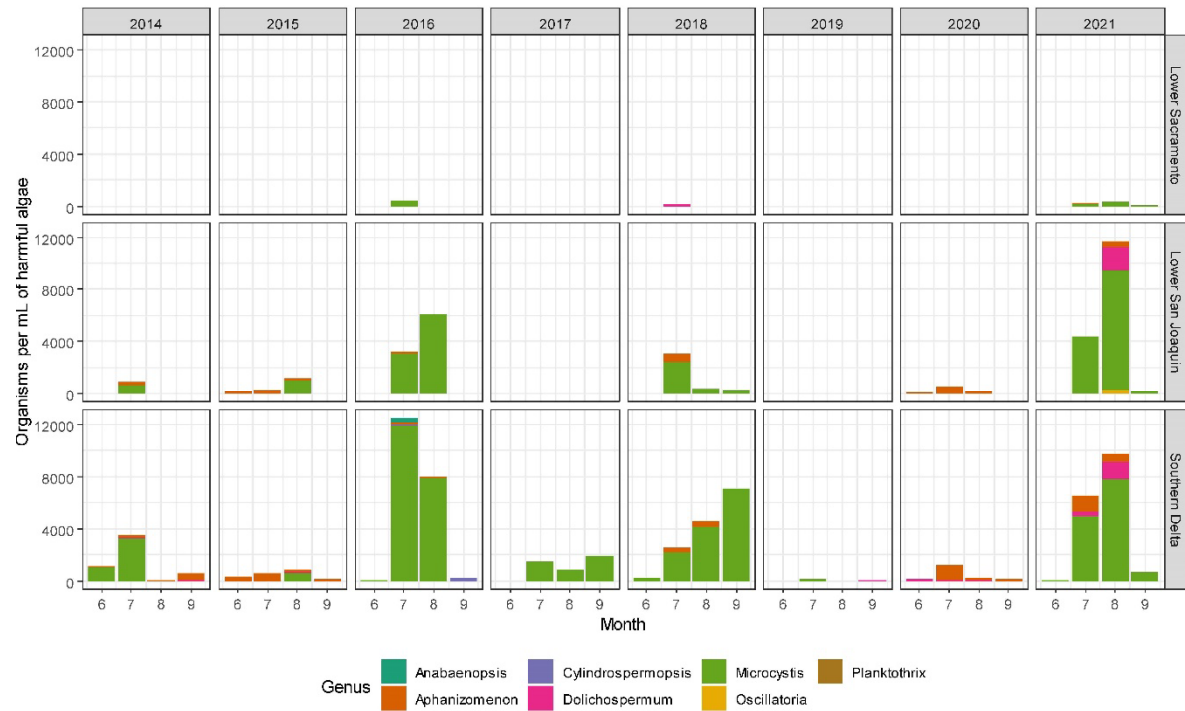


Figure 9
Concentration (organisms/mL) of potentially toxic cyanobacteria collected by the Environmental Monitoring Program in regions adjacent to the emergency drought barrier by month, region, and year.

The zero-inflated negative binomial model of concentration of total potentially toxic cyanobacteria found significant differences in both the incidence and the abundance of potentially toxic cyanobacteria between regions and years (Table 6, Figure 10). 2017 and 2019 had the lowest incidence of cyanobacteria, and 2014, 2015, 2016, 2018, 2020, and 2021 had higher incidence (zero inflation contrasts; Appendix A, Table A-4). 2015, 2017, 2019, and 2020 had lower abundance of cyanobacteria, while 2014, 2016, 2018, and 2021 had higher abundance (count model contrasts; Appendix A, Table A-4).

TABLE 6
COEFFICIENTS FOR ZERO-INFLATED NEGATIVE BINOMIAL MIXED MODEL ON TOTAL POTENTIALLY TOXIC CYANOBACTERIA CONCENTRATION COLLECTED BY THE ENVIRONMENTAL MONITORING PROGRAM IN THE REGIONS SURROUNDING THE BARRIER

Predictor	X ²	Degrees of Freedom	P-value	Coefficient Type
Year	121.22	7	<0.0001	Count
Region	30.355	2	<0.0001	Count
Year	41.989	7	<0.0001	Zero Inflation
Region	40.535	2	<0.0001	Zero Inflation



Figure 10
 Mean (+/- 1 SE) total concentration of selected potentially toxic cyanobacteria (*Aphanizomenon*, *Dolichospermum*, *Cylindrospermopsis*, *Anabaenopsis*, *Microcystis*, *Oscillatoria*, and *Planktothrix*) from EMP microscopy samples collected in summer (June–September) in regions adjacent to the barrier by year.

2.3.4 Nutrients

Nutrient samples collected in 2021 mostly showed similar levels to the previous seven years, though these were not tested statistically (Figure 11). Ammonium was somewhat higher in summer and fall of 2021 than in 2020, but within the range of 2014-2018. Dissolved orthophosphate was also slightly higher in spring and summer of 2021 than 2020, though it was similar to 2014 and 2015.

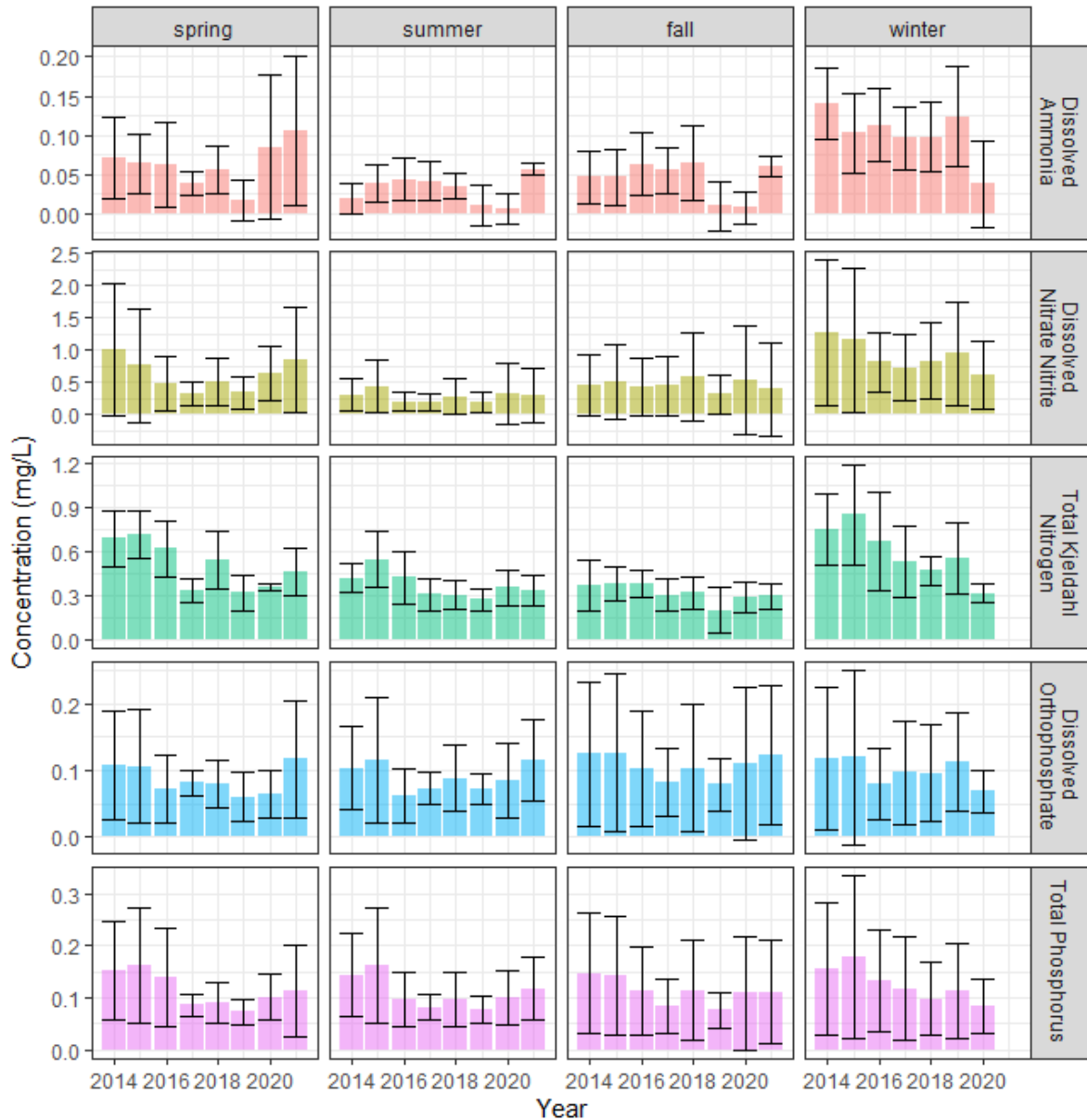
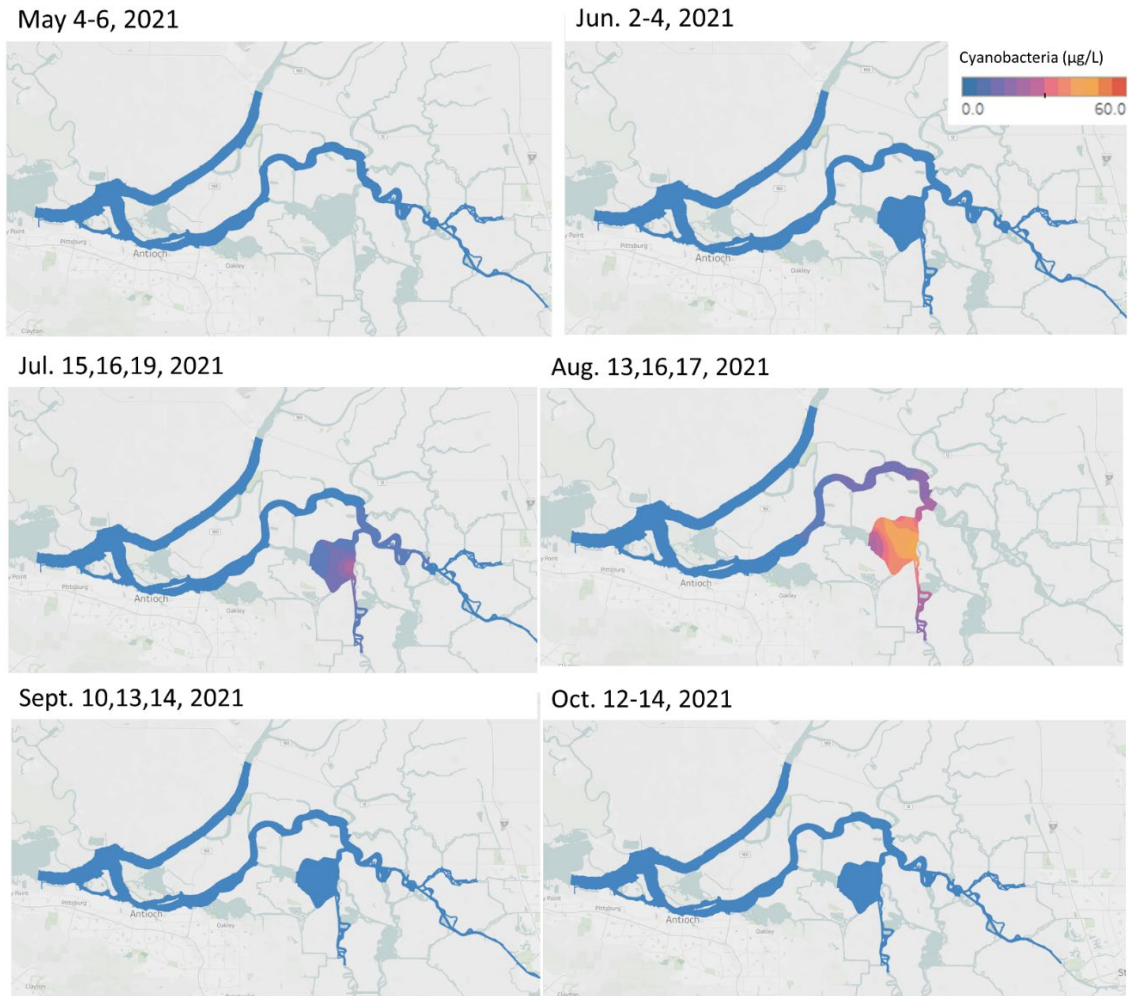


Figure 11
Average concentration (+/- 1 SD) of nutrients collected by EMP in the South Delta by season.

2.3.5 FluoroProbe Data

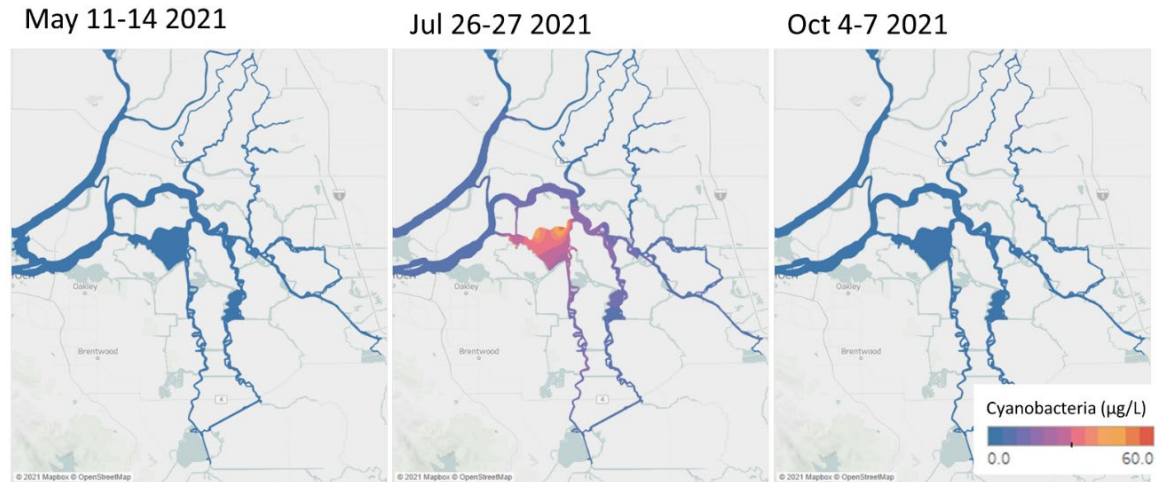
Spatial maps of cyanobacteria pigment concentration as measured by the FluoroProbe showed low concentrations (less than 5 $\mu\text{g/L}$) of cyanobacteria in May and June 2021 (Figure 12, Figure 13). Measurements taken in July, however, detected increasing amounts of cyanobacteria in the interior Delta around Franks Tract. Notably, the concentration of cyanobacteria measured by the EMP in this area on July 16 was substantially lower than the concentration measured by USGS later in the month. EMP collected data from the 15th through the 19th, while USGS

mapped the 26th through the 30th. The highest concentration of cyanobacterial pigments measured by the EMP occurred in August, with concentrations peaking at 60.2 $\mu\text{g/L}$ in the eastern part of Franks Tract at the mouth of Old River before subsiding below 5 $\mu\text{g/L}$ in September. Both data sets show the highest cyanobacterial biomass around Franks Tract and south into Holland Cut. The USGS survey also measured values of cyanobacterial pigment ranging from 10 to 30 $\mu\text{g/L}$ in the San Joaquin River and Mildred Island in July.



NOTE: Data were collected by DWR and analyzed in ArcGIS and Tableau by USGS.

Figure 12
 Monthly maps (May–October 2021) showing concentrations of cyanobacteria in the confluence and interior Delta, as measured using a FluoroProbe (bbe Moldenaek GmbH) during the Environmental Monitoring Program’s water quality cruises.



NOTE: Data were collected and analyzed by USGS.

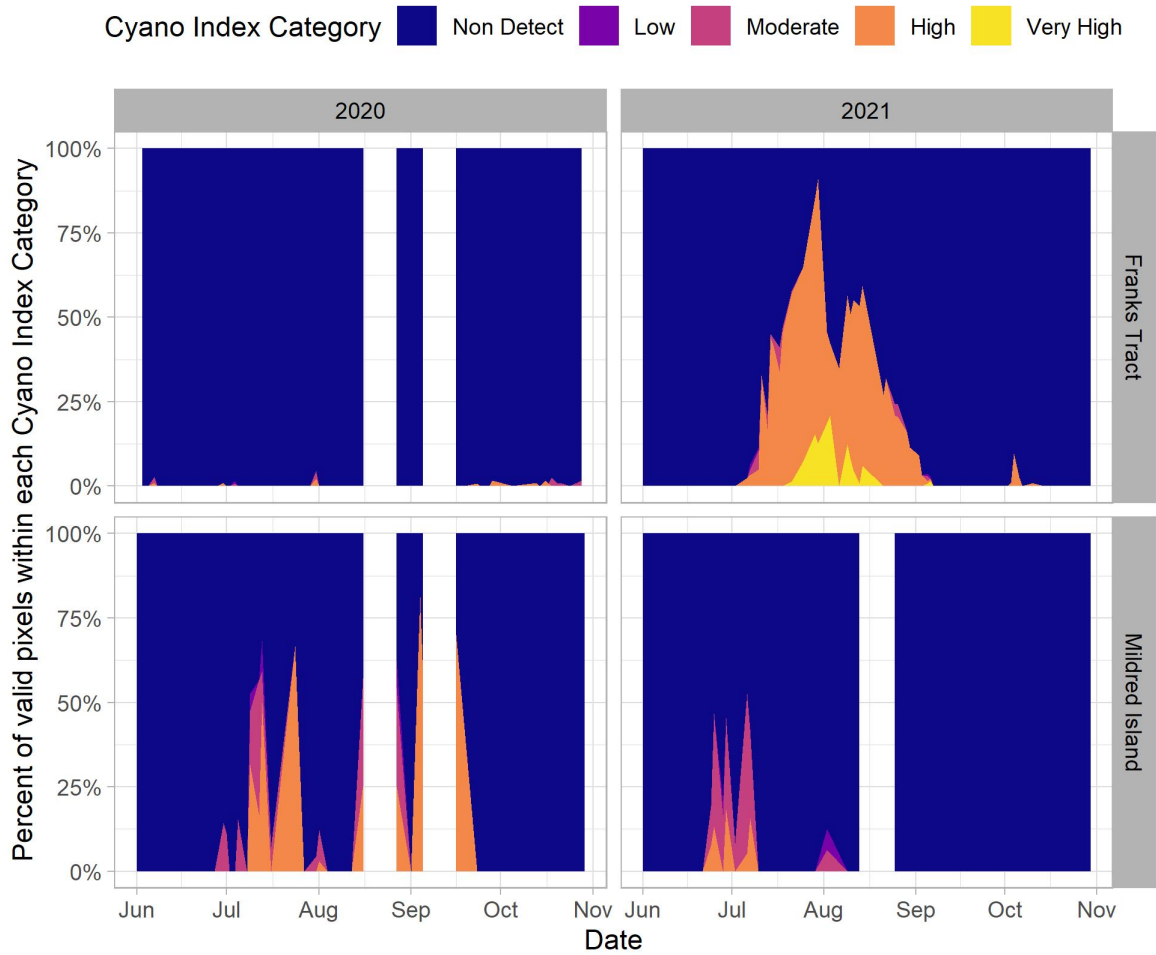
Figure 13

Monthly maps (May, July, and October 2021) showing concentrations of cyanobacteria in the confluence, interior, and southern Delta, as measured using a FluoroProbe (bbe Moldenaek GmbH) on U.S. Geological Survey rapid water quality cruises.

2.3.6 Satellite Data

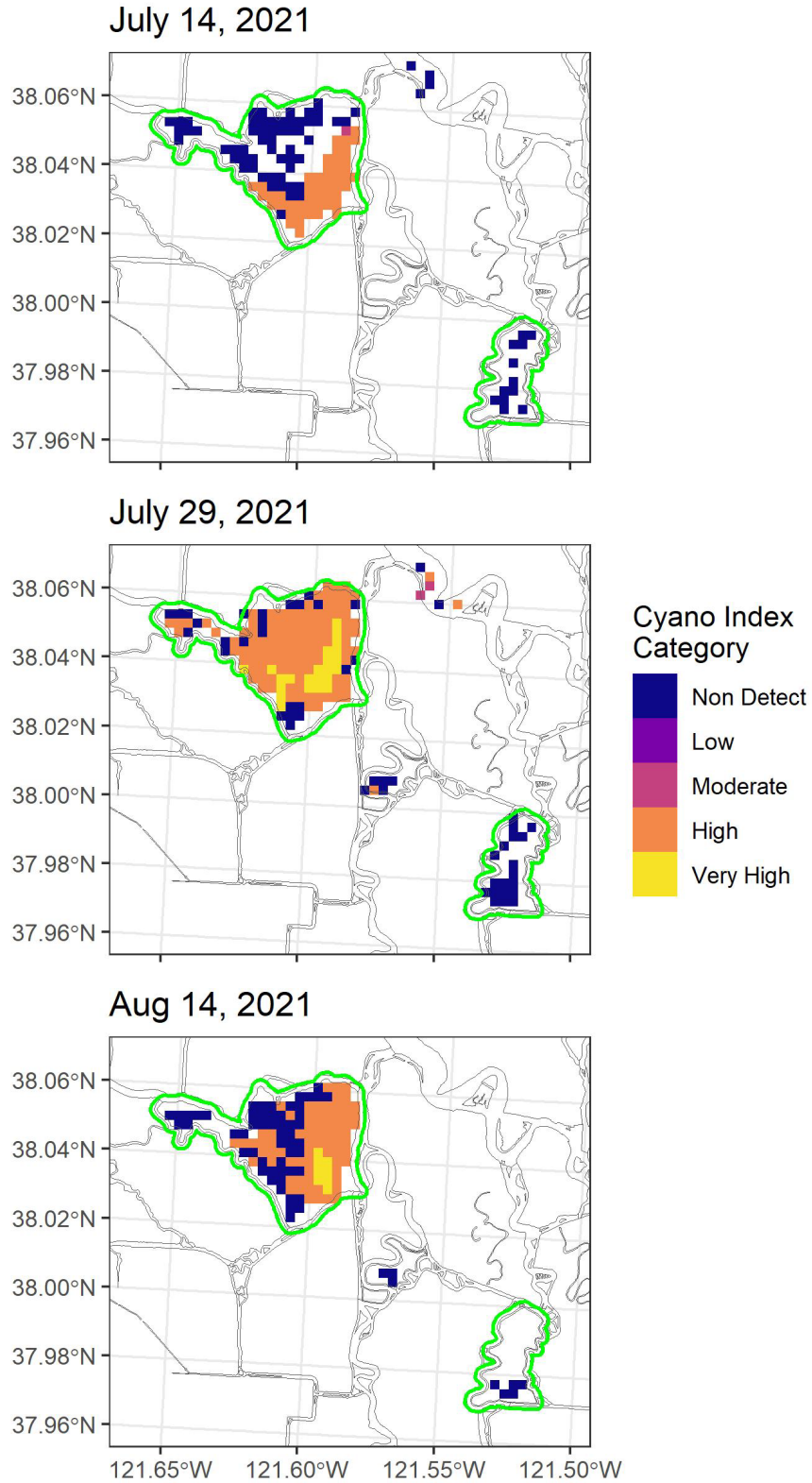
The July-August cyanobacteria bloom in Franks Tract documented by the EMP and USGS surveys was also apparent in the satellite data. These data indicated by a high percentage of its Franks Tract pixels within the High and Very High CI categories (Figure 14). During the peak of this bloom from mid-July through mid-August, at least 35 percent of the pixels were in the High or Very High categories, with a maximum of 90 percent in late July 2021. The bloom in Franks Tract in 2021 was the only time period in 2020–2021 at the two regions investigated when there were pixels in the Very High CI category. Spatially, the pixels with the highest CI categories appeared to be concentrated in the southeast corner of Franks Tract throughout the bloom in 2021 (Figure 15). In contrast, almost all pixels were in the Non Detect category within Franks Tract in 2020, with no apparent cyanobacteria bloom (Figure 14).

Nearby, Mildred Island had two cyanobacterial blooms of shorter duration during summer 2021: one in late June through early July and another in early August (Figure 14). These blooms appeared to be lower in concentration than in Franks Tract in 2021. Other than the Non Detect category, most of the pixels were within the Moderate CI category during the blooms observed at Mildred Island in 2021. During summer 2020, Mildred Island appeared to have a couple of longer duration blooms, with a greater percentage of pixels in the High CI category. Unfortunately, there were a few gaps in the satellite data set toward the end of August and beginning of September 2020 that may have obscured the extent of the cyanobacterial bloom in Mildred Island during this time. These gaps were greater than a week in duration and may have been during times when there was dense smoke in the area from regional wildfires.



NOTE: Gaps in the time series are moments when data were either missing or invalid for more than a week. These could have been during times when there was dense smoke in the area from regional wildfires.

Figure 14
Time series of the percent of valid pixels within each Cyanobacteria Index category for summer-fall in 2020 and 2021 within Franks Tract and Mildred Island.

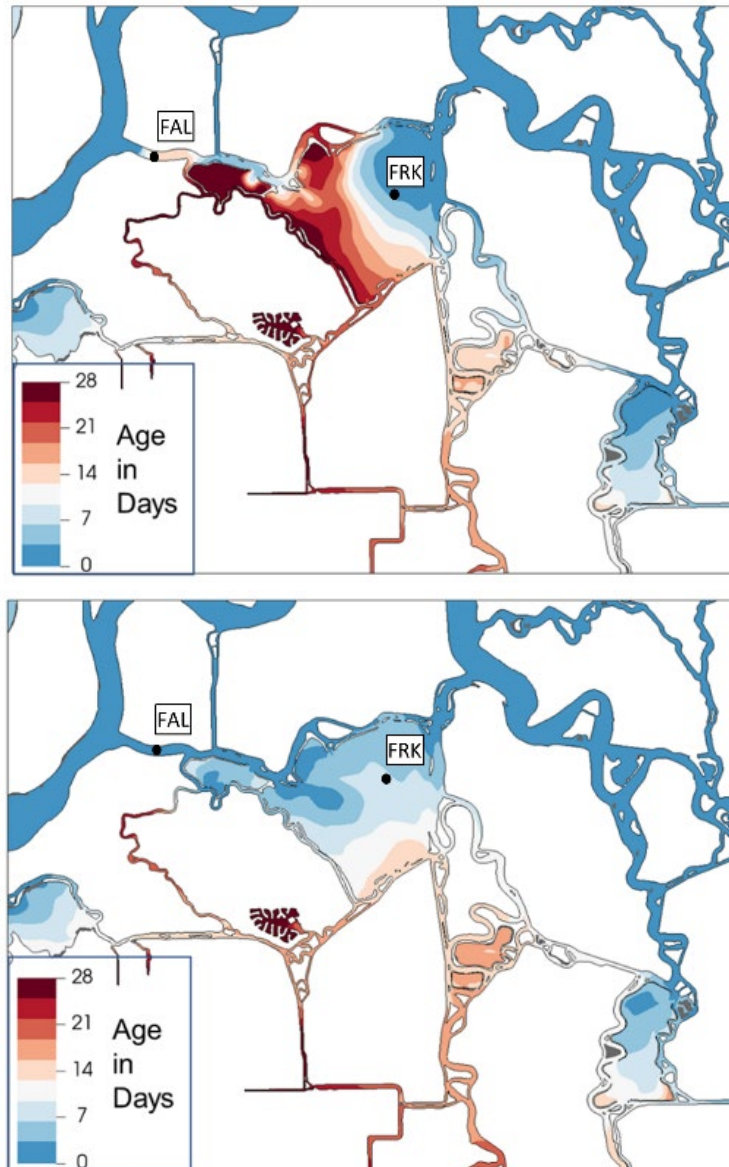


NOTE: The bright green polygons represent Franks Tract (top, left) and Mildred Island (bottom, right).

Figure 15
 Maps of Cyanobacteria Index categories at the beginning (top), peak (middle), and end (bottom) of the cyanobacteria bloom in Franks Tract during summer 2021.

2.3.7 Models of Water Age and Temperature

Figure 16 shows simulated mean age on August 17, 2021, with and without a barrier. The selected date coincides with a medium-strength spring tide and is timed sufficiently long after the closure of the barrier that the longest reported ages are developed entirely with the barrier in place. The images show that there is greater spatial organization of residence time within Franks Tract, with a clear gradient developing from northeast to southwest when the barrier is in place.



NOTE: "Age" is defined as time since contact with freshening flows from the San Joaquin River using the implementation described by Delhez et al. (2014). FAL and FRK are CDEC stations shown in Figure 15.

Figure 16
Modeled daily averaged age of water in Franks Tract with the barrier (top) and without the barrier (bottom) on August 17, 2021.

The enhanced gradient in age is readily explainable in terms of changes in tidal flow on the two sides of Franks Tract. **Figure 17** shows time series of tidal flows for a period straddling the installation of the barrier at False River to the west (USGS 11313440, CDEC FAL) and Old River to the east (USGS 11313452, CDEC OSJ). Model flow is also shown to allow comparison with a no-barrier case and corroborate that the simulation correctly captures the very large changes that occur. Without the barrier, the tidal range of flow is generated through connections to the San Joaquin River, both on False River to the northwest and on Old River in the northeast. With two connections open, water is renewed from both sides and some net circulation is fostered. With the barrier installed, tidal flow from False River is mostly eliminated and the tidal range at Old River is nearly doubled. Because of the dominance of Old River in supplying replenishing flow, age in the With Barrier case becomes proportional to distance from that inlet. The resulting changes in age are not zero-sum; overall, age is increased in Franks Tract. However, there are significant areas of greater flushing to the east.

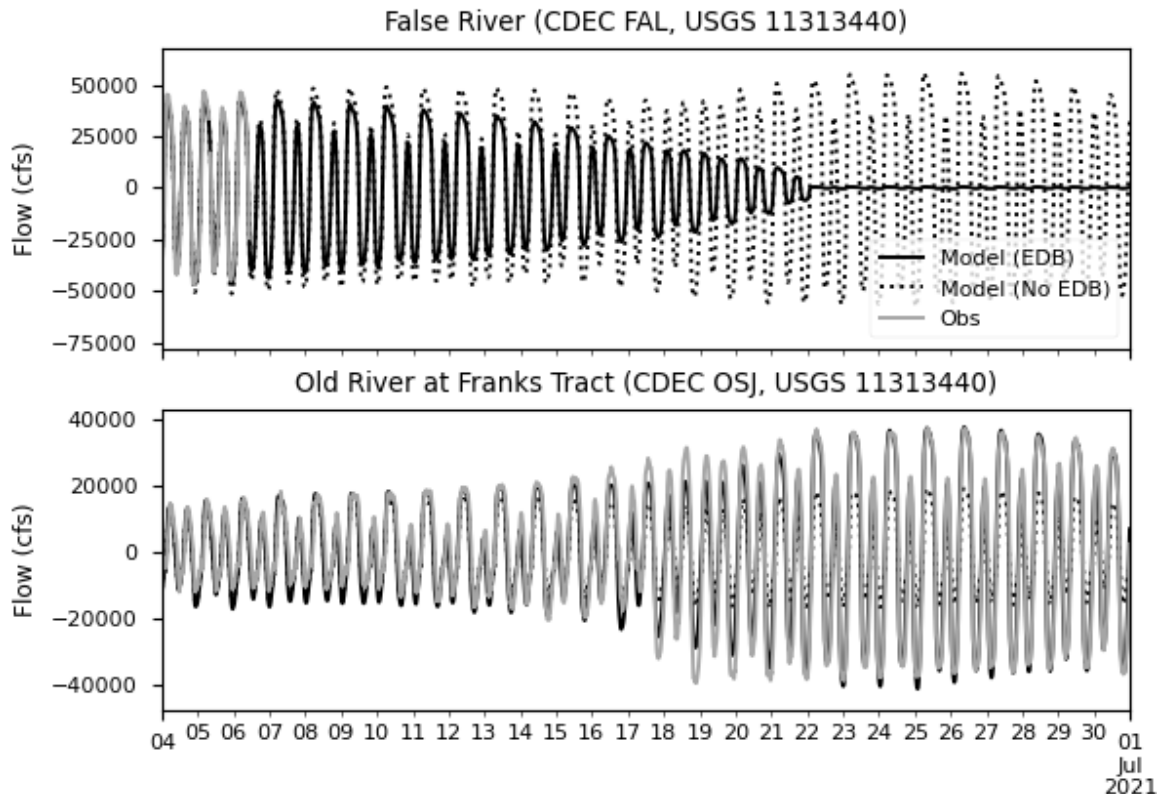


Figure 17
Modeled flow with and without the emergency drought barrier at False River and at Old River at Franks Tract.

Differences in July mean temperature are shown in Figure 18. Mean temperature in Franks Tract is not as affected by the barrier as mean age is, with changes in the range of 0.1° to 0.3°C. The reason for this more modest change is that water tends to reside in Franks Tract for a period that is long compared to the diel heat cycle. Local radiation and heat balance are therefore more important to temperature than advection of colder water. The exception to this generalization

occurs right at the inlet of False River, where exchanges with colder San Joaquin River water have their greatest effect. There, the difference in temperature with the barrier is +0.59°C.

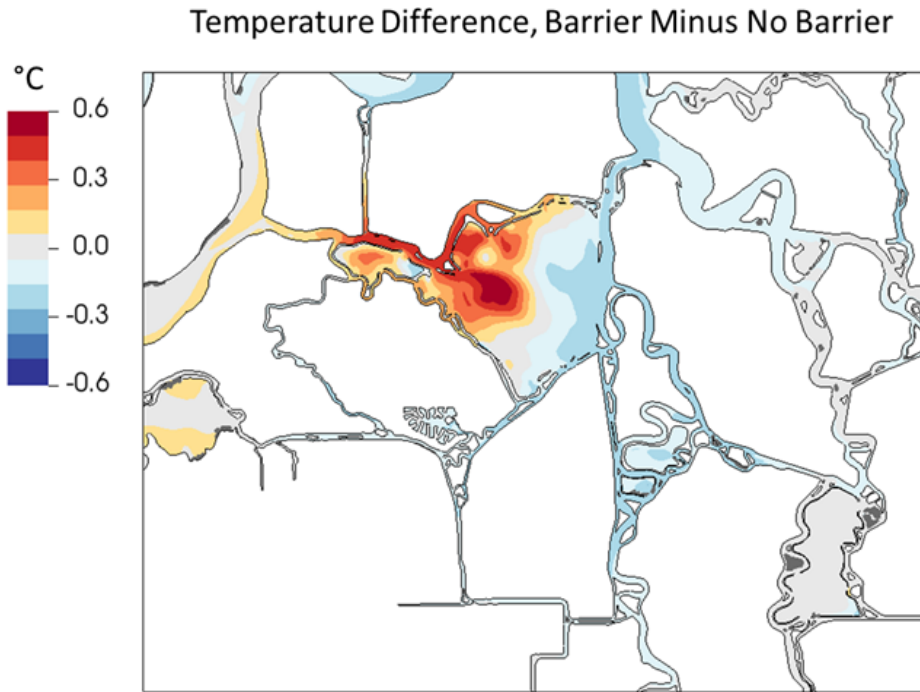


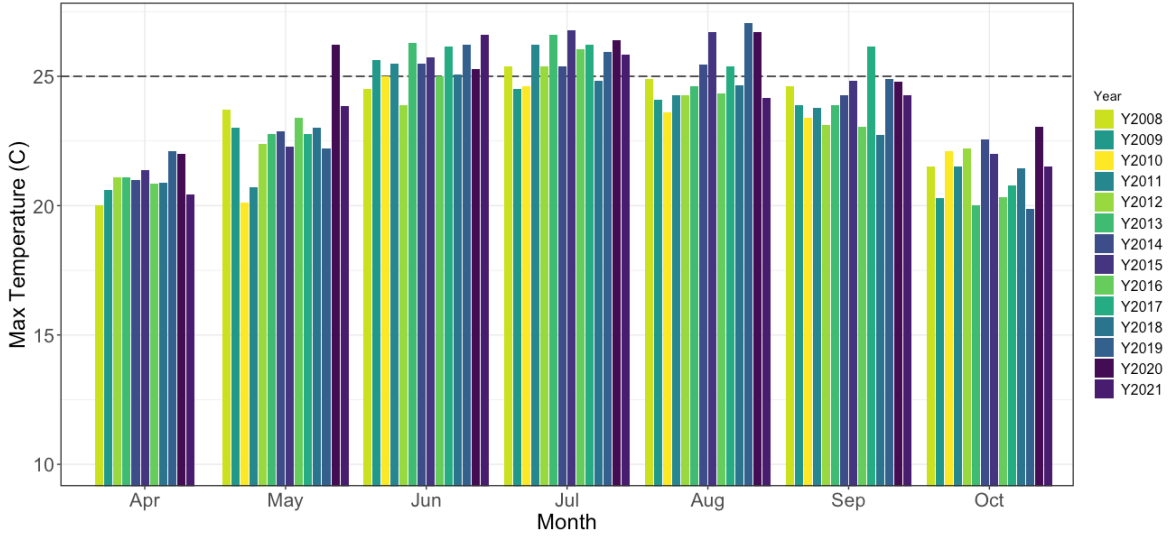
Figure 18

Modeled difference in water temperature for scenarios with and without the West False River Barrier.

2.3.8 Continuous Water Quality

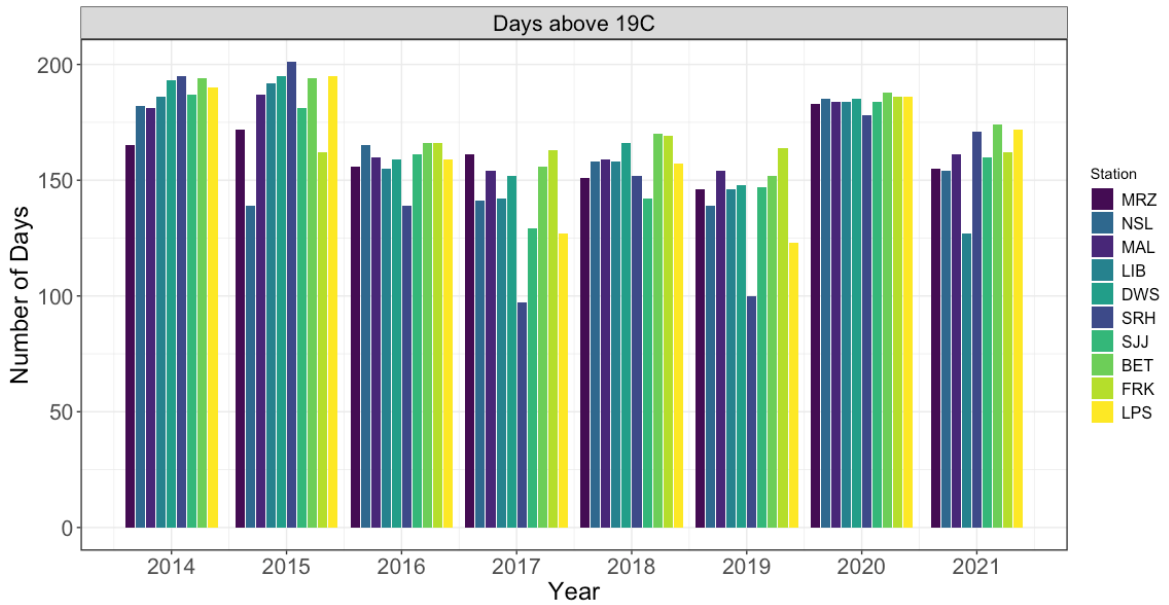
Water temperature data recorded at the Bethel Island continuous monitoring station since 2008 indicate that maximum water temperature in late spring and early summer has been increasing in the Central Delta. While water temperatures in the Central Delta typically do not exceed 25°C in May, maximum temperatures in 2020 reached above 25°C (Figure 19). Data from 2008 to the present demonstrate a consistent increase in maximum temperatures measured in June, at the start of summer, with the highest maximum occurring in 2021 (Figure 19). During August, when growth rates of *Microcystis* typically are highest (i.e., Lehman et al. 2018), temperatures reached maxima both in 2014–2015 and in 2020–2021 at Bethel Island near Franks Tract (Figure 19).

Years 2014 and 2015 were both warm years, as measured by the number of days in the calendar year that water temperatures reached 19°C or warmer across most stations (Figure 20). The same was true for 2020, while 2021, also considered a drought year, had slightly fewer 19°C days (Figure 20).



NOTE: Drought years (2014, 2015, 2020, and 2021) are indicated using darker shading.

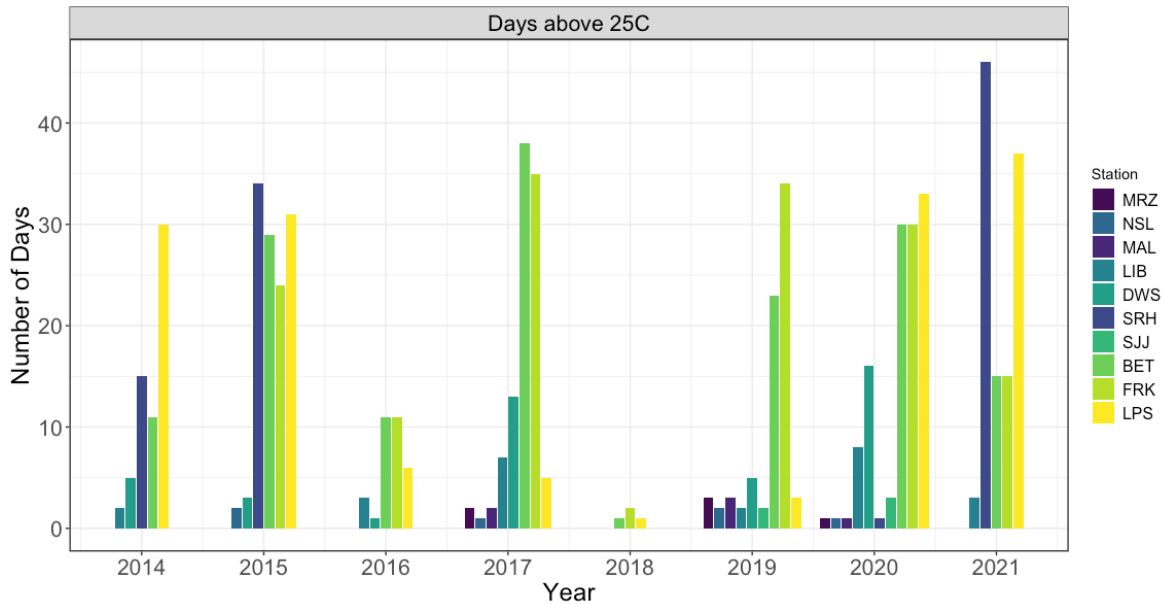
Figure 19
Maximum water temperatures by month at station BET, 2008–2021.



NOTE: Stations include three in Suisun Bay and the western Delta (MRZ, NSL, MAL), two within the Cache Slough/Liberty Island complex (DWS, LIB), one in the Sacramento River at Hood (SRH), and four stations in the Central and eastern Delta (SJJ, BET, FRK, LPS). See text for station abbreviations.

Figure 20
Number of days in the calendar year that water temperature reached 19°C or above across 10 stations in Suisun Bay, the Sacramento River, and the Delta.

There were differences in number of days above 19°C between years, though there were few differences between stations, with the exception of the Sacramento River (SRH), which consistently demonstrated lower temperatures and fewer days above 19°C in non-drought years (2016–2019). In contrast, the number of days with water temperatures of 25°C or above varied by stations more than between years. Only stations BET and FRK in the Franks Tract region, and station LPS in the eastern Delta, consistently reached 20 days or more of water temperatures 25°C and warmer in a calendar year (Figure 21). During the 2014, 2015, and 2021 drought years, SRH also reached a relatively high number of days with temperatures of 25°C and warmer (Figure 21).



NOTE: This figure refers to the same stations as identified for Figure 18.

Figure 21

Number of days in the calendar year that water temperature reached 25°C or above across 10 stations in Suisun Bay, the Sacramento River, and the Delta.

The binomial model of *Microcystis* presence in each region in each year versus days above 19°C did show a significant increase in presence with number of warm days (coefficient = 0.072, se = 0.026, z = 2.68, p = 0.007; Figure 22). However, days above 25°C were not a significant predictor of *Microcystis* presence (z = -0.219, p = 0.826; Figure 22).

A focused assessment of continuous water quality collected by the EMP at Franks Tract over the summer months of 2021 found substantial differences in parameters linked to increased levels of photosynthesis, i.e., DO and pH, from previous years. Beginning in July 2021, both the pH (Table 7, Figure 23) and concentration of DO (Figure 24) in Franks Tract began to increase, and by August had reached higher levels than previously recorded at this station (collected since 2015). The maximum daily pH peaked in early September before declining rapidly, while the DO peak was reached later in that month before also declining.

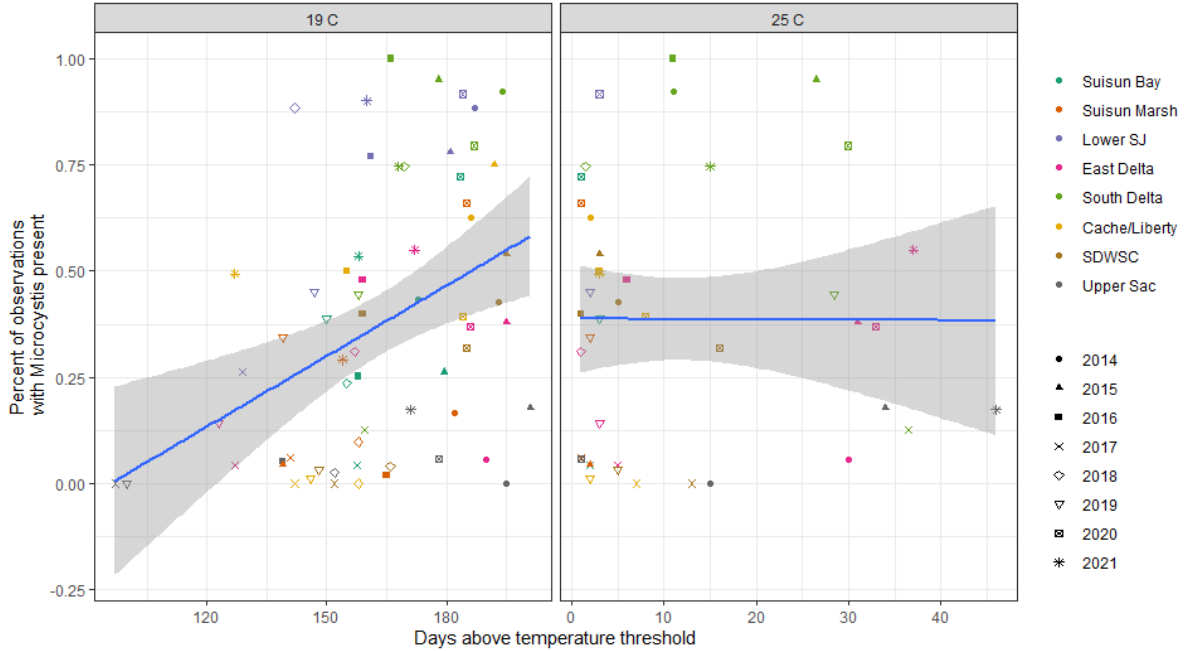
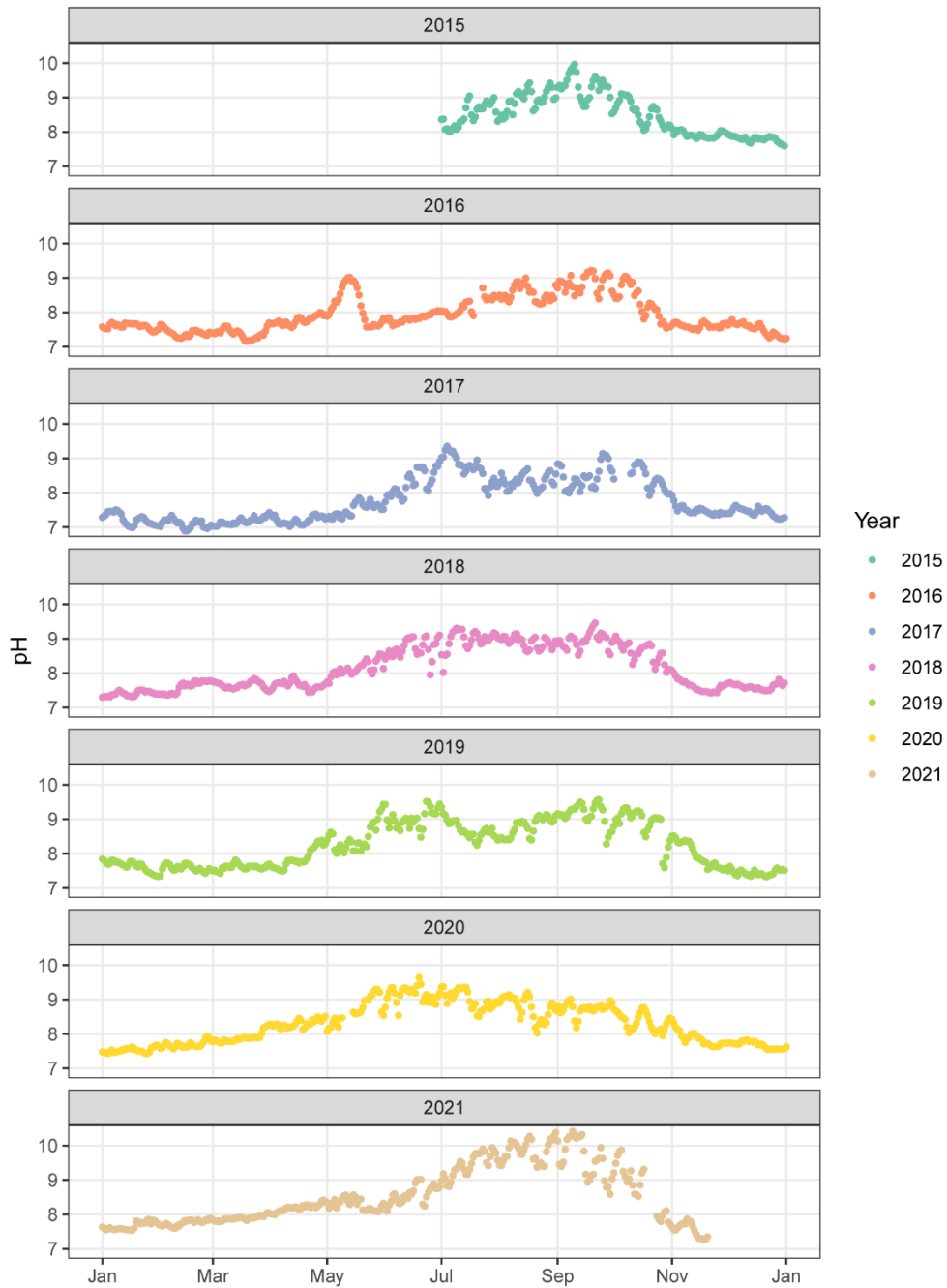


Figure 22
 Comparison of Delta-wide days above 19°C and 25°C per year with total percent of visual observations with *Microcystis* present.

TABLE 7
MEAN MONTHLY VALUE OF DAILY MAXIMUM PH (PH UNITS)

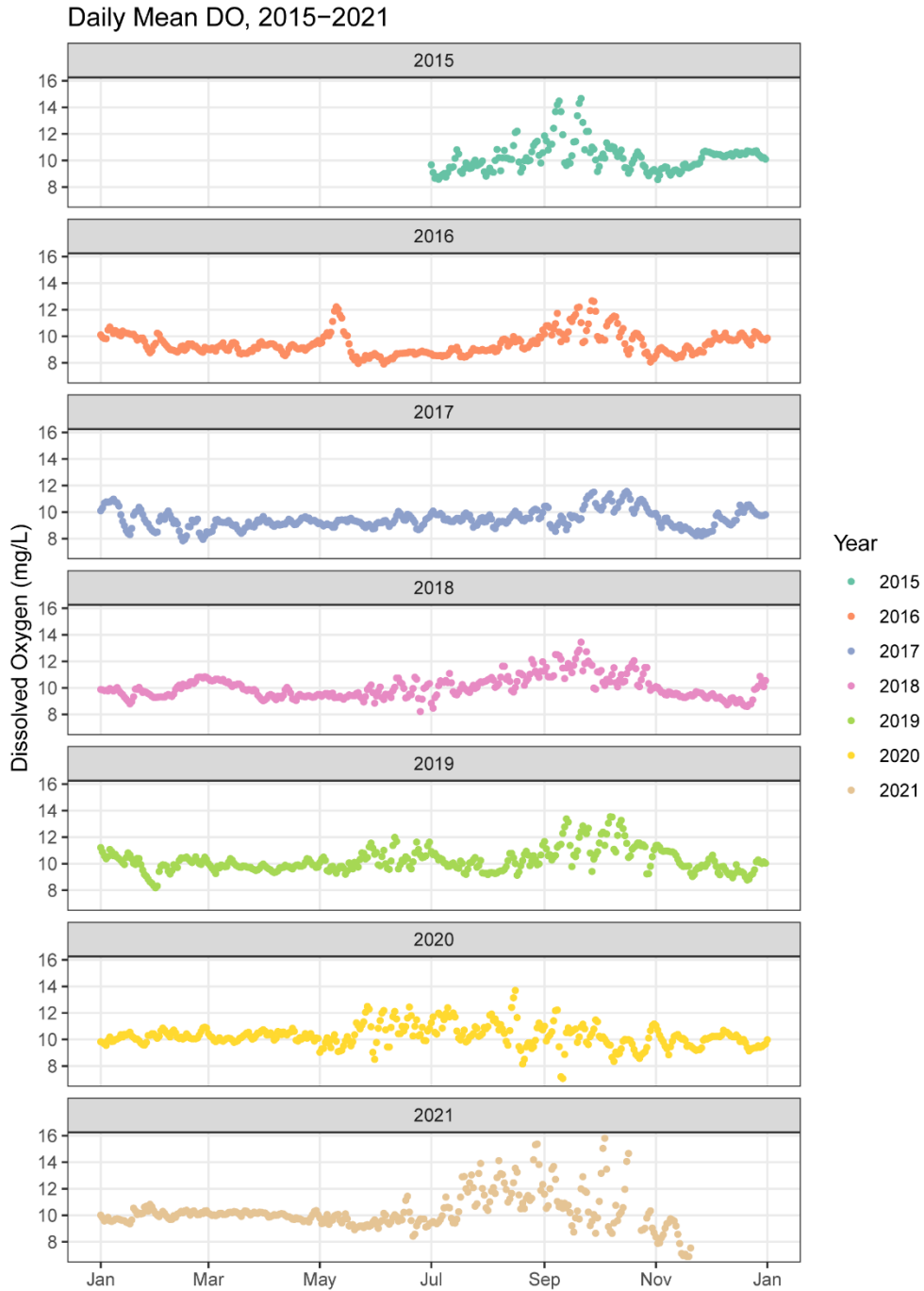
	2015	2016	2017	2018	2019	2020	2021
May	-	8.5	7.9	8.4	9.0	9.1	8.6
June	-	8.2	8.7	9.1	9.5	9.5	8.9
July	8.8	8.6	9.3	9.3	9.2	9.3	9.7
August	9.2	9.0	9.1	9.2	9.3	9.2	10.1
September	9.5	9.2	9.0	9.3	9.5	9.1	10.0
October	8.8	8.5	8.7	8.9	9.2	8.7	9.1

Daily Mean pH, 2015–2021



NOTE: Data were collected by the Environmental Monitoring Program using a YSI EXO2 water quality sonde equipped with a pH Smart Sensor.

Figure 23
Daily mean pH (2015–2021) at the continuous water quality monitoring station in Franks Tract.



NOTE: Data were collected by the Environmental Monitoring Program using a YSI EXO2 water quality sonde equipped with an optical dissolved oxygen Smart Sensor.

Figure 24
Daily mean concentration of dissolved oxygen (2015–2021) at the continuous water quality monitoring station in Franks Tract.

During the bloom, daily DO maxima peaked at more than 200 percent of saturation with atmospheric oxygen and averaged more than 170 percent for the months of July and August, the highest on record for this station (Table 8). Values of DO saturation greater than 100 percent indicate that photosynthesis is active in the water column. Daily chlorophyll levels, while higher than in summer 2020 (Figure 25), did not match the elevated levels detected using the FluoroProbe (Figure 12, Figure 13) and were in fact lower than in previous years (Table 9).

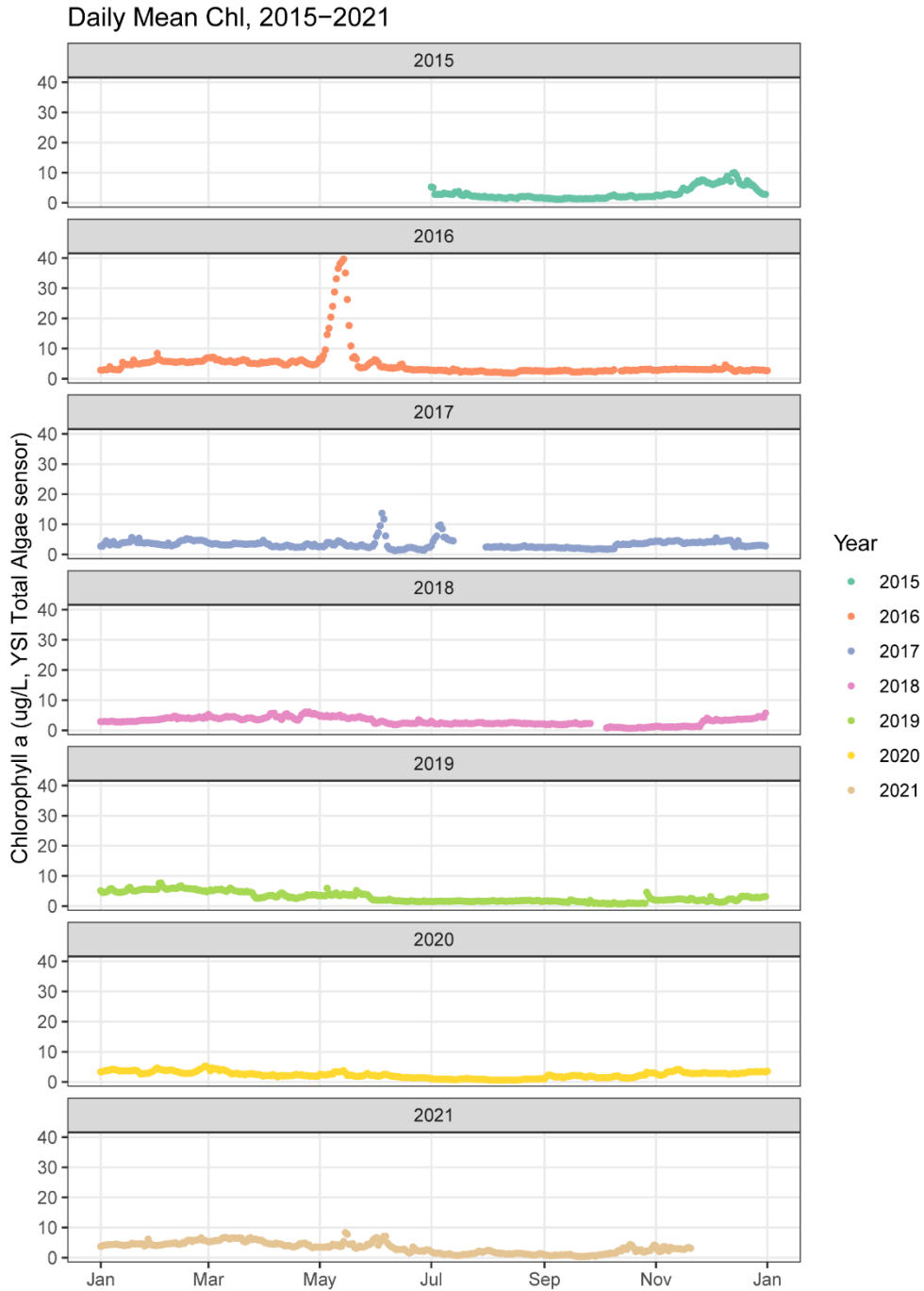
TABLE 8
MEAN MONTHLY VALUE OF DAILY MAXIMUM DISSOLVED OXYGEN (% SATURATION)

	2015	2016	2017	2018	2019	2020	2021
May	-	119.3	108.4	111.8	122.1	133.8	115.7
June	-	110.6	119.0	132.5	141.6	154.3	127.5
July	127.2	119.1	130.0	135.4	145.1	153.9	171.4
August	142.3	126.7	135.3	147.9	152.7	160.1	176.2
September	160.7	144.0	133.0	159.5	164.8	148.9	157.8
October	127.6	116.9	123.0	133.3	141.8	125.9	135.5

TABLE 9
MEAN MONTHLY VALUE OF DAILY MAXIMUM CHLOROPHYLL A (µg/L) AT THE CONTINUOUS WATER QUALITY MONITORING STATION IN FRANKS TRACT (FRK)

	2015	2016	2017	2018	2019	2020	2021
May	-	24.0	5.3	6.3	8.0	3.5	9.2
June	-	5.2	5.7	4.4	3.4	2.1	6.6
July	4.3	4.4	11.1	5.5	2.7	1.4	2.4
August	2.9	3.9	3.7	5.5	3.2	1.4	3.4
September	2.6	4.0	3.4	4.8	5.2	2.9	2.9
October	3.2	4.0	4.8	2.1	4.4	3.0	4.4

NOTE: µg/L = micrograms per liter



NOTE: Data were collected by the Environmental Monitoring Program using a YSI EXO2 water quality sonde equipped with a Total Algae sensor.

Figure 25
Daily mean concentration chlorophyll a (2015–2021) at the continuous water quality monitoring station in Franks Tract.

2.4 Discussion/Interpretation

Collectively, the data assembled from multiple sources for this report indicate no significant difference in the Delta-wide occurrence of harmful algal blooms in years with and without the TUCP or barrier. However, a local high density of cyanobacteria was found within and around Franks Tract in 2021, which may have been partially attributable to the increase in residence time of water within the tract caused by the barrier.

2.4.1 Impact of the Drought

Both the visual index data and microscopy data found a significantly higher incidence and abundance of cyanoHABs in dry years (2014, 2015, 2016, 2018, 2020, 2021) than in wet years (2017, 2019) (Figure 4, Figure 6, Figure 9, Figure 10), and a significant relationship between monthly Delta outflow and *Microcystis* observations (Figure 7). This is consistent with previous research indicating a strong inverse relationship between *Microcystis* concentrations in the Delta and freshwater flows through the Delta (Lehman et al. 2013).

Interestingly, there was a slightly higher incidence of high *Microcystis* observations in 2020 than in 2021 on a Delta-wide scale (Figure 4), while 2021 had a higher abundance of harmful cyanobacteria in grab samples in the region surrounding the barrier (Figure 10). Some of this difference may be attributed to *Microcystis* being most common in surface scum and the EMP samples being collected 1 meter below the surface. Additional surface samples targeting *Microcystis* began in August 2021 and will continue through 2022 to better capture this difference. The visual *Microcystis* observations should be analyzed with realization of the inherent biases in the data – there may be differences between observers, observations may change with light or turbidity, and the observations may fail to pick up taxa other than *Microcystis*. However, they provide a high-frequency, broad-scale data not available with other methods (1,431 observations in 2021 alone).

Another key observation was that 2021 had significantly more *Dolichospermum* than previous years (Figure 9, Table 5). cyanoHAB research in the Delta to date has focused primarily on *Microcystis*; however, other harmful cyanobacteria, such as *Dolichospermum* and *Aphanizomenon* are becoming increasingly prevalent (Lehman et al. 2021). *Aphanizomenon* produces cylindrospermopsin, saxitoxin, and anatoxins, while *Dolichospermum* can produce microcystins and anatoxins (Chorus and Welker 2021). Anatoxins are toxic at much lower concentrations than microcystins, and act on the nervous system instead of the liver (Chorus and Welker 2021). No anatoxins or cylindrospermopsins were detected in Franks Tract or Clifton Court Forebay during summer 2021 (Table 4, Table 9), but low concentrations of anatoxins and saxitoxins have been found in the Delta in previous studies (Lehman et al. 2021). The lack of these toxins in 2021 could have been attributable to the relatively low concentrations of these cyanobacteria, strains of these genera without toxin-producing genes, or sampling during time periods of low toxin production. Increased sampling in future years may help explain this result.

Based on the physiological capabilities of these different genera, one would expect *Aphanizomenon* to dominate early in the bloom, with *Microcystis* gaining a competitive advantage as water temperature rises, because the temperature optimum for *Microcystis* is 28°C

whereas for *Aphanizomenon* it is 20°C (Reynolds 2006). In other systems, *Aphanizomenon* often precedes *Microcystis* (Konopka and Brock 1978; Paerl and Otten 2016; Zhang et al. 2020a), which aligns with the decrease in *Aphanizomenon* in the Delta in August and September. This may be caused by temperature, because other studies have found that *Microcystis* dominates at warmer temperatures (higher than 17°C) and *Dolichospermum* at cooler temperatures (Zhang et al. 2020a). Nitrogen fixation by *Aphanizomenon* and *Dolichospermum* may provide a competitive advantage in low-nitrogen conditions; however, most cyanoHAB species, including those that fix nitrogen, thrive under high nutrient concentrations and continue to increase with increased eutrophication of freshwater systems (Li et al. 2016; Paerl and Paul 2012). Furthermore, nitrogen fixation is shut down in the presence of ammonium (Herrero et al. 2004; Moisaner et al. 2008), limiting its potential for conferring a competitive advantage in environments with relatively high ammonium, such as the Delta (Figure 10). Phosphorus is also often a limiting nutrient, and *Microcystis* is very efficient at acquiring phosphorus and been shown to outcompete *Dolichospermum* at low phosphorus concentrations (Wan et al. 2019), though concentrations in the Delta are not likely to be low enough for this competitive advantage to kick in (Figure 11). Allelopathic effects by *Microcystis* on other cyanobacteria have also been posited to contribute to *Microcystis* dominance and could partially explain the subdominant abundance of *Dolichospermum* and *Aphanizomenon* during *Microcystis* dominance (Chia et al. 2018; Ma et al. 2015). The presence of all three genera during summer 2021 may be attributable to concentrations of the various species at the start of a bloom, combined with environmental factors and differences in intrinsic growth rates that may interact in unpredictable ways.

2.4.2 Impact of the Drought Barrier and Temporary Urgency Change Petition

When comparing years with a West False River barrier (2015, 2021) to dry years without a barrier (2014, 2016, 2018, and 2020), no clear patterns were seen in visual observations of *Microcystis* or concentrations of potentially toxic cyanobacteria from grab samples. Analysis of visual observations in the area immediately surrounding the barrier did not find significant differences between 2020 and 2021 but 2015 had lower index values than 2014 or 2016 (Figure 6, Table 3; Appendix A, Table A-4). Concentrations of harmful cyanobacteria in grab samples were higher in 2021, but 2015 had very low concentrations compared to other dry years (Table 6, Figure 9). These observations are supported by previous studies of cyanoHABs during the 2014–2015 drought, which found that cyanobacterial concentrations were much lower in 2015 than in 2014 (Lehman et al. 2018), nor did the 2015 barrier appear to enhance blooms in September–November 2015 (Kimmerer et al. 2019). Looking on a monthly scale, higher outflow was associated with lower *Microcystis* observations (Figure 7), and this is supported by Lehman et al. (2013; 2008). Change in outflow due to the TUCP would have predicted a change in the probability of *Microcystis* observations (~10%), but this relationship had only a weak fit to the data (r-squared of 0.068) and overpredicted *Microcystis* observations in June of 2021, the first month of the TUCP. Furthermore, months with high outflow also tend to have low temperatures, so the extent to which flow drives the observation remains to be explored. So, while flow is an important factor in cyanoHABs, taken together, these data do not support a role for the TUCP or barrier for driving widespread impacts of cyanoHABs on the landscape scale beyond the impact of the drought itself.

Although no impacts were detected Delta-wide, some localized impacts of the barrier on cyanoHABs within Franks Tract were detected. A large cyanoHAB began forming within Franks Tract in July 2021 and peaked in August before subsiding in September (Figure 12, Figure 13, Figure 14). The bloom appears to have initiated in mid-July (as seen in the satellite data as well [Figure 14]), before the EMP sampled, and then was accruing biomass through mid-August, when the EMP recorded its highest biomass values. No large blooms were detected in Franks Tract in 2020, despite the high incidence of *Microcystis* in visual assessments across the Delta (Figure 4). Smaller blooms occurred in Mildred Island in July of both 2020 and 2021 (Figure 14). The large shift in cyanobacterial abundance in Franks Tract from 2020 to 2021, and lack of shift at Mildred Island, provide a strong indication that the barrier may have played a role in bloom development within Franks Tract.

It is important to note that both the Fluoroprobe data and the satellite data record concentrations of total cyanobacteria, however not all cyanobacteria are harmful. The most frequent cyanobacteria found in grab samples collected by EMP is *Eucapsis sp.* (Brown 2021; Perry and Brown 2020), which does not produce toxins. Grab samples taken during EMP's July and August surveys show that some of this bloom certainly contained *Microcystis*, *Aphanizomenon*, and *Dolichospermum* (Figure 9), but *Eucapsis* was also present in high abundance (data not shown).

These findings correspond to other changes in water quality as well, which indicates a large increase in photosynthesis around the end of June, as shown by increases in pH and DO above the thresholds seen in previous years before subsiding in September. Similar patterns in water quality have long been associated with cyanoHABs in water bodies worldwide (Talling 1976; Wilhelm et al. 2020), as the consumption of dissolved inorganic carbon by photosynthesis can drive pH levels near 11 (Ibelings and Maberly 1998; Verspagen et al. 2014). Research has indicated that these changes in water quality can benefit *Microcystis* and other toxin-producing taxa over other algae and cyanobacteria (Ji et al. 2020).

Although DO in Franks Tract is frequently supersaturated even in the absence of a bloom (Figure 24), a finding that is unsurprising given the amount of aquatic vegetation present, the levels of supersaturation seen in 2021 surpass those of previous years and correspond directly with the other observations of cyanoHAB formation shown here.

The residence time of water within Franks Tract was significantly increased based on the model shown in Figure 16. Decreased flow is a well-known driver of algal blooms of all kinds (Glibert et al. 2014; Lehman et al. 2013), so the major restriction of flow within Franks Tract could have been a factor in allowing the bloom to establish. *Microcystis* have slow growth rates and need longer residence times to accrue biomass than other algae (Carey et al. 2012; Reynolds 2006). The increased residence time caused by the EDB may have afforded *Microcystis* the opportunity to reach higher biomass before being flushed from the system.

There are also complex interactions between residence time, water quality, light availability, nutrients, SAV, and cyanoHABs that may produce unexpected results. Franks Tract has become more and more inundated with aquatic vegetation in recent years (see Section 3, *Weeds*), which can further reduce flow and increase residence time (Boyer and Sutula 2015 and references cited

therein). Submerged vegetation also reduces turbidity (Hestir et al. 2015), potentially increasing the availability of light for cyanoHABs, although it will reduce light availability under the canopy. SAV may also compete with cyanobacteria for nutrients (Dahm et al. 2016), and reduction in water flow may reduce the transport of nutrients into the area, limiting the growth of phytoplankton of all types (Berg and Sutula 2015; Glibert et al. 2014). While both nitrogen and phosphorus concentrations in the south Delta were similar to previous years (Figure 11), sampling within Franks Tract was limited to a few points. There may have been spatially variable drawdown of nutrients within the weed bed. SAV may also provide a substrate for epiphytic cyanoHABs. Cyanobacteria associated with SAV have become a problem for wildlife health in other areas (Wilde et al. 2014), but remain understudied in the Delta.

2.4.3 Impact of Temperature

Another major driver of cyanoHABs in the Delta is water temperature. *Microcystis* growth rates increase rapidly between 15°C and 20°C, with low to no growth below 15°C and maximum growth rates at higher than 25°C (Carey et al. 2012; Coles and Jones 2000; Konopka and Brock 1978; Lurling et al. 2013). In particular, 19°C has been identified as the threshold above which *Microcystis* is likely to increase in the Delta (Lehman et al. 2013). In addition, Lehman et al. (2018) found an interesting association between greater *Microcystis* biomass in 2014 compared with 2015, based on the increased frequency of temperatures above 25°C in 2014.

High temperatures throughout the Delta, particularly high temperatures in Franks Tract and the South Delta in 2020 and 2021, likely contributed to the severity of cyanoHABs seen in these years. Looking at the impact of temperature across years, years with more days above 19°C were positively correlated with more visual observations of *Microcystis*, but there was no trend associated day above 25°C (Figure 22). In particular, 2014, 2015, and 2020 had more days above 19°C at all stations than most other years. 2020 also warmed earlier, with a May maximum temperature of 26.2°C at Bethel Island, and temperatures stayed warm late into the fall (Figure 19). However, these high temperatures are unlikely to be caused by the TUCP or barrier, because modeling indicated temperature changes of less than 0.6°C attributable to the barrier, and these effects were very localized (Figure 16). Water temperatures in the Delta are driven primarily by air temperature (Vroom et al. 2017), so the relatively small impact of the barrier on temperature is not surprising.

Regionally, the South Delta and Lower San Joaquin River have consistently higher levels of cyanoHABs (both visual indices and concentrations of cyanobacteria in grab samples; Figure 6, Figure 9). These regions are also warmer, on average, than other areas of the Delta (Figure 20; Bashevkin et al. 2021; Pien et al. in prep). If a strong interaction had been seen between regions and years with and without emergency drought barriers (i.e., higher cyanobacteria in the Central Delta during years with a barrier than without a barrier when compared to other areas of the Delta), it would suggest an impact of the barrier on the regional distribution of cyanoHABs. Although the authors of this report did not have enough degrees of freedom to statistically test an interaction between region and year, the relative difference in cyanoHAB abundance between regions was relatively consistent between years (Figure 6, Figure 9). The South and Central Delta have consistently been the areas of highest cyanobacteria, as identified in multiple other studies

(Berg and Sutula 2015; Lehman et al. 2005; Spier et al. 2013), indicating no support for an effect of the barrier.

2.4.4 Impacts of CyanoHABs on Beneficial Uses

Despite the higher accumulation of cyanobacteria in Franks Tract during late summer 2021 than any previously seen in this location, the magnitude of this bloom was still less than seen elsewhere in California (e.g., Clear Lake). Furthermore, during the peak of the Franks Tract bloom (early August), the concentration of cyanotoxins was below the levels thought to cause problems for recreational use, although it was slightly above EPA drinking water standards (Table 2, Table 4). No toxins were detected at Clifton Court Forebay or Banks Pumping Plant (Table 9). Cyanotoxin sampling, however, was conducted only twice at Franks Tract and may not have captured the most toxic period of the bloom. Any visible accumulation of *Microcystis* and *Dolichospermum* in the water may have also negatively affected recreational use of the area.

For fish and wildlife, the thresholds at which cyanoHABs may cause problems are less well understood. Reported LD₅₀ levels of microcystins for fishes are species-dependent and range from 20 to 1,500 µg/L (OEHHA Ecotoxicology et al. 2009), and nonlethal effects have been reported at much lower levels. Microcystins cause harmful effects on the liver, kidneys, gills, growth, and behavior (Acuna et al. 2012a; Acuna et al. 2012b; OEHHA Ecotoxicology et al. 2009). Liver lesions are frequently found in fish throughout the Delta (Fong et al. 2016; Johnson et al. 2010; Teh et al. 2020), and while these lesions may be caused by a number of toxic contaminants, microcystins may be part of the overall toxicity of the Delta, particularly in drought years.

Less research has been done on the impact of cyanotoxins on invertebrates. Studies of the dominant calanoid copepods in the estuary (*Eurytemora affinis* and *Pseudodiaptomus forbesi*) found LD₅₀ levels greater than 520 µg/L of microcystins, with chronic, nonlethal effects at 140 µg/L (Ger et al. 2009), much higher than levels observed at Franks Tract in summer 2021 (0.6 µg/L). However, ingestion of *Microcystis* did cause significant mortality in both species, with higher mortality in the native *E. affinis* than the non-native *P. forbesi* (Ger et al. 2010b). This is an area of active research, and recent evidence suggests that some types of cyanobacteria may actually be preferred food for copepods (Kimmerer et al. 2018). Because the cyanoHABs recorded in Franks Tract were made up of multiple taxa, the full impact on invertebrates is hard to predict.

Other research has implicated *Microcystis* in broad changes to both phytoplankton and zooplankton communities in the Delta when it is present in high abundance (Lehman et al. 2010; Lehman et al. 2021). Many cyanobacteria have allelopathic effects on other phytoplankton (Chia et al. 2018; Lehman et al. 2010; Otten et al. 2017), or may affect both the phytoplankton and zooplankton communities by differential toxicity to zooplankton, which, in turn, feed on different phytoplankton. This report did not analyze potential impacts of cyanoHABs on other phytoplankton, zooplankton, or fishes, but this is an important area for future research.

2.4.5 Potential Mitigation of CyanoHABs

To better predict and respond to future cyanoHABs in the central Delta that may be related to departmental drought actions, DWR is increasing monitoring of cyanoHABs and associated toxins in the Delta. Whole-water grab samples will be collected at several additional stations in Franks Tract, Mildred Island, and other cyanoHAB hot spots in the South and Central Delta. In addition, a new SPATT station will be established in Franks Tract, which will be part of an existing study of cyanotoxins throughout the Delta currently being conducted by USGS and DWR (see the updated Emergency Drought Barrier monitoring plan for details).

Actions that can be taken to mitigate and/or prevent cyanoHAB occurrences in months where the risk of occurrence is high, and the barrier is in place (i.e., July–October), are still experimental. Some possible avenues are to reduce nutrient inputs, investigate biological controls such as cyanophages or grazers (Pal et al. 2020), implement mechanical control methods to increase turbidity and mixing (Kibuye et al. 2021b), or reduce a bloom after it has started through chemical control methods (Kibuye et al. 2021a).

Preventing blooms from forming is often more effective than trying to reduce a bloom after it is initiated. The least intrusive and most effective method of preventing cyanoHABs from occurring is usually to limit nutrient availability (Kibuye et al. 2021b). However, in a region like the Central and South Delta where agricultural nonpoint-source inputs of nutrients dominate, this is an option that is challenging to implement at the source. Moreover, this method may prevent other phytoplankton from growing, including eukaryotic species that are important food sources for higher trophic levels (Dahm et al. 2016). Nutrient levels are not generally limiting to phytoplankton production in the Delta, and reductions in point-source nitrogen from the Stockton and Sacramento wastewater treatment plants have failed to prevent increases in cyanoHABs over the last 10 years (Cloern et al. 2020; Senn et al. 2020), so this strategy may not be as effective in the Delta as it has been elsewhere.

Top-down control of cyanoHABs may also be difficult. Most grazers (such as copepods) preferentially avoid small cyanobacteria or toxic species (Ger et al. 2010a; Lucas et al. 2016). Some research has shown that cyanophages may be able to control cyanoHABs in laboratory settings, but this has not been tried at the field scale (Pal et al. 2020).

Mechanical methods for controlling cyanoHABs take advantage of the fact that, compared with eukaryotic phytoplankton such as diatoms, cyanobacteria have poor light absorption efficiencies and therefore have low rates of photosynthesis for a given light intensity (Visser et al. 2016). This is particularly the case for *Microcystis*, which has one of the lowest photosynthetic efficiencies compared with other cyanoHABs (Wu et al. 2009). It is important to note that mechanical control methods are particularly well-suited for the control of buoyant cyanoHAB genera, in contrast with nonbuoyant cyanoHAB genera such as *Planktothrix* and *Cylindrospermopsis* (Burford and O'Donohue 2006; Reynolds et al. 1983). In addition to physically moving cyanoHABs around in the water column, mechanical/artificial mixing may increase sediment suspension and turbidity, shading the water column and lowering cyanoHAB growth rates.

Mechanical control of cyanoHABs through mixing has been proven effective on small scales, such as ponds or small lakes (Burford and O'Donohue 2006; Visser et al. 2016); however, it has not been attempted in a large, tidal environment such as Franks Tract. Mechanical mixing on the scale of Franks Tract would be cost-prohibitive, and high densities of SAV in the tract are likely to make mechanical mixing ineffective.

If a bloom has already developed, artificial control methods that arrest a bloom include decreasing residence times, reducing the availability of nutrients, and directly killing the cyanoHAB species via an algicide. With respect to Franks Tract, a decrease in the residence time of the water may be accomplished by a temporary notch in the barrier, if feasible while maintaining other water quality standards. Reducing the availability of phosphorus can be accomplished by adding aluminum salts, which form flocs that bind both phosphate and cyanobacterial cells and clear the water column (Kibuye et al. 2021a). The efficacy over time of this method is not well understood and repeated applications will most likely be necessary. Using algicide in a region with special-status species may not be possible, depending on nontarget effects.

SECTION 3

Weeds

3.1 Introduction

Aquatic vegetation provides important structure and function for aquatic organisms and waterfowl and greatly influences nutrient cycling, water quality, and the stability of sediments (Caraco and Cole 2002; Miranda et al. 2000). Diversity of fish and invertebrate species tends to be greater in native aquatic plant beds, and water quality conditions are generally more favorable for native fish and invertebrates (Boyer et al. 2013; Kuehne et al. 2016; Toft et al. 2003). Alternatively, non-native aquatic plants can have dramatic spatial and temporal effects on DO, temperature, and pH (Caraco and Cole 2002; Frodge et al. 1990) and can affect fish and macroinvertebrates (Brown 2003; Nobriga et al. 2005; Schultz and Dibble 2012).

Aquatic vegetation is commonly discussed in terms of their growth forms: submerged aquatic vegetation (SAV), emergent aquatic vegetation (EAV), and (3) floating aquatic vegetation (FAV) (Boyer and Sutula 2015). SAV grows predominantly below the water's surface and may or may not be rooted in the sediment. Examples of SAV found in the Delta include Brazilian waterweed (*Egeria densa*), coontail (*Ceratophyllum demersum*), and Canadian waterweed (*Elodea canadensis*). EAV is rooted in shallow water, with the majority of its growth occurring above the water's surface. Examples include cattail (*Typha* sp.), tules (*Schoenoplectus actutus*), and giant reed (*Arundo donax*). FAV floats on the water's surface and is not rooted in the sediment. An example of FAV in the Delta is water hyacinth (*Eichhornia crassipes*). Coverage by FAV and SAV in the Delta has increased over the past 20 years (Ta et al. 2017), with particularly high increases seen during the last drought (Kimmerer et al. 2019). From 2008 to 2019, aquatic vegetation increased in coverage by 2.4 times (7,100 acres to 17,300 acres), occupying nearly one-third of the area of Delta waterways (Ta et al. 2017; Ustin et al. 2020).

Factors contributing to the successful growth and establishment of SAV include temperature, light, water depth, sediment nutrient availability, and water velocity (Barko and Smart 1981; Chambers et al. 1991; Riis et al. 2012). In general, photosynthesis rates are largely driven by light levels; they increase from sunrise, peak at midday, then slowly decline in a fairly predictable manner. Some invasive SAV species, such as Brazilian waterweed, are adapted to low-light conditions, which enables rapid elongation of shoots and subsequent canopy formation that further blocks light to other native SAV species.

The maximum depth of plant growth is typically driven by the maximum depth to which light penetrates to support photosynthesis and can vary greatly between species (Chambers and Kalff 1987). Increased water clarity allows for greater light penetration for photosynthesis to occur. In

many cases, the presence of SAV can lower water velocity and increase sediment deposition which, in combination, increases water clarity and promotes further growth (Hestir et al. 2015; Petticrew and Kalff 1992). Increased water clarity in the Delta has been implicated in the increased spread of Brazilian waterweed (Durand et al. 2016), and the increase in Brazilian waterweed has been implicated in increasing water clarity and the reduction in sediment transport to tidal wetlands (Drexler et al. 2020; Hestir et al. 2015).

Different species of SAV also have varying temperature tolerances that factor into their life history patterns. For example, curlyleaf pondweed (*Potamogeton crispus*) commonly sprouts early in the growing season and can outcompete native SAV species that are not tolerant of lower water temperatures (Stuckey 1979). Rooted SAV and EAV obtain the majority of their nutrients from the sediment, particularly nitrogen and phosphorus (Barko et al. 1991). During plant decomposition, this interface provides a mechanism for nutrient recycling between the sediment and the overlying water column. Factors that can affect rates of decomposition, and hence nutrient cycling, include the diversity of the plant community (Banks and Frost 2017) and water temperature (Carvalho et al. 2005).

Both SAV and EAV establish more readily in slower-moving water, so low-flow conditions that occur during droughts have been linked to increases in coverage of invasive vegetation. Increases in nutrients, such as those seen during 2013–2014 (Figure 11), may also facilitate the expansion of aquatic vegetation, although this effect is less conclusive (Boyer and Sutula 2015; Dahm et al. 2016). Changes to flow patterns caused by the 2015 emergency drought barrier were implicated in the expansion of submerged vegetation in Franks Tract (Kimmerer et al. 2019).

The increase in aquatic vegetation may be mitigated by control methods. The Aquatic Invasive Plant Control Program of the California Department of Parks and Recreation, Division of Boating and Waterways (DBW) is chiefly responsible for aquatic vegetation control in the Delta and employs primarily chemical control tools. DBW is permitted to treat up to 15,000 acres per year of aquatic vegetation, but typically treats only about 40 percent of that limit (DBW 2020). For control of FAV, DBW most commonly uses glyphosate but also uses some imazamox and 2,4-D. For SAV control, fluridone is by far the most commonly applied herbicide in the Delta. However, recent studies have shown the use of fluridone on SAV in tidal environments such as the Delta to be generally ineffective (Khanna et al. in review; Rasmussen et al. in review). Therefore, this treatment program may increase the loading of herbicides into the system without significantly affecting weed abundance. Treatment of FAV with herbicides is thought to be somewhat more effective, although there are noticeable changes in water quality post-treatment (Tobias et al. 2019).

The authors of this report predicted that drought conditions would cause an increase in invasive FAV and SAV. An increase in aquatic vegetation in Franks Tract after installation of the 2021 EDB was also predicted, considering the decrease in water velocity in the tract. Although Durand et al. (2016) failed to detect a relationship between the establishment of aquatic vegetation and velocity, in 2015, coverage by weeds increased within Franks Tract, and the area was not cleared when high flows returned (Kimmerer et al. 2019). This was attributed to the decrease in water velocity through the center of the tract. The report authors expected a similar response to the 2021 EDB, although the high coverage by weeds within Franks Tract over the past several years will

make detecting a response difficult. It will also be difficult to extract the response to the 2021 EDB from the response to the drought.

3.2 Methods

Three sources of data were used to evaluate whether the 2021 EDB contributed to changes in the abundance and/or species composition of aquatic weeds. The first two data sets are from the Center for Spatial Technologies and Remote Sensing (CSTARS) at the University of California, Davis. These data sets consist of (1) hyperspectral imagery that classifies the types of aquatic vegetation growing across the Bay-Delta landscape and (2) the vegetation field surveys used to ground-truth this hyperspectral imagery. The third data set, collected by SePRO Corporation (SePRO), consists of annual field surveys of SAV in Franks Tract and is used to assess the efficacy of herbicide treatments at this site.

3.2.1 Hyperspectral Imagery

Since 2004, hyperspectral airborne imagery has been collected by fixed-wing aircraft over the Delta in many years, although the time of year and spatial extent of these surveys has varied. Franks Tract has been included in all surveyed years (2004, 2008, 2014–2021). It generally takes a year or longer from the time of imagery collection to produce finalized maps. Therefore, 2020 imagery is preliminary, and the 2021 imagery will not be available until spring 2022.

It is difficult to differentiate potential impacts of the 2021 EDB on the abundance and composition of aquatic vegetation from impacts simply caused by drought. However, it is useful to compare changes in Franks Tract to those at similar sites not influenced by the barrier (Figure 26). Previous studies have used Big Break as a reference site for Franks Tract because it is near Franks Tract but not influenced by the barriers (Kimmerer et al. 2019). Clifton Court Forebay was also chosen because it shares some similarities to Franks Tract in size, bathymetry, and hydrology and is far from the influence of the 2021 EDB. Imagery for this site is available for seven of the 10 years for which there is Franks Tract imagery: 2004, 2008, 2014, 2015, and 2019–2021. All Clifton Court Forebay imagery is included in this draft of the report except imagery from 2021, which is currently undergoing analysis. Mildred Island was also considered as a candidate reference site, but was ultimately rejected because this site is too turbid to produce accurate classification maps of SAV using hyperspectral imagery.

Another challenge to isolating impacts of the 2021 EDB on aquatic vegetation is the use of herbicides for vegetation management. Herbicide treatments have been conducted at Franks Tract, Clifton Court Forebay, and Big Break, and the timing, type, and amounts of chemicals used in these treatments have varied among sites and years (Table 10).

Survey and analysis methods for the hyperspectral imagery have varied somewhat among years, but the approach generally proceeds as described here for the 2018 survey. During this survey, HyVista Corporation (Sydney, Australia) used the HyMap sensor (126 bands: 450–2,500 nanometers, bandwidth: 10–15 nanometers) to collect imagery at a resolution of 1.7 meters by 1.7 meters. A diverse suite of inputs was derived from these images to capture reflectance properties across different regions of the electromagnetic spectrum, which track biophysiological

characteristics useful for distinguishing types of plants. These intermediate inputs were generated using IDL scripts (IDL 8.01, ITT Visual Information Solutions) in ENVI (ENVI 4.8, ITT Visual Information Solutions).

Concurrent with imagery collection, ground-truthing surveys were conducted to determine species composition at points across the Delta region (e.g., 2018: 950 points; see the *Hyperspectral Imagery Ground-Truthing* section for details). Field data were divided into training and validation subsets for image classification and independent validation of class maps. Training and validation polygons were overlaid on the raster images with generated inputs, and corresponding pixels within the raster images were extracted using the R statistical computing language (version 4.0.2, R Core Team 2021) and packages ‘sp’ (version 1.4.5) (Pebesma and Bivand 2021), ‘rgdal’ (version 0.5.5) (Bivand et al. 2021), and ‘rgeos’ (version 1.5.23).

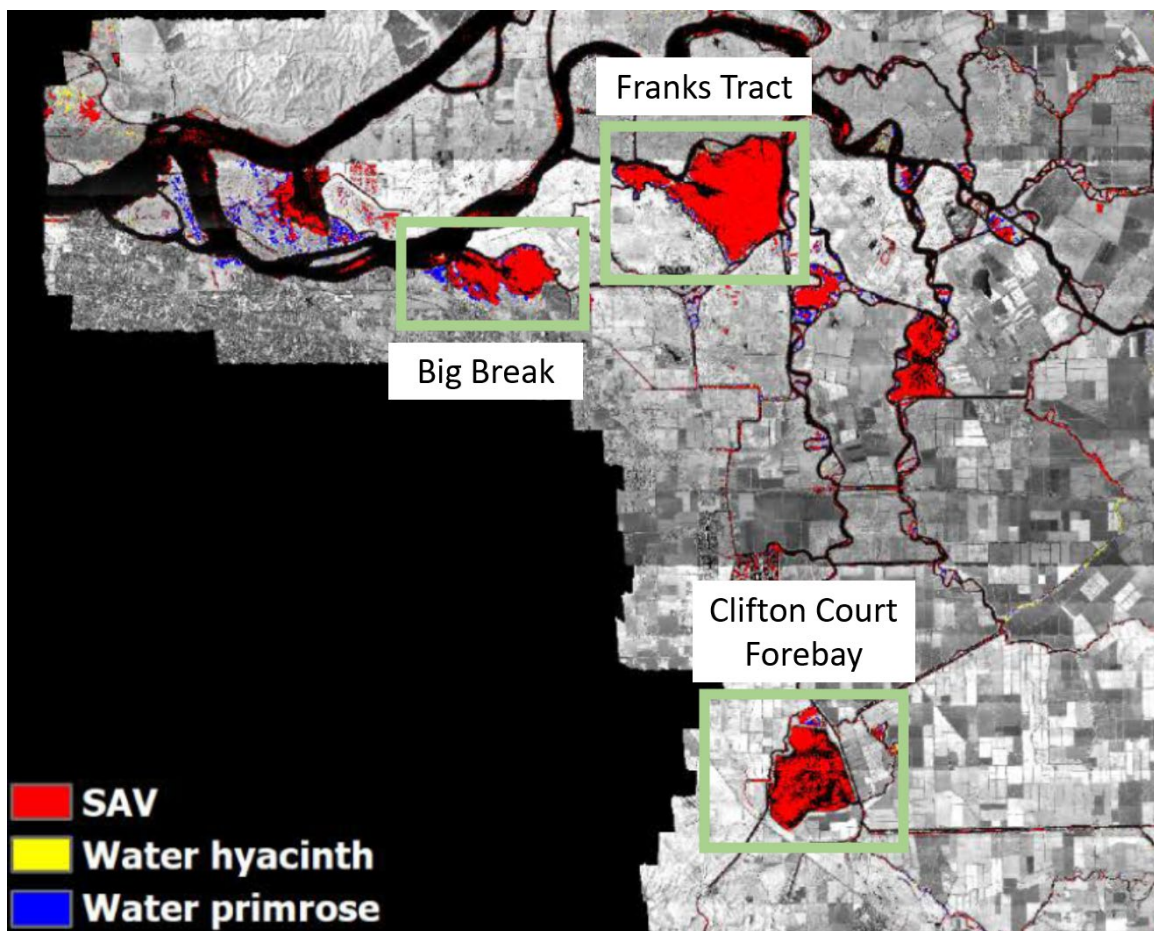


Figure 26
Map of the central and south regions of the Delta for 2019 showing the locations of Franks Tract and the two reference sites, Big Break and Clifton Court Forebay.

TABLE 10
AREA OF FRANKS TRACT TREATED BY THE DIVISION OF BOATING AND WATERWAYS
WITH THE HERBICIDE FLURIDONE, BY YEAR

Year	Area Treated (hectares)
2006	57
2007	1,314
2008	1,314
2009	0
2010	202
2011	977
2012	283
2013	0
2014	758
2015	0
2016	421
2017	444
2018	456
2019	0
2020	0
2021	0

Training data were fed into a Random Forests classifier (packages ‘raster’: version 3.4.5 (Hijmans 2021) and ‘randomforest’: version 4.6.14 (Breiman 2001)). The best-fit class type (e.g., open water, SAV, water hyacinth, water primrose) for each pixel was chosen based on consistency across tree predictions. The accuracy of the final maps was assessed using confusion matrices and Kappa coefficients. The area of SAV was calculated per year per site as the number of pixels classified as SAV multiplied by the area of a single pixel. These area calculations were then used to make comparisons among sites and years. For additional details about the imagery analysis methodology, see Khanna et al. (2018).

3.2.2 Hyperspectral Imagery Ground-Truthing

Around the time that hyperspectral imagery is collected each year, the CSTARS staff collects ground-truthing field data on the community composition of aquatic vegetation across the Delta, including areas in and around Franks Tract (Figure 27). In 2021, this field survey took place from late July to mid-August. At sites where SAV was present, they collected data on the species present at the water's surface and the fraction of surface area covered, Secchi depth, depth of the plant below the water surface, species, and fractional cover using a standard rake sample for vegetation. They also estimated the percentage of aquatic plants covered with epiphytic algae. At sites where FAV and EAV were present, they recorded the species present, the fraction of surface area covered, the state of the plant (in a flowering or vegetative state versus senescent), and the mat density (classified as sparse, medium, or thick).

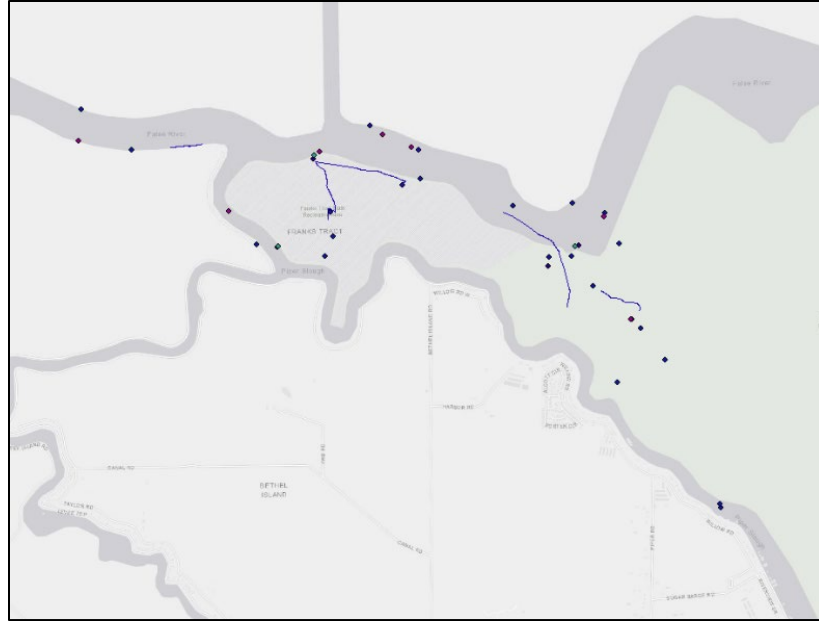


Figure 27
Locations near the 2021 emergency drought barrier where CSTARS sampled aquatic vegetation to ground-truth the hyperspectral imagery.

3.2.3 SePRO Vegetation Survey

Since 2006, DBW has collaborated with SePRO to manage SAV in Franks Tract using the herbicide fluridone (Survey and analysis methods for the hyperspectral imagery have varied somewhat among years, but the approach generally proceeds as described here for the 2018 survey). During this survey, HyVista Corporation (Sydney, Australia) used the HyMap sensor (126 bands: 450–2,500 nanometers, bandwidth: 10–15 nanometers) to collect imagery at a resolution of 1.7 meters by 1.7 meters. A diverse suite of inputs was derived from these images to capture reflectance properties across different regions of the electromagnetic spectrum, which track biophysiological characteristics useful for distinguishing types of plants. These intermediate inputs were generated using IDL scripts (IDL 8.01, ITT Visual Information Solutions) in ENVI (ENVI 4.8, ITT Visual Information Solutions).

Concurrent with imagery collection, ground-truthing surveys were conducted to determine species composition at points across the Delta region (e.g., 2018: 950 points; see the *Hyperspectral Imagery Ground-Truthing* section for details). Field data were divided into training and validation subsets for image classification and independent validation of class maps. Training and validation polygons were overlaid on the raster images with generated inputs, and corresponding pixels within the raster images were extracted using the R statistical computing language (version 4.0.2, R Core Team 2021) and packages ‘sp’ (version 1.4.5) (Pebesma and Bivand 2021), ‘rgdal’ (version 0.5.5) (Bivand et al. 2021), and ‘rgeos’ (version 1.5.23).

) (Caudill et al. 2019). SePRO monitors changes in SAV community composition using point-intercept surveys (Madsen and Wersal 2018) conducted on one date annually in the fall. Sampling points are chosen by generating a grid of evenly spaced points projected over the full area of

Franks Tract (Figure 28). The number of sampling points varies among years but is usually 100 (range: 50–200 samples). Most surveys have been conducted in mid-October (range: October 1–October 13). To sample each point, SePRO uses a weighted, double-headed, 0.33-meter-wide rake, which is dragged for approximately 3 meters along the bottom and then pulled up to the boat for analysis. All SAV present on the rake is identified to species and species-specific abundances are estimated based on the percentage of the rake each covers. Abundances are recorded using ordinal scores (1 = 1–19 percent, 2 = 20–39 percent, 3 = 40–59 percent, 4 = 60–79 percent, 5 = 80–100 percent). Monitoring data for 2014–2021 were available and used for analyses in this report.

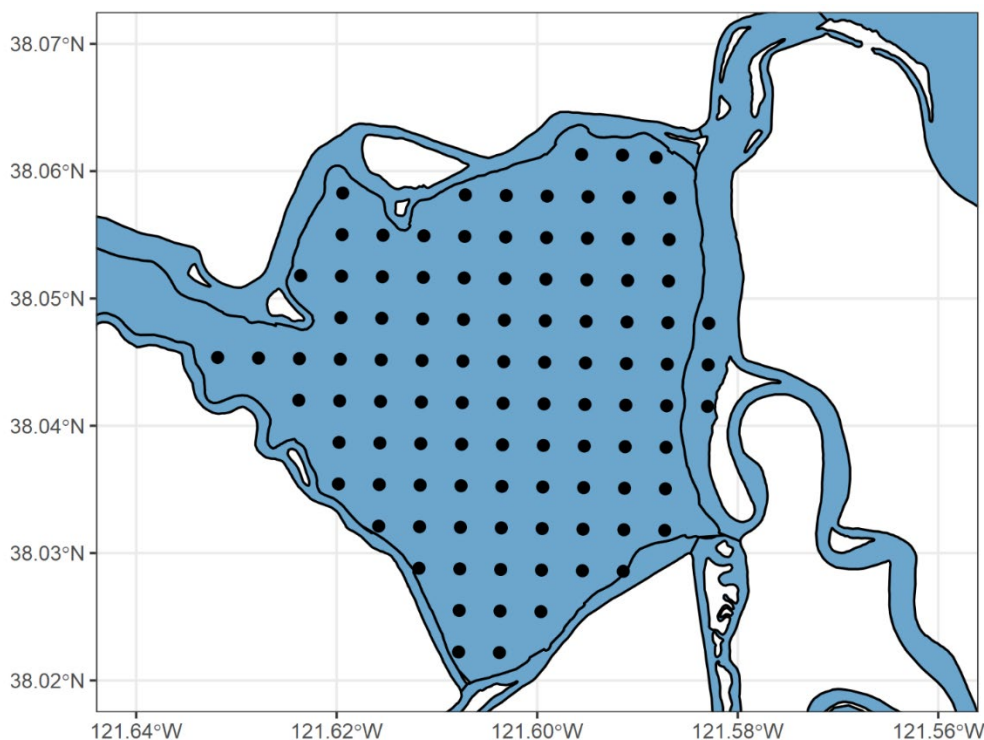


Figure 28
Sampling design for SePRO’s long-term monitoring of submerged aquatic vegetation in Franks Tract, conducted in conjunction with herbicide treatments.

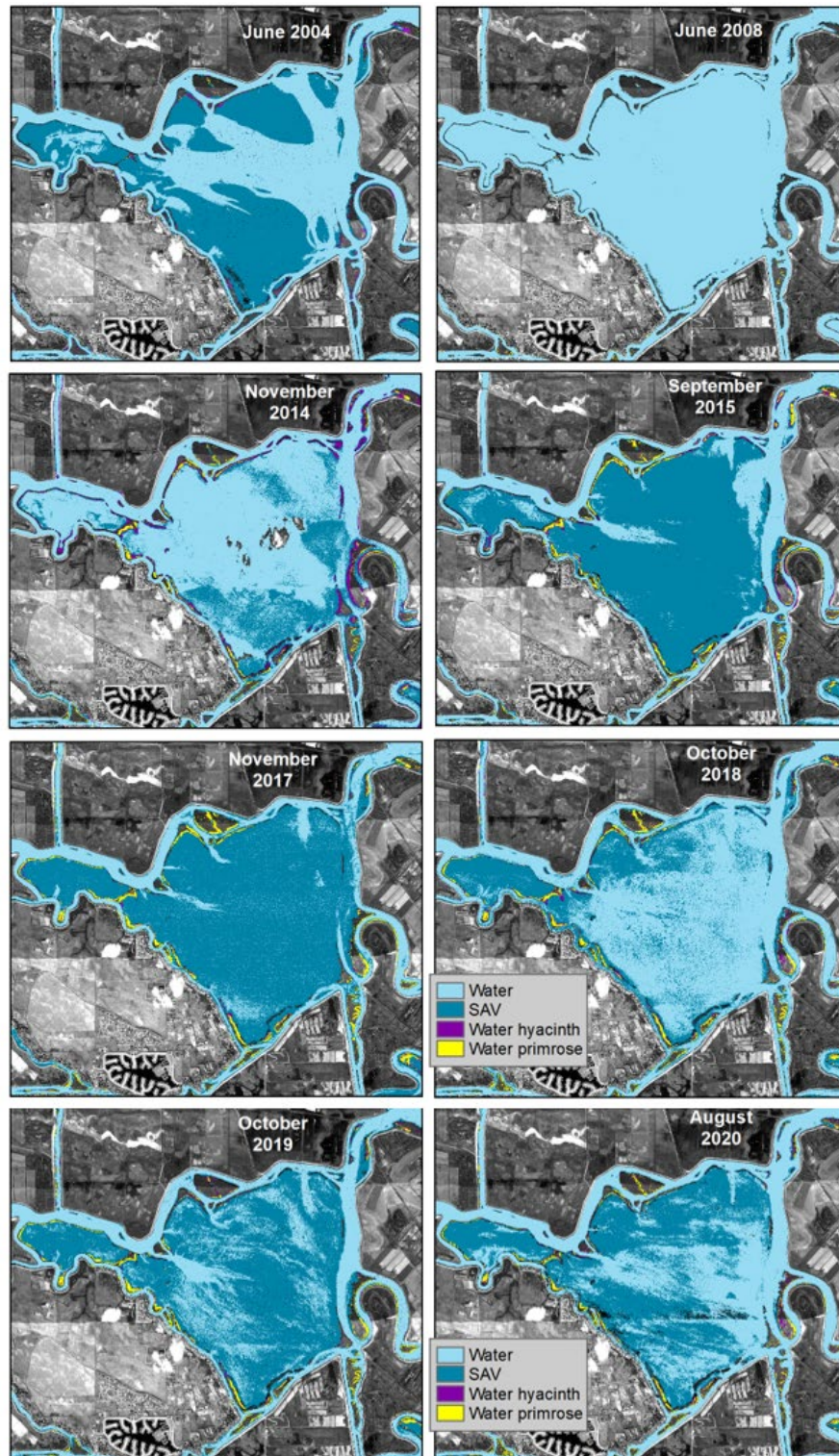
3.2.4 Data Analysis

For this report, total coverage by aquatic weeds in each region (Sacramento, San Joaquin, and Central) was calculated for 2014–2021, along with the change in coverage between years using hyperspectral imagery as described above. The change in coverage for drought years with no barrier to drought years with a barrier and wet years will be compared when 2021 data are complete. The change in community composition over time from DBW/SePro sample data was assessed via graphs of changes in the relative abundance of each species collected in rake samples.

3.3 Results

3.3.1 Hyperspectral Imagery

Based on this time series of imagery, SAV coverage in Franks Tract has changed markedly over time (Figure 29). When monitoring was initiated in 2004, Franks Tract contained a mix of areas of open water and SAV, with water velocities likely driving these spatial patterns. Data from 2005 to 2014 are sparse, but based on the two years of available data (2008 and 2014), it appears that SAV coverage may have been fairly low during this period, perhaps as a result of herbicide treatments (Table 10). During 2015, SAV increased in coverage to fill nearly the entire site, which likely occurred because of a combination of drought conditions and the presence of the drought barrier (Kimmerer et al. 2019), and possibly also the lack of herbicide treatments that year. SAV coverage remained high through the next few years despite wetter conditions, the absence of drought barriers, and the use of herbicide treatments. From 2018 to 2020, SAV coverage was variable, ranging from low to moderately high.



NOTE: The map for 2016 is being updated and will be in the final version of this report. The 2020 map is preliminary.

Figure 29
Time series of hyperspectral imagery for Franks Tract.

The dynamics of SAV coverage at Big Break, one of the reference sites, appear to be simpler than those at Franks Tract (Figure 30). Before 2015, SAV coverage was generally low. In 2015, SAV spread to cover most of the site, and this site has remained infested with SAV during all subsequent years.

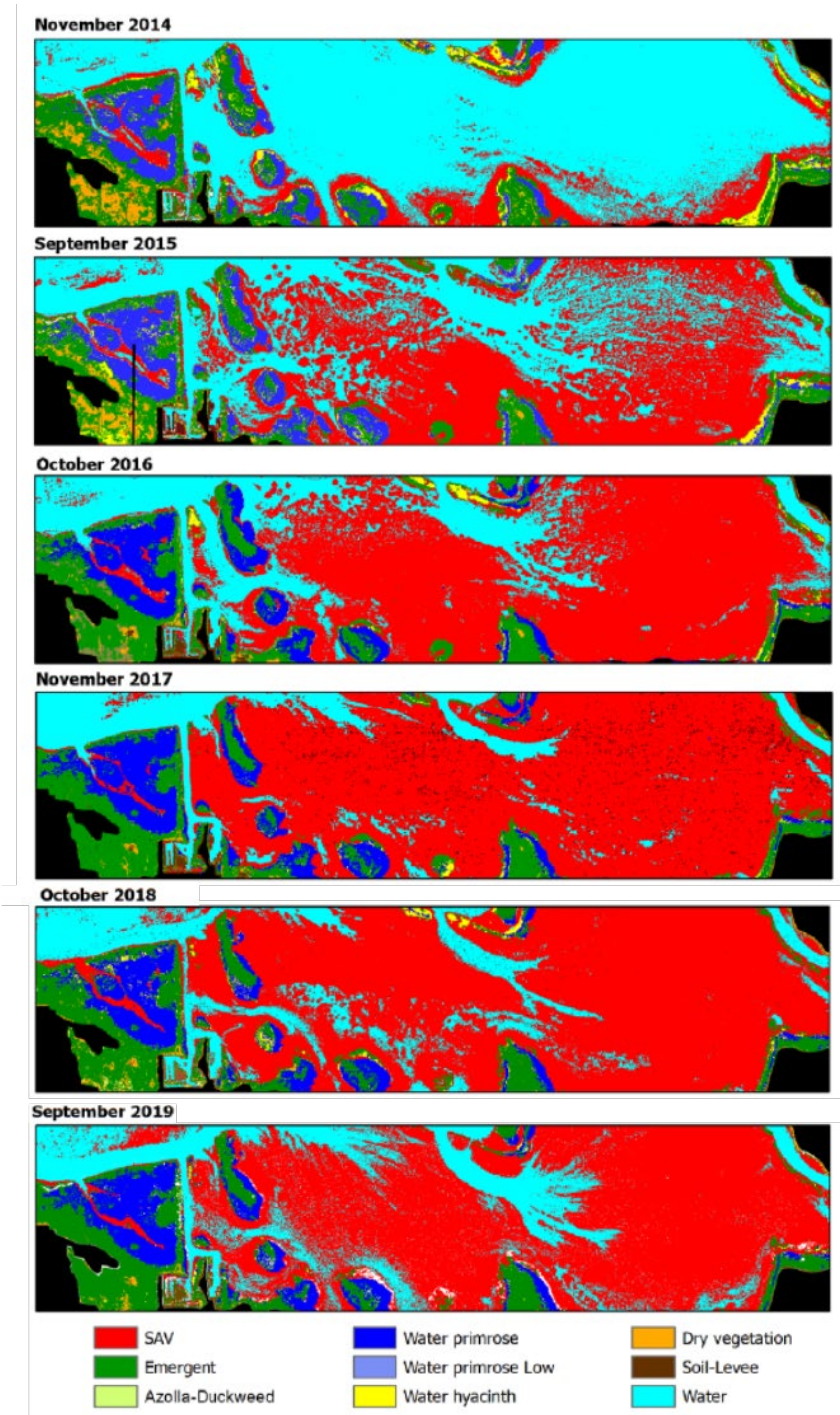
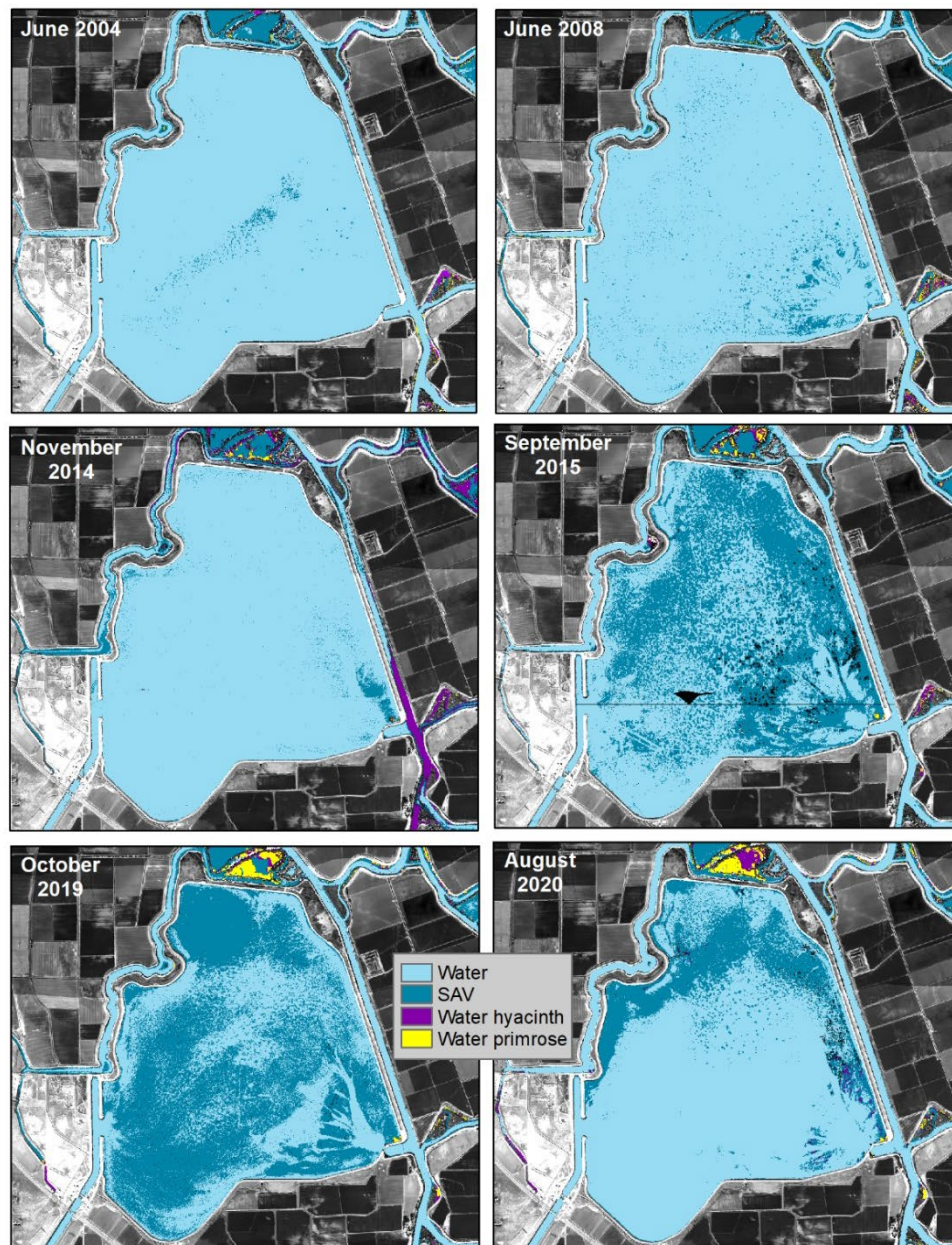


Figure 30
Time series of hyperspectral imagery for Big Break, which serves as a reference site for Franks Tract.

Clifton Court Forebay, the other reference site, exhibited SAV coverage patterns qualitatively similar to those of the other sites (Figure 31 and Figure 32). Before 2015, the site contained large areas of open water, and from 2015 onward, the site generally had higher levels of SAV. Figure 33 shows the change in vegetation percent coverage of Delta waterways over time. The generally similar dynamics in SAV across the three sites suggests that the 2015 drought may have been the most important factor driving SAV coverage patterns, although it is possible that, in Franks Tract, the emergency drought barrier magnified effects of the drought.



NOTE: Only six years of imagery were collected for this region, which represents a subset of years for which there is imagery for Franks Tract. The 2020 map is preliminary.

Figure 31
Time series of hyperspectral imagery for Clifton Court Forebay, which serves as a reference site for Franks Tract.

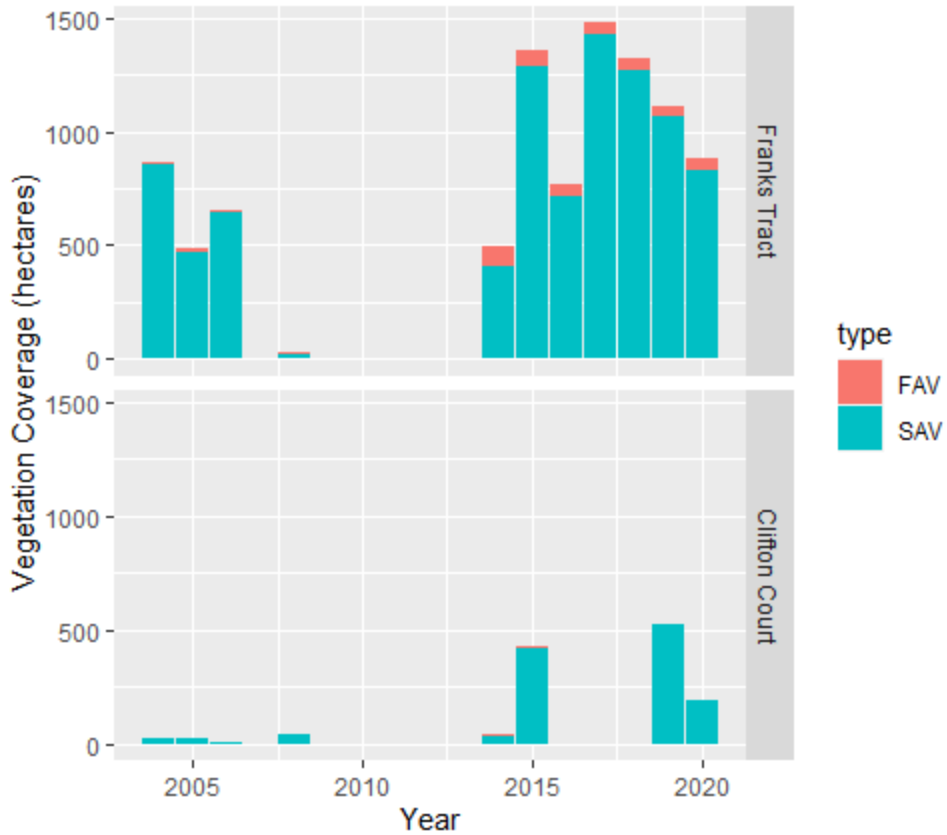
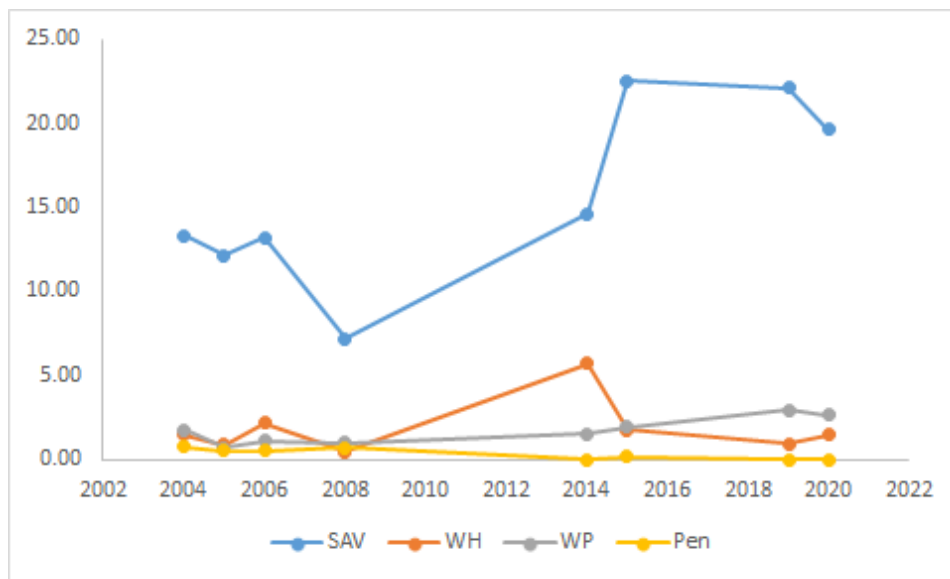


Figure 32
Coverage of floating aquatic vegetation (FAV) and submerged aquatic vegetation (SAV) in Franks Tract and Clifton Court Forebay.



NOTES: Pen = water pennywort; SAV = submerged aquatic vegetation (all species); WH = water hyacinth; WP = water primrose.

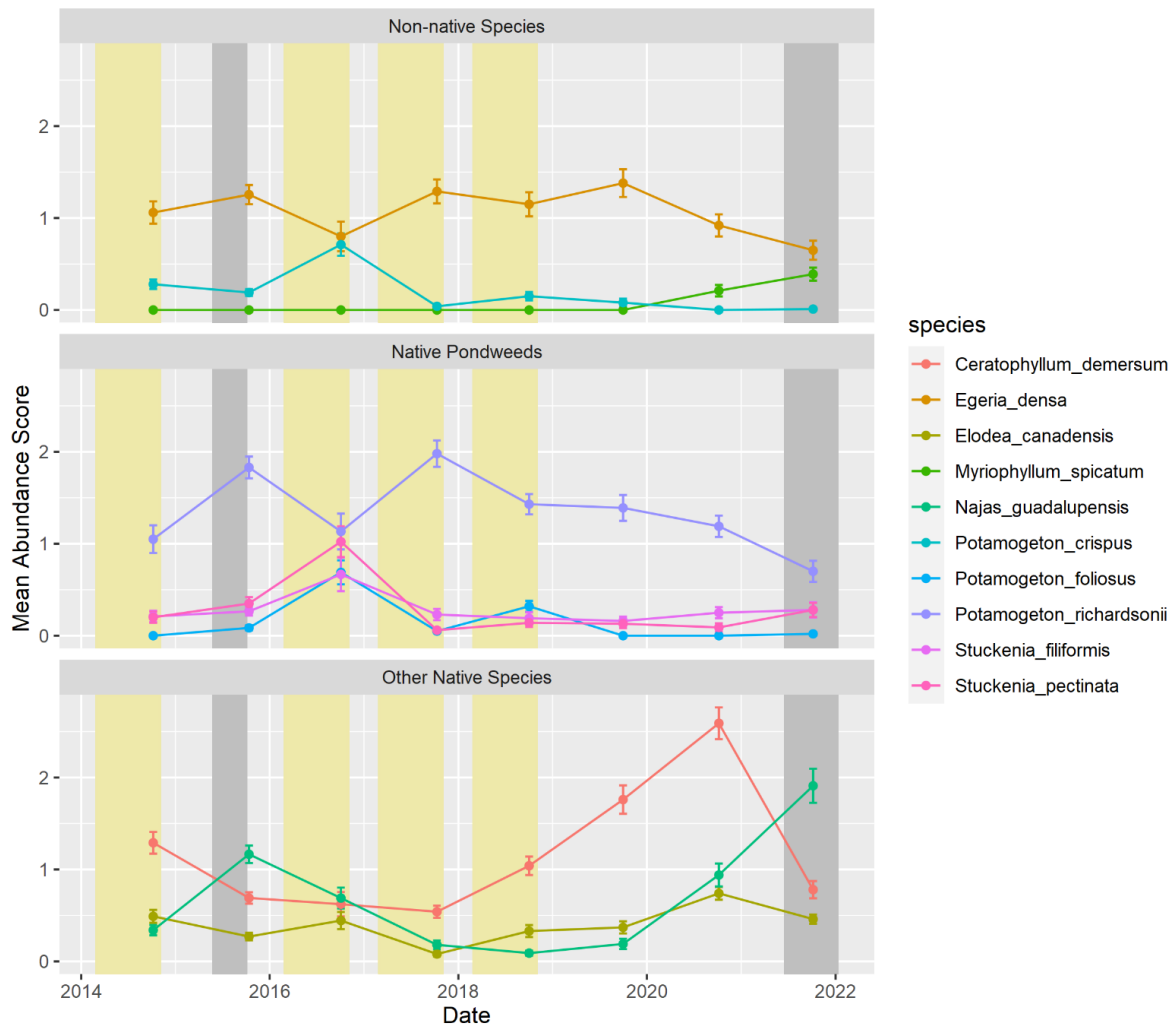
Figure 33
Change in vegetation percent coverage of Delta waterways over time (assuming 55,500 acres of waterways total).

3.3.2 Hyperspectral Imagery Ground-Truthing

The analysis of the 2021 data will be included in the next draft of this report.

3.3.3 SePRO Vegetation Survey

Figure 34 summarizes the results of the SePRO annual surveys as a mean abundance score (\pm standard error) overlain with the time frame when the barriers were in place in 2015 and 2021 (vertical gray bars) and when herbicide treatments occurred (vertical yellow bars). The dates and area of annual herbicide applications using fluridone are provided in Table 10.



NOTE: Points are means of the ordinal abundance scores (range: 1–5) and error bars are standard errors. Five species were excluded from the plot because they were detected 10 or fewer times in total across the eight-year survey period: *Heteranthera dubia*, *Nitella* sp., *Potamogeton pusillus*, *P. zosteriformis*, and *P. nodosus*. Yellow regions indicate periods of fluridone applications and gray regions indicate periods with the emergency drought barrier installed.

Figure 34
Changes in composition of submerged aquatic vegetation species during 2014–2021 based on SePRO Corporation rake surveys.

In total, 15 species of SAV were identified and measured during sampling. Five species were excluded from the plot because they were detected 10 or fewer times in total across the eight-year survey period: *Heteranthera dubia*, *Nitella* sp., *Potamogeton pusillus*, *P. zosteriformis*, and *P. nodosus*. By far, the most dominant non-native species has been *Egeria densa*, which has maintained a fairly consistent abundance score over the years despite repeated herbicide applications and the presence of the barrier. The abundance of *P. crispus* was generally quite low, with the exception of 2017 when levels were similar to those of *E. densa*. *Myriophyllum spicatum*, another non-native, had been absent from all rake tosses since an observation in 2006 (Caudill et al. 2019), but was found again in 2020 and 2021. Also in 2006, *Cabomba caroliniana* was observed, but the species has not been noted on rake samples since that time.

The abundance of the native *P. richardsonii* exceeded that of *E. densa* in all years surveyed. Interestingly, in 2017 there was a decline in its abundance and a slight increase in the abundance of some other native species, including *Stuckenia filiformis*, *S. pectinata*, and *P. foliosus*. Trends in other native species include a relatively consistent abundance of *Ceratophyllum demersum*, *Elodea canadensis*, and *Najas guadalupensis* from 2014 to 2017. The abundance of *C. demersum* then increased greatly until the 2021 survey, when abundance dropped greatly.

Teasing out the effects of the barrier on the abundance of native and non-native SAV species is confounded by the application of aquatic herbicides in some years. Table 10 indicates that herbicide applications between 2006 and 2018 ranged in extent from 57 hectares (ha) in 2006 to 1,314 ha in both 2007 and 2008. Treatments in more recent years have been on the order of 450 ha. The aquatic herbicide fluridone is labeled to control *C. demersum*, *Elodea canadensis*, *Egeria densa*, *Potamogeton* spp., and *Myriophyllum* spp. (Corporation 2017). However, the application of fluridone does not appear to have been highly efficacious in controlling *E. densa* and it is unclear whether the treatments played a role in the decline in *P. crispus* in 2017. The application of fluridone in 2017 could explain the decline in the abundance of native *S. filiformis*, *S. pectinata*, and *P. foliosus*; however, knowing the exact dates of applications would better inform this conclusion. Because fluridone is a relatively slow-acting herbicide, the effects of treatment may not be observed for weeks. Further, information on the exact location of treatments is not known. Franks Tract is approximately 1,347 ha in size; thus, recent years' treatments that were less than 500 ha would have affected only a portion of the area. Of the other native species, the recovery of *C. demersum* when herbicide treatments were halted is evident. The presence of the barrier could have reduced the abundance of this species, as seen in the sharp decline in 2021.

3.4 Discussion/Interpretation

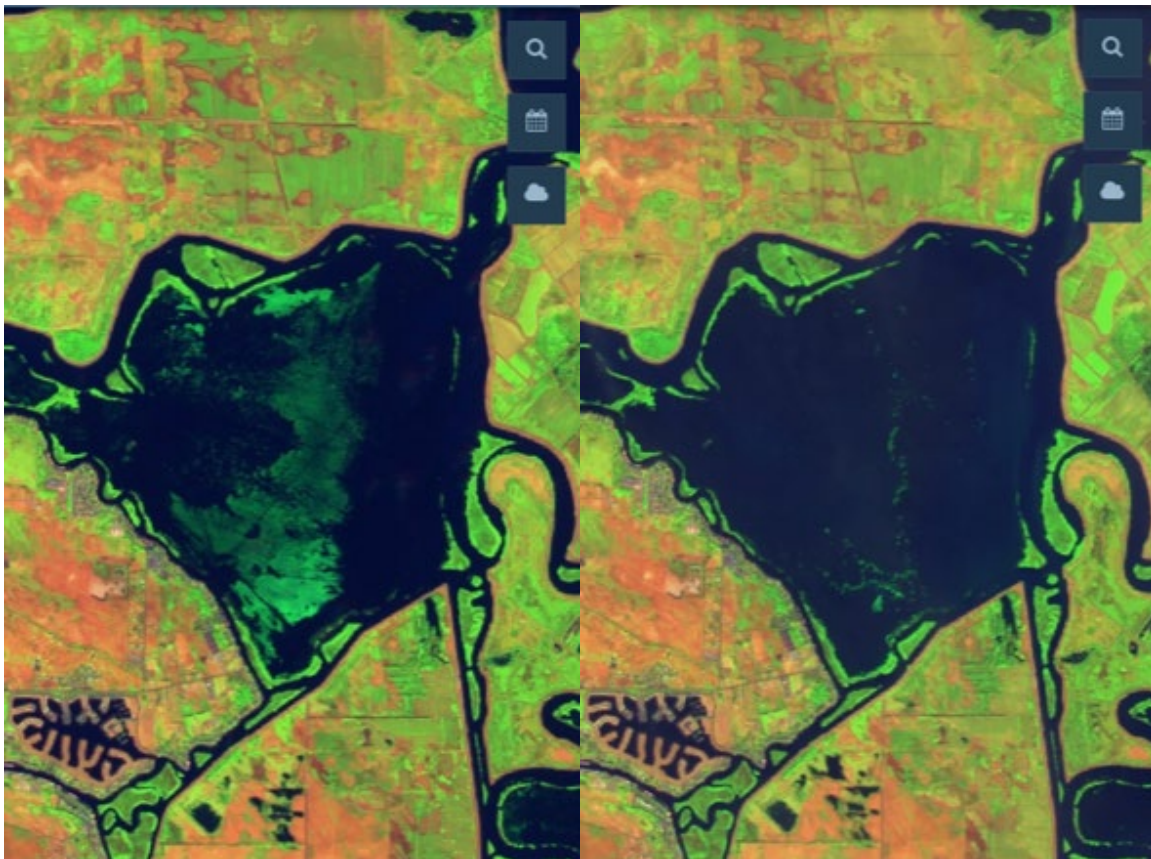
3.4.1 Impact of Drought

The extended, frequent droughts over the past 20 years have coincided with increases in the abundance of aquatic weeds. This is particularly apparent in the expansion of SAV between 2014 and 2016 (Figure 29, Figure 30, Figure 31, Figure 32, Figure 33). While the wet years of 2017 and 2019 showed some reduction in SAV within Franks Tract and the Delta as a whole, SAV abundance remains significantly higher than in the early 2000s (Figure 29, Figure 30, Figure 31, Figure 32, Figure 33).

3.4.2 Impact of Drought Barrier

The 2015 drought barrier may have caused a regime shift in Franks Tract in which the middle of the tract filled in with aquatic plants as flows decreased, and this condition persisted after the drought and barrier removal (Kimmerer et al. 2019). The open channel through the center of the island that was present in 2004 and 2014 had filled in by fall 2015 and did not re-form after removal of the 2015 barrier (Figure 29). However, similar expansions of aquatic weeds have been seen in other large Delta islands (such as Big Break or Clifton Court Forebay; Kimmerer et al. 2019; Figure 30, Figure 31). Therefore, the shift in weeds within Franks Tract may have been driven primarily by the drought, though likely exacerbated by the presence of the barrier.

The level of further expansion of aquatic weeds within Franks Tract with the 2021 EDB is unknown pending finalization of 2021 hyperspectral imagery. However, existing satellite data and surveys can provide some information about the state of weeds at the site (Figure 35, Figure 36). The western side of the tract had particularly thick filamentous algae at the surface in fall 2020 (Figure 35, Figure 36). This coincided with increased residence time in the same area of the tract observed in hydrodynamic models (Figure 16).



NOTE: Large mats of filamentous green algae are visible in the early-October image, but much of this algae was washed out during the large atmospheric river that occurred October 23–25, 2021. Images courtesy of SePRO Corporation.

Figure 35
Satellite images of Franks Tract in early October 2021 (left)
and late October 2021 (right).



Figure 36
Photo provided by SePRO Corporation showing the amount of vegetation and algae present in Franks Tract on October 6, 2021.

Franks Tract has particularly good data on SAV community composition, thanks to the SePRO surveys (Figure 34). In 2021, three species exhibited lower abundances than in previous years: *Egeria densa* (non-native), *Ceratophyllum demersum* (native), and *Potamogeton richardsonii* (native). Conversely, two species exhibited higher abundances: *Najas guadalupensis* (native) and *Myriophyllum spicatum* (non-native). However, only *C. demersum* showed a strong change in the trajectory of its abundance compared to recent years. This species had increased in abundance by nearly five times during 2017–2020 but dropped back nearly to 2017 abundance levels in 2021 which may be attributable to the effects of the drought barrier. This dramatic increase in 2021 could also be caused by very high levels of *N. guadalupensis* outcompeting *C. demersum*. The salinity barrier may be favoring *N. guadalupensis* because of lower salinity and flow, and lack of fluridone treatment may be favoring annual species (such as *N. guadalupensis*), because it is highly effective on plants sprouting from seeds.

3.4.3 Interaction between Weed Treatment and Drought

The treatment of weeds with herbicides makes it difficult to identify impacts of hydrologic conditions versus treatment effects. The area treated annually by DBW’s SAV and FAV

treatment program has varied depending on funding, permits, plant community composition, and distribution of weeds (Caudill et al. 2021; Moran et al. 2021; Ta et al. 2017). Therefore, increases and decreases in weeds may be a combination of environmental parameters (e.g., water temperature, salinity, flow, water clarity) and treatment effects.

Weed treatment may also have negative effects on water quality, phytoplankton, and invertebrate populations, as well as potential fish health effects, although the extent to which this is a problem in the Delta is an area of active research (Jin et al. 2018; Marineau et al. 2019; Rasmussen et al. 2020; Tobias et al. 2019).

3.4.4 Impacts of Weeds on Beneficial Uses

Increases in aquatic vegetation have had multiple serious implications for both human uses and native fish habitat. SAV and FAV obstruct water diversions, with more than 30,000 cubic meters of vegetation removed from the State Water Project and Central Valley Project per year (Khanna et al. 2019). SAV also obstructs boat traffic, clogging propellers and jet engines, and control efforts can be extremely expensive, causing major economic impacts in the Delta (Moran et al. 2021).

Most native fish in the Delta are adapted to an ecosystem with high turbidity and without SAV. Changes to fish communities linked to SAV have been documented as SAV has expanded (Brown and Michniuk 2007; Conrad et al. 2016). Delta Smelt preferentially seek out turbid habitat, where they have higher feeding success and lower risk of predation (Ferrari et al. 2014; Hestir et al. 2015; Tigan et al. 2020). Aquatic vegetation slows water flow, which decreases turbidity, and provides habitat for non-native predatory fish such as Largemouth Bass (Conrad et al. 2016). The ability of SAV to trap sediment may also reduce sediment transported to emergent tidal wetlands, reducing their ability to keep pace with sea level rise (Drexler et al. 2020).

The extent to which native SAV may provide different impacts from those of invasive SAV is not well understood. Some evidence has found that certain native species, such as *Stuckenia pectinata*, may have less of an impact on fish habitat than invasive SAV such as *Egeria densa* (Boyer et al. 2013). There is also some evidence that native floating vegetation provides better habitat for fish and native invertebrates than invasive *Eichhornia crassipes* (Toft et al. 2003). However, research on the interactions of many of the native species in Franks Tract—including *N. guadalupensis*, which dominated in 2021—and the native fish community is lacking. Given the similarities in structure between many of the SAV species within Franks Tract, pelagic fish presumably will be negatively affected by both native and invasive SAV species.

These impacts of weeds on beneficial uses have been increasing over time. There is some indication of localized impacts of the barrier on weeds (Figure 29), and data for 2021 are not available yet, but the extent to which the TUCP may influence weeds will be very hard to detect over the background increases in weeds. Franks Tract and the South Delta, the areas most influenced by the barrier, are already regions with low turbidity, high temperatures, and low pelagic fish populations (CDFW data; Bashevkin et al., in review; Moyle et al. 2012; Sommer and Mejia 2013). Therefore, any change in aquatic weeds in these regions is unlikely to have major impacts on the bulk of pelagic fish populations. The barrier may also divert migrating

salmon from the Sacramento River away from Franks Tract (CDFW 2021), although this is still to be determined.

3.4.5 Potential Mitigation Actions for the Future

Management of aquatic vegetation is an area of active research, and no clear solutions for control of weeds in the Delta have been identified to date. The existing control program run by DBW is permitted to treat a limited area with a limited number of methods. Treatment for FAV, chiefly by the use of glyphosate herbicide, is relatively effective in killing weeds but requires large investments of time and money (Caudill et al. 2021), introduces toxic contaminants into the waterways, and does not remove dead plant material, which will continue to alter aquatic habitats (Marineau et al. 2019; Tobias et al. 2019). The use of herbicides for SAV is much less effective in a tidal environment (Rasmussen et al. 2020). New control strategies are currently under investigation, including new herbicides (Madsen and Kyser 2020; Madsen et al. 2021), biocontrol agents (Hopper et al. 2017), and physical barriers (Moran et al. 2021).

SAV treatment within Franks Tract while the barrier is in place may be somewhat more effective than SAV treatment in other areas of the Delta, because flows on the west side of the tract will be significantly reduced (Figure 16). Longer residence times may allow aquatic herbicides to reach effective concentrations for a longer period, thus increasing their efficacy (Netherland et al. 1991; Rasmussen et al. 2020; Slade et al. 2008). Currently, use of herbicides within Franks Tract is precluded by the presence of many species not listed in DBW's permit (E. Hard, DBW, pers. comm.), but some investigation on reduced flow and herbicide efficiency may be an area ripe for future research.

SECTION 4

References

- Acuña, S., D. Baxa, P. Lehman, F.-C. Teh, D.-F. Deng, and S. Teh. 2020. Determining the exposure pathway and impacts of *Microcystis* on threadfin shad, *Dorosoma petenense*, in San Francisco Estuary. *Environmental Toxicology and Chemistry* 39(4):787–798. Viewed online at <https://doi.org/10.1002/etc.4659>.
- Acuña, S., D. Baxa, and S. Teh. 2012a. Sublethal dietary effects of microcystin producing *Microcystis* on threadfin shad, *Dorosoma petenense*. *Toxicon* 60:1191–1202.
- Acuña, S., D. F. Deng, P. Lehman, and S. Teh. 2012b. Sublethal dietary effects of *Microcystis* on Sacramento splittail, *Pogonichthys macrolepidotus*. *Aquatic Toxicology* 110–111:1–8.
- APHA (American Public Health Association). 2017. *Standard Methods for the Examination of Water and Wastewater*, 23rd edition. American Public Health Association, American Water Works Association, and Water Environment Federation.
- Ateljevich, E., K. Nam, Y. Zhang, R. Wang, and Q. Shu. 2014. Bay Delta Calibration Overview. In: *Methodology for Flow and Salinity Estimates in the Sacramento-San Joaquin Delta and Suisun Marsh. 35th Annual Progress Report*. Sacramento: California Department of Water Resources.
- Banerjee, S., S. Maity, R. Guchhait, A. Chatterjee, C. Biswas, M. Adhikari, and K. Pramanick. 2021. Toxic effects of cyanotoxins in teleost fish: A comprehensive review. *Aquatic Toxicology* 240:105971. Viewed online at: <https://doi.org/10.1016/j.aquatox.2021.105971>.
- Banks, L. K., and P. C. Frost. 2017. Biomass loss and nutrient release from decomposing aquatic macrophytes: effects of detrital mixing. *Aquatic Sciences* 79(4):881-890. Viewed online at: [doi:10.1007/s00027-017-0539-y](https://doi.org/10.1007/s00027-017-0539-y).
- Barko, J. W., D. Gunnison, and S. R. Carpenter. 1991. Sediment interactions with submersed macrophyte growth and community dynamics. *Aquatic Botany* 41(1):41–65. Viewed online at: [https://doi.org/10.1016/0304-3770\(91\)90038-7](https://doi.org/10.1016/0304-3770(91)90038-7).
- Barko, J. W., and R. M. Smart. 1981. Sediment-based nutrition of submersed macrophytes. *Aquatic Botany* 10:339–352. Viewed online at: [https://doi.org/10.1016/0304-3770\(81\)90032-2](https://doi.org/10.1016/0304-3770(81)90032-2).
- Bashevkin, S. M., B. Mahardja, and L. R. Brown. 2021. Warming in the Upper San Francisco Estuary: Patterns of Water Temperature Change from 5 Decades of Data. Viewed online at: https://www.researchgate.net/publication/351195769_Warming_in_the_upper_San_Francisco_Estuary_Patterns_of_water_temperature_change_from_5_decades_of_data.

-
- Baston, D. 2021. exactextractr: Fast Extraction from Raster Datasets using Polygons. Comprehensive R Archive Network (CRAN). Viewed online at: <https://cran.r-project.org/web/packages/exactextractr/index.html>.
- Bates, D., M. Maechler, B. Bolker, and S. Walker. 2020. lme4: Linear Mixed-Effects Models using 'Eigen' and S4. The Comprehensive R Archive Network (CRAN). Viewed online at: <https://github.com/lme4/lme4/>.
- Berg, M., and M. Sutula. 2015. *Factors Affecting the Growth of Cyanobacteria with Special Emphasis on the Sacramento–San Joaquin Delta*. Southern California Coastal Water Research Project. 100 pp.
- Bergamaschi, B. A., T. E. Kraus, B. D. Downing, J. Soto Perez, K. O'Donnell, J. A. Hansen, A. M. Hansen, A. D. Gelber, and E. B. Stumpner. 2020. Assessing spatial variability of nutrients and related water quality constituents in the California Sacramento–San Joaquin Delta at the landscape scale. High resolution mapping surveys: U.S. Geological Survey data release. Viewed online at: <https://doi.org/10.5066/P9FQEUAL>.
- Bivand, R., T. Keitt, and B. Rowlingson. 2021. Package 'rgdal': Bindings for the 'Geospatial' Data Abstraction Library. Comprehensive R Archive Network (CRAN). Viewed online at: <http://rgdal.r-forge.r-project.org/>.
- Boyer, K., E. Borgnis, J. Miller, J. Moderan, and M. Patten. 2013. *Habitat Values of Native SAV (Stukenia spp.) in the Low Salinity Zone of San Francisco Estuary*, Final Project Report. Sacramento: Delta Stewardship Council.
- Boyer, K., and M. Sutula. 2015. *Factors Controlling Submersed and Floating Macrophytes in the Sacramento–San Joaquin Delta*. Southern California Coastal Water Research Project, Technical Report 870. Costa Mesa, CA.
- Breiman, L. 2001. Random Forests. *Machine Learning* 45(1):5–32. Viewed online at: [doi:10.1023/A:1010933404324](https://doi.org/10.1023/A:1010933404324).
- Brooks, M. L., E. Fleishman, L. Brown, P. Lehman, I. Werner, N. L. Scholz, C. Mitchelmore, J. R. Lovvorn, M. L. Johnson, D. Schlenk, S. van Drunick, J. I. Derver, D. M. Stoms, A. E. Parker, and R. Dugdale. 2011. Life histories, salinity zones, and sublethal contributions of contaminants to pelagic fish declines illustrated with a case study of San Francisco Estuary, California, USA. *Estuaries and Coasts* 35(2):603–621.
- Brown, L. R. 2003. Will tidal wetland restoration enhance populations of native fishes? *San Francisco Estuary and Watershed Science* 1(1):43 pages. Viewed online at: <https://doi.org/10.15447/sfew.2003v1iss1art2>.
- Brown, L. R., and D. Michniuk. 2007. Littoral fish assemblages of the alien-dominated Sacramento–San Joaquin Delta, California, 1980–1983 and 2001–2003. *Estuaries and Coasts* 30(1):186–200.
- Burford, M. A., and M. J. O'Donohue. 2006. A comparison of phytoplankton community assemblages in artificially and naturally mixed subtropical water reservoirs. *Freshwater Biology* 51(5):973–982. Viewed online at: <https://doi.org/10.1111/j.1365-2427.2006.01536.x>.

- Caraco, N. F., and J. J. Cole. 2002. Contrasting impacts of a native and alien macrophyte on dissolved oxygen in a large river. *Ecological Applications* 12(5):1496–1509. Viewed online at: [https://doi.org/10.1890/1051-0761\(2002\)012\[1496:CIOANA\]2.0.CO;2](https://doi.org/10.1890/1051-0761(2002)012[1496:CIOANA]2.0.CO;2).
- Carey, C. C., B. W. Ibelings, E. P. Hoffmann, D. P. Hamilton, and J. D. Brookes. 2012. Ecophysiological adaptations that favour freshwater cyanobacteria in a changing climate. *Water Research* 46(5):1394–1407. Viewed online at: <https://doi.org/10.1016/j.watres.2011.12.016>.
- Carmichael, W. 2008. A world overview—One-hundred-twenty-seven years of research on toxic cyanobacteria—Where do we go from here? Pages 105–125 in H. K. Hudnell (ed.), *Cyanobacterial Harmful Algal Blooms: State of the Science and Research Needs*. New York: Springer.
- Carvalho, P., S. M. Thomaz, and L. M. Bini. 2005. Effects of temperature on decomposition of a potential nuisance species: the submerged aquatic macrophyte *Egeria najas* Planchon (Hydrocharitaceae). *Brazilian Journal of Botany* 65(1):51–60.
- Caudill, J., A. R. Jones, L. Anderson, J. D. Madsen, P. Gilbert, S. Shuler, and M. A. Heilman. 2019. Aquatic plant community restoration following the long-term management of invasive *Egeria densa* with fluridone treatments. *Management of Biological Invasions* 10(3):473–485. Viewed online at: <https://doi.org/10.3391/mbi.2019.10.3.05>.
- Caudill, J., J. Madsen, and W. Pratt. 2021. Operational aquatic weed management in the California Sacramento–San Joaquin River Delta. *Journal of Aquatic Plant Management* 59:112–122.
- CDFW (California Department of Fish and Wildlife). 2021. California Endangered Species Act Incidental Take Permit No. 2081-2021-041-03-A1. Amendment No. 1. California Department of Water Resources. 2021 Emergency Drought Salinity Barrier in Contra Costa County. Sacramento, CA.
- Chambers, P. A., and J. Kalff. 1987. Light and nutrients in the control of aquatic plant community structure. I. *In situ* experiments. *Journal of Ecology* 75(3):611–619. Viewed online at: [doi:10.2307/2260193](https://doi.org/10.2307/2260193).
- Chambers, P. A., E. E. Prepas, H. R. Hamilton, and M. L. Bothwell. 1991. Current velocity and its effect on aquatic macrophytes in flowing waters. *Ecological Applications* 1(3):249–257. Viewed online at: <https://doi.org/10.2307/1941754>.
- Chia, M. A., J. G. Jankowiak, B. J. Kramer, J. A. Goleski, I. S. Huang, P. V. Zimba, M. do Carmo Bittencourt-Oliveira, and C. J. Gobler. 2018. Succession and toxicity of *Microcystis* and *Anabaena* (*Dolichospermum*) blooms are controlled by nutrient-dependent allelopathic interactions. *Harmful Algae* 74:67–77. Viewed online at: <https://doi.org/10.1016/j.hal.2018.03.002>.
- Chorus, I., and M. Welker. 2021. *Toxic Cyanobacteria in Water: A Guide to Their Public Health Consequences, Monitoring and Management*. Taylor & Francis.

-
- Cloern, J. E., T. S. Schraga, E. Nejad, and C. Martin. 2020. Nutrient status of San Francisco Bay and its management implications. *Estuaries and Coasts*. Viewed online at: doi:10.1007/s12237-020-00737-w.
- Coles, J. F., and R. C. Jones. 2000. Effect of temperature on photosynthesis-light response and growth of four phytoplankton species isolated from a tidal freshwater river. *Journal of Phycology* 36(1):7–16. Viewed online at: <https://doi.org/10.1046/j.1529-8817.2000.98219.x>.
- Conrad, J. L., A. J. Bibian, K. L. Weinersmith, D. De Carion, M. J. Young, P. Crain, E. L. Hestir, M. J. Santos, and A. Sih. 2016. Novel species interactions in a highly modified estuary: Association of largemouth bass with Brazilian waterweed *Egeria densa*. *Transactions of the American Fisheries Society* 145:249–263. Viewed online at: doi:10.1080/00028487.2015.1114521.
- Dahm, C. N., A. E. Parker, A. E. Adelson, M. A. Christman, and B. A. Bergamaschi. 2016. Nutrient dynamics of the Delta: Effects on primary producers. *San Francisco Estuary and Watershed Science* 14(4). Viewed online at: <http://www.escholarship.org/uc/item/1789c0mz>.
- DBW (California Department of Parks and Recreation, Division of Boating and Waterways). 2020. *Aquatic Invasive Plant Control Program 2019 Annual Monitoring Report*. Sacramento, CA.
- Deleersnijder, E., J.-M. Campin, and E. J. M. Delhez. 2001. The concept of age in marine modelling: I. Theory and preliminary model results. *Journal of Marine Systems* 28(3):229–267. Viewed online at: [https://doi.org/10.1016/S0924-7963\(01\)00026-4](https://doi.org/10.1016/S0924-7963(01)00026-4).
- Delhez, É. J. M., B. de Brye, A. de Brauwere, and É. Deleersnijder. 2014. Residence time vs influence time. *Journal of Marine Systems* 132:185–195. Viewed online at: <https://doi.org/10.1016/j.jmarsys.2013.12.005>.
- Deng, D. F., K. Zheng, F. C. Teh, P. W. Lehman, and S. J. Teh. 2010. Toxic threshold of dietary microcystin (-LR) for quart medaka. *Toxicol* 55:787–794.
- Drexler, J. Z., S. Khanna, and J. R. Lacy. 2020. Carbon storage and sediment trapping by *Egeria densa* Planch., a globally invasive, freshwater macrophyte. *Science of the Total Environment*. Viewed online at: doi:10.1016/j.scitotenv.2020.142602.
- Durand, J., W. Fleenor, R. McElreath, M. J. Santos, and P. Moyle. 2016. Physical controls on the distribution of the submersed aquatic weed *Egeria densa* in the Sacramento–San Joaquin Delta and implications for habitat restoration. *San Francisco Estuary and Watershed Science* 14(1). Viewed online at: <http://www.escholarship.org/uc/item/85c9h479>.
- DWR (California Department of Water Resources). 2019. *Efficacy Report—2015 Emergency Drought Barrier Project*. Bay-Delta Office, West Sacramento, CA. 106 pp.
- Ferrari, M. C. O., L. Ranaker, K. L. Weinersmith, M. J. Young, A. Sih, and J. L. Conrad. 2014. Effects of turbidity and an invasive waterweed on predation by introduced largemouth bass. *Environmental Biology of Fishes* 97:79–90.

- Fong, S., S. Louie, I. Werner, J. Davis, and R. E. Connon. 2016. Contaminant effects on California Bay–Delta species and human health. *San Francisco Estuary and Watershed Science* 14(4). Viewed online at: <http://www.escholarship.org/uc/item/52m780xj>.
- Foss, A. J., and M. T. Aubel. 2015. Using the MMPB technique to confirm microcystin concentrations in water measured by ELISA and HPLC (UV, MS, MS/MS). *Toxicon* 104:91–101. Viewed online at: <https://doi.org/10.1016/j.toxicon.2015.07.332>.
- Frodge, J. D., G. L. Thomas, and G. B. Pauley. 1990. Effects of canopy formation by floating and submergent aquatic macrophytes on the water quality of two shallow Pacific Northwest lakes. *Aquatic Botany* 38(2):231–248. Viewed online at: [https://doi.org/10.1016/0304-3770\(90\)90008-9](https://doi.org/10.1016/0304-3770(90)90008-9).
- Ger, K. A., P. Arneson, C. R. Goldman, and S. J. Teh. 2010a. Species specific differences in the ingestion of *Microcystis* cells by the calanoid copepods *Eurytemora affinis* and *Pseudodiaptomus forbesi*. *Journal of Plankton Research*.
- Ger, K. A., S. J. Teh, D. V. Baxa, S. Lesmeister, and C. R. Goldman. 2010b. The effects of dietary *Microcystis aeruginosa* and microcystin on the copepods of the upper San Francisco Estuary. *Freshwater Biology* 55:1548–1559.
- Ger, K. A., S. J. Teh, and C. R. Goldman. 2009. Microcystin-LR toxicity on dominant copepods *Eurytemora affinis* and *Pseudodiaptomus forbesi* of the upper San Francisco Estuary. *Science of the Total Environment* 407:4852–4857.
- Glibert, P. M., R. Dugdale, F. P. Wilkerson, A. E. Parker, J. Alexander, E. Antell, S. Blaser, A. Johnson, J. Lee, T. Lee, S. Murasko, and S. Strong. 2014. Major—but rare—spring blooms in 2014 in San Francisco Bay Delta, California, a result of the long-term drought, increased residence time, and altered nutrient loads and forms. *Journal of Experimental Marine Biology and Ecology* 460:8–18.
- Herrero, A., A. M. Muro-Pastor, A. Valladares, and E. Flores. 2004. Cellular differentiation and the NtcA transcription factor in filamentous cyanobacteria. *FEMS Microbiology Reviews* 28(4):469–487. Viewed online at: [doi:10.1016/j.femsre.2004.04.003](https://doi.org/10.1016/j.femsre.2004.04.003).
- Hestir, E. L., D. H. Schoellhamer, J. Greenberg, T. Morgan-King, and S. L. Ustin. 2015. The effect of submerged aquatic vegetation expansion on a declining turbidity trend in the Sacramento–San Joaquin River Delta. *Estuaries and Coasts* 39(4):1100–1112. Viewed online at: [doi:10.1007/s12237-015-0055-z](https://doi.org/10.1007/s12237-015-0055-z).
- Hijmans, R. J. 2021. Package 'raster': Geographic Data Analysis and Modeling. Comprehensive R Archive Network (CRAN). Viewed online at: <https://rspatial.org/raster>.
- Hopper, J. V., P. D. Pratt, K. F. McCue, M. J. Pitcairn, P. J. Moran, and J. D. Madsen. 2017. Spatial and temporal variation of biological control agents associated with *Eichhornia crassipes* in the Sacramento–San Joaquin River Delta, California. *Biological Control* 111:13–22. Viewed online at: <https://doi.org/10.1016/j.biocontrol.2017.05.005>.
- Huber, V., C. Wagner, D. Gerten, and R. Adrian. 2012. To bloom or not to bloom: contrasting responses of cyanobacteria to recent heat waves explained by critical thresholds of abiotic drivers. *Oecologia* 169(1):245–256. Viewed online at: [doi:10.1007/s00442-011-2186-7](https://doi.org/10.1007/s00442-011-2186-7).

-
- Hudnell, H. (ed.). 2008. *Cyanobacterial Harmful Algal Blooms: State of the Science and Research Needs*, Volume 619. New York: Springer.
- Hudnell, H. K. 2010. The state of U.S. freshwater harmful algal blooms assessments, policy and legislation. *Toxicon* 55(5):1024–1034. Viewed online at: <https://doi.org/10.1016/j.toxicon.2009.07.021>.
- Ibelings, B. W., and S. C. Maberly. 1998. Photoinhibition and the availability of inorganic carbon restrict photosynthesis by surface blooms of cyanobacteria. *Limnology and Oceanography* 43(3):408–419. Viewed online at: <https://doi.org/10.4319/lo.1998.43.3.0408>.
- IEP et al. (Interagency Ecological Program, S. Lesmeister, and M. Martinez). 2020. Interagency Ecological Program: Discrete water quality monitoring in the Sacramento–San Joaquin Bay-Delta, collected by the Environmental Monitoring Program, 2000–2018. Ver. 2. Environmental Data Initiative. Viewed online at: <https://doi.org/10.6073/pasta/a215752cb9ac47f9ed9bb0fdb7fc7c19>.
- Ji, X., J. M. H. Verspagen, D. B. V. d. Waal, B. Rost, and J. Huisman. 2020. Phenotypic plasticity of carbon fixation stimulates cyanobacterial blooms at elevated CO₂. *Science Advances* 6(8):eaax2926. Viewed online at: [doi:10.1126/sciadv.aax2926](https://doi.org/10.1126/sciadv.aax2926).
- Jin, J., T. Kurobe, W. F. Ramírez-Duarte, M. B. Bolotaolo, C. H. Lam, P. K. Pandey, T.-C. Hung, M. E. Stillway, L. Zweig, J. Caudill, L. Lin, and S. J. Teh. 2018. Sub-lethal effects of herbicides penoxsulam, imazamox, fluridone and glyphosate on Delta Smelt (*Hypomesus transpacificus*). *Aquatic Toxicology* 197:79–88. Viewed online at: <https://doi.org/10.1016/j.aquatox.2018.01.019>.
- Johnson, M. L., I. Werner, S. Teh, and F. Loge. 2010. *Evaluation of Chemical, Toxicological and Histopathologic Data to Determine Their Role in the Pelagic Organism Decline*. University of California, Davis. 296 pp.
- Khanna, S., S. Acuña, D. Contreras, W. K. Griffiths, S. Lesmeister, R. C. Reyes, B. Schreier, and B. J. Wu. 2019. Invasive aquatic vegetation impacts on Delta operations, monitoring, and ecosystem and human health. *IEP Newsletter* 36(1):8–19.
- Khanna, S., M. J. Santos, J. D. Boyer, K. D. Shapiro, J. Bellvert, and S. L. Ustin. 2018. Water primrose invasion changes successional pathways in an estuarine ecosystem. *Ecosphere* 9(9):e02418. Viewed online at: [doi:10.1002/ecs2.2418](https://doi.org/10.1002/ecs2.2418).
- Khanna, S., J. W. Gaeta, J. L. Conrad, and E. Gross. In review. Multi-year landscape-scale efficacy analysis of herbicide treatment of invasive submerged aquatic vegetation in a California estuary using fluridone. *Biological Invasions*.
- Kibuye, F. A., A. Zamyadi, and E. C. Wert. 2021a. A critical review on operation and performance of source water control strategies for cyanobacterial blooms: Part II—Mechanical and biological control methods. *Harmful Algae* 109:102119. Viewed online at: <https://doi.org/10.1016/j.hal.2021.102119>.
- Kibuye, F. A., A. Zamyadi, and E. C. Wert. 2021b. A critical review on operation and performance of source water control strategies for cyanobacterial blooms: Part I—

- Chemical control methods. *Harmful Algae* 109:102099. Viewed online at: <https://doi.org/10.1016/j.hal.2021.102099>.
- Kimmerer, W., T. R. Ignoffo, B. Bemowski, J. Modéran, A. Holmes, and B. Bergamaschi. 2018. Zooplankton dynamics in the Cache Slough Complex of the Upper San Francisco Estuary. *San Francisco Estuary and Watershed Science* 16(3). Viewed online at: <https://doi.org/10.15447/sfew.2018v16iss3art4>.
- Kimmerer, W., F. Wilkerson, B. Downing, R. Dugdale, E. S. Gross, K. Kayfetz, S. Khanna, A. E. Parker, and J. K. Thompson. 2019. Effects of drought and the emergency drought barrier on the ecosystem of the California Delta. *San Francisco Estuary and Watershed Science* 17(3). Viewed online at: <https://doi.org/10.15447/sfew.2019v17iss3art2>.
- Konopka, A., and T. D. Brock. 1978. Effect of temperature on blue-green algae (cyanobacteria) in Lake Mendota. *Applied and Environmental Microbiology* 36(4):572–576. Viewed online at: [doi:10.1128/aem.36.4.572-576.1978](https://doi.org/10.1128/aem.36.4.572-576.1978).
- Kuehne, L. M., J. D. Olden, and E. S. Rubenson. 2016. Multi-trophic impacts of an invasive aquatic plant. *Freshwater Biology* 61(11):1846–1861. Viewed online at: <https://doi.org/10.1111/fwb.12820>.
- Lehman, P., K. Marr, G. Boyer, S. Acuña, and S. Teh. 2013. Long-term trends and causal factors associated with *Microcystis* abundance and toxicity in San Francisco Estuary and implications for climate change impacts. *Hydrobiologia* 718:141–158.
- Lehman, P., S. Teh, G. Boyer, M. Nobriga, E. Bass, and C. Hogle. 2010. Initial impacts of *Microcystis aeruginosa* blooms on the aquatic food web in the San Francisco Estuary. *Hydrobiologia* 637(1):229–248.
- Lehman, P., and S. Waller. 2003. *Microcystis* blooms in the Delta. *Interagency Ecological Program for the San Francisco Estuary Newsletter* 16:18–19.
- Lehman, P. W., G. Boyer, C. Hall, S. Waller, and K. Gehrts. 2005. Distribution and toxicity of a new colonial *Microcystis aeruginosa* bloom in the San Francisco Estuary, California. *Hydrobiologia* 541:87–99.
- Lehman, P. W., G. Boyer, M. Satchwell, and S. Waller. 2008. The influence of environmental conditions on the seasonal variation of *Microcystis* cell density and microcystins concentration in San Francisco Estuary. *Hydrobiologia* 600(1):187–204. Viewed online at: [doi:10.1007/s10750-007-9231-x](https://doi.org/10.1007/s10750-007-9231-x).
- Lehman, P. W., T. Kurobe, K. Huynh, S. Lesmeister, and S. J. Teh. 2021. Covariance of phytoplankton, bacteria, and zooplankton communities within *Microcystis* blooms in San Francisco Estuary. *Frontiers in Microbiology* 12(1184). Viewed online at: [doi:10.3389/fmicb.2021.632264](https://doi.org/10.3389/fmicb.2021.632264).
- Lehman, P. W., T. Kurobe, S. Lesmeister, C. Lam, A. Tung, M. Xiong, and S. J. Teh. 2018. Strong differences characterize *Microcystis* blooms between successive severe drought years in the San Francisco Estuary, California, USA. *Aquatic Microbial Ecology* 81(3):293–299. Viewed online at: <https://www.int-res.com/abstracts/ame/v81/n3/p293-299>.

-
- Lehman, P. W., T. Kurobe, and S. J. Teh. 2020. Impact of extreme wet and dry years on the persistence of *Microcystis* harmful algal blooms in San Francisco Estuary. *Quaternary International*.
- Lenth, R. V., P. Buerkner, M. Herve, J. Love, H. Riebl, and H. Singmann. 2021. Package 'emmeans': Estimated Marginal Means, aka Least-Squares Means. Version 1.6.2. Comprehensive R Archive Network, CRAN. Viewed online at: <https://cran.r-project.org/web/packages/emmeans/index.html>.
- Li, X., T. W. Dreher, and R. Li. 2016. An overview of diversity, occurrence, genetics and toxin production of bloom-forming *Dolichospermum* (*Anabaena*) species. *Harmful Algae* 54:54–68. Viewed online at: <https://doi.org/10.1016/j.hal.2015.10.015>.
- Lucas, L. V., J. E. Cloern, J. K. Thompson, M. T. Stacey, and J. R. Koseff. 2016. Bivalve grazing can shape phytoplankton communities. *Frontiers in Marine Science* 3:14.
- Lurling, M., F. Eshutu, E. J. Faassen, S. Kosten, and V. L. M. Huszar. 2013. Comparison of cyanobacterial and green algal growth rates at different temperatures. *Freshwater Biology* 58(3):552–559. Viewed online at: <https://doi.org/10.1111/j.1365-2427.2012.02866.x>.
- Ma, H., Y. Wu, N. Gan, L. Zheng, T. Li, and L. Song. 2015. Growth inhibitory effect of *Microcystis* on *Aphanizomenon flos-aquae* isolated from cyanobacteria bloom in Lake Dianchi, China. *Harmful Algae* 42:43–51. Viewed online at: <https://doi.org/10.1016/j.hal.2014.12.009>.
- Madsen, J. D., and G. B. Kyser. 2020. Herbicides for management of waterhyacinth in the Sacramento–San Joaquin River Delta, California. *Journal of Aquatic Plant Management* 58:98–104.
- Madsen, J. D., C. Morgan, J. Miskella, G. Kyser, P. Gilbert, J. O'Brien, and K. D. Getsinger. 2021. Brazilian egeria herbicide mesocosm and field trials for managing the Sacramento–San Joaquin River Delta. *Journal of Aquatic Plant Management* 59(01s):90–97.
- Madsen, J. D., and R. M. Wersal. 2018. Proper survey methods for research of aquatic plant ecology and management. *Journal of Aquatic Plant Management* 56:90–96.
- Magnusson, A., H. Skaug, A. Nielsen, C. Berg, K. Kristensen, M. Maechler, K. v. Bentham, N. Sadat, B. Bolker, and M. Brooks. 2019. Package 'glmmTMB': Generalized Linear Mixed Models using Template Model Builder. The Comprehensive R Archive Network. Viewed online at: <https://github.com/glmmTMB>.
- Marineau, E. D., M. J. Perryman, S. Lawler, R. Hartman, and P. D. Pratt. 2019. Management of invasive water hyacinth as both a nuisance weed and invertebrate habitat. *San Francisco Estuary and Watershed Science* 17(2):1–19. Viewed online at: <https://doi.org/10.15447/sfews.2019v17iss5>.
- Mioni, C., R. Kudela, and D. Baxa. 2012. *Harmful Cyanobacteria Blooms and Their Toxins in Clear Lake and the Sacramento–San Joaquin Delta (California)*. Surface Water Ambient Monitoring Program Report 10-058-150.

- Miranda, L. E., M. P. Driscoll, and M. S. Allen. 2000. Transient physicochemical microhabitats facilitate fish survival in inhospitable aquatic plant stands. *Freshwater Biology* 44(4):617–628. Viewed online at: <https://doi.org/10.1046/j.1365-2427.2000.00606.x>.
- Moisander, P., P. Lehman, M. Ochiai, and S. Corum. 2009. Diversity of *Microcystis aeruginosa* in the Klamath River and San Francisco Bay Delta, California, USA. *Aquatic Microbial Ecology* 57:19–31. Viewed online at: [doi:10.3354/ame01320](https://doi.org/10.3354/ame01320).
- Moisander, P. H., M. Ochiai, and J. E. Stajich. 2020. Draft genome sequence of the non-microcystin-producing *Microcystis aeruginosa* strain KLA2, isolated from a freshwater reservoir in Northern California, USA. *Microbiology Resource Announcements* 9(3):e01086-19. Viewed online at: [doi:10.1128/MRA.01086-19](https://doi.org/10.1128/MRA.01086-19).
- Moisander, P. H., H. W. Paerl, and J. P. Zehr. 2008. Effects of inorganic nitrogen on taxa-specific cyanobacterial growth and nifH expression in a subtropical estuary. *Limnology and Oceanography* 53(6):2519–2532. Viewed online at: <https://doi.org/10.4319/lo.2008.53.6.2519>.
- Moran, P. J., J. D. Madsen, P. D. Pratt, D. L. Bubenheim, E. Hard, T. Jabusch, and R. I. Carruthers. 2021. An overview of the Delta Region Areawide Aquatic Weed Project for improved control of invasive aquatic weeds in the Sacramento–San Joaquin Delta. *Journal of Aquatic Plant Management* 59:2–15.
- Moyle, P., W. Bennett, J. Durand, W. Fleenor, B. Gray, E. Hanak, J. Lund, and J. Mount. 2012. *Where the Wild Things Aren't: Making the Delta a Better Place for Native Species*. San Francisco, CA: Public Policy Institute of California.
- Netherland, M. D., W. R. Green, and K. D. Getsinger. 1991. *Endothall Concentration and Exposure Time Relationships for the Control of Eurasian Watermilfoil and Hydrilla*. Vicksburg, MS: Environmental Laboratory, Department of the Army, Waterways Experiment Station, Corps of Engineers.
- Nobriga, M., F. Feyrer, R. Baxter, and M. Chotkowski. 2005. Fish community ecology in an altered river delta: Spatial patterns in species composition, life history strategies, and biomass. *Estuaries* 28(5):776–785.
- O'Neil, J. M., T. W. Davis, M. A. Burford, and C. J. Gobler. 2012. The rise of harmful cyanobacteria blooms: The potential roles of eutrophication and climate change. *Harmful Algae* 14:313–334. Viewed online at: <https://doi.org/10.1016/j.hal.2011.10.027>.
- OEHHA and CCHAB (Office of Environmental Health Hazard Assessment and California Cyanobacteria and Harmful Algal Bloom Network). 2021. California Voluntary Guidance for Response to HABs in Recreational Inland Waters. Viewed online at: mywaterquality.ca.gov/habs/resources/habs_response.html.
- OEHHA Ecotoxicology, N. Butler, J. C. Carlisle, R. Linville, and B. Washburn. 2009. *Microcystins: A Brief Overview of Their Toxicity and Effects, with Special Reference to Fish, Wildlife, and Livestock*. Sacramento: California Environmental Protection Agency, Office of Environmental Health Hazard Assessment, Integrated Risk Assessment Branch. 21 pp.

-
- Oksanen, J., F. G. Blanchet, R. Kindt, P. Legendre, P. R. Minchin, R. B. O'Hara, G. L. Simpson, and P. Solymos. 2020. Community Ecology Package "vegan." Version 2.5-7. Comprehensive R Archive Network (CRAN). Viewed online at: <https://github.com/vegandevs/vegan>.
- Otten, T. G., H. W. Paerl, T. W. Dreher, W. J. Kimmerer, and A. E. Parker. 2017. The molecular ecology of *Microcystis* sp. blooms in the San Francisco Estuary. *Environmental Microbiology* 19(9):3619–3637. Viewed online at: <https://doi.org/10.1111/1462-2920.13860>.
- Paerl, H. W., N. S. Hall, and E. S. Calandrino. 2011. Controlling harmful cyanobacterial blooms in a world experiencing anthropogenic and climatic-induced change. *Science of the Total Environment* 409(10):1739–1745. Viewed online at: <https://doi.org/10.1016/j.scitotenv.2011.02.001>.
- Paerl, H. W., and T. G. Otten. 2016. Duelling 'CyanoHABs': unravelling the environmental drivers controlling dominance and succession among diazotrophic and non-N₂-fixing harmful cyanobacteria. *Environmental Microbiology* 18(2):316–324.
- Paerl, H. W., and V. J. Paul. 2012. Climate change: Links to global expansion of harmful cyanobacteria. *Water Research* 46(5):1349–1363. Viewed online at: <https://doi.org/10.1016/j.watres.2011.08.002>.
- Pal, M., P. J. Yesankar, A. Dwivedi, and A. Qureshi. 2020. Biotic control of harmful algal blooms (HABs): A brief review. *Journal of Environmental Management* 268:110687. Viewed online at: <https://doi.org/10.1016/j.jenvman.2020.110687>.
- Pebesma, E., and R. Bivand. 2021. Package 'sp': Classes and Methods for Spatial Data. Version 1.4-6. Comprehensive R Archive Network (CRAN). Viewed online at: <https://github.com/edzer/sp/> <https://edzer.github.io/sp/>.
- Perry, S., and T. Brown. 2020. Phytoplankton, Chlorophyll-a and Pheophytin-a Status and Trends 2018. IEP Newsletter 37(2):16-23.
- Petticrew, E. L., and J. Kalff. 1992. Water flow and clay retention in submerged macrophyte beds. *Canadian Journal of Fisheries and Aquatic Sciences* 49(12):2483–2489. Viewed online at: <https://doi.org/10.1139/f92-274>.
- Pien, C., B. Davis, P. Lehman, E. Bush, and R. Hartman. In prep. Continuous water temperature trends and implications in the San Francisco Estuary.
- Rasmussen, N., J. L. Conrad, H. Green, S. Khanna, J. Caudill, P. Gilbert, P. Goertler, H. Wright, K. Hoffmann, S. Lesmeister, J. Jenkins, L. Takata, D. Boswort, T. Flynn, E. Hard, and T. Sommer. 2020. 2017–2018 Delta Smelt Resiliency Strategy Action for Enhanced Control of Aquatic Weeds and Understanding Effects of Herbicide Treatment on Habitat. Interagency Ecological Program Technical Report. 324 pp.
- Rasmussen, N., J. L. Conrad, H. Green, S. Khanna, H. Wright, K. Hoffmann, J. Caudill, and P. Gilbert. In review. Efficacy and fate of fluridone applications for control of invasive submersed aquatic vegetation in the estuarine environment of the Sacramento–San Joaquin Delta.

- Reynolds, C., S. Wiseman, B. Godfrey, and C. Butterwick. 1983. Some effects of artificial mixing on the dynamics of phytoplankton populations in large limnetic enclosures. *Journal of Plankton Research* 5(2):203–234.
- Reynolds, C. S. 2006. Growth and replication of phytoplankton. In *The Ecology of Phytoplankton*, 178–238. Cambridge, UK: Cambridge University Press.
- Riis, T., B. Olesen, J. S. Clayton, C. Lambertini, H. Brix, and B. K. Sorrell. 2012. Growth and morphology in relation to temperature and light availability during the establishment of three invasive aquatic plant species. *Aquatic Botany* 102:56–64. Viewed online at: <https://doi.org/10.1016/j.aquabot.2012.05.002>.
- Ripley, B., B. Venables, D. M. Bates, K. Hornik, A. Gebhardt, and D. F. [ctb]. 2021. Package MASS, Support Functions and Datasets for Venables and Ripley's MASS. Version 7.3-54. R Project. CRAN. Viewed online at: <http://www.stats.ox.ac.uk/pub/MASS4/>.
- Schultz, R., and E. Dibble. 2012. Effects of invasive macrophytes on freshwater fish and macroinvertebrate communities: the role of invasive plant traits. *Hydrobiologia* 684(1):1–14. Viewed online at: <https://doi.org/10.1007/s10750-011-0978-8>.
- Senn, D., T. Kraus, A. Richey, B. Bergamaschi, L. Brown, L. Conrad, C. Francis, W. Kimmerer, R. Kudela, T. Otten, A. Parker, A. Robinson, A. Mueller-Solger, D. Stern, and J. Thompson. 2020. *Changing Nitrogen Inputs to the Northern San Francisco Estuary: Potential Ecosystem Responses and Opportunities for Investigation*. SFEI Contribution #973. Richmond, CA: San Francisco Estuary Institute.
- SePRO (SePRO Corporation). 2017. Sonar PR Precision Release Specimen Label. Viewed online at: https://sepro.com/Documents/Sonar-PR_Label.pdf.
- SFEI (San Francisco Estuary Institute). 2021. HAB Satellite Analysis Tool. Viewed online at: <https://fhab.sfei.org/>.
- Slade, J. G., A. G. Poovey, and K. D. Getsinger. 2008. Concentration–exposure time relationships for controlling sago pondweed (*Stuckenia pectinata*) with endothall. *Weed Technology* 22(1):146–150. Viewed online at: <https://doi.org/10.1614/WT-07-121.1>.
- Sommer, T., and F. Mejia. 2013. A place to call home: a synthesis of Delta Smelt habitat in the upper San Francisco Estuary. *San Francisco Estuary and Watershed Science* 11(2):25 pages. Viewed online at: <https://doi.org/10.15447/sfew.2013v11iss2art4>.
- Spier, C., W. Stringfellow, J. Hanlon, M. Estiandan, T. Koski, and J. Kaaria. 2013. Unprecedented Bloom of Toxin-Producing Cyanobacteria in the Southern Bay-Delta Estuary and Its Potential Negative Impact on the Aquatic Food Web. University of the Pacific Ecological Engineering Research Program Report 4.5.1.
- Stal, L. J., P. Albertano, B. Bergman, K. von Bröckel, J. R. Gallon, P. K. Hayes, K. Sivonen, and A. E. Walsby. 2003. BASIC: Baltic Sea cyanobacteria. An investigation of the structure and dynamics of water blooms of cyanobacteria in the Baltic Sea—responses to a changing environment. *Continental Shelf Research* 23(17–19):1695–1714.

-
- State Water Board (State Water Resources Control Board). 2021. Order Conditionally Approving a Petition for Temporary Urgency Changes in License and Permit Terms and Conditions Requiring Compliance with Delta Water Quality Objectives in Response to Drought Conditions. Sacramento, CA. Viewed online at: https://www.waterboards.ca.gov/waterrights/water_issues/programs/drought/docs/tucp/2015/tucp_order070315.pdf.
- Stuckey, R. L. 1979. Distributional history of *Potamogeton crispus* (curly pondweed) in North America. *Bartonia* (46):22–42. Viewed online at: <http://www.jstor.org/stable/41610371>.
- Ta, J., L. W. J. Anderson, M. A. Christman, S. Khanna, D. Kratville, J. D. Madsen, P. J. Moran, and J. A. Viers. 2017. Invasive aquatic vegetation management in the Sacramento–San Joaquin River Delta: Status and recommendations. *San Francisco Estuary and Watershed Science* 15(4). Viewed online at: <https://doi.org/10.15447/sfews.2017v15iss4art5>.
- Talling, J. F. 1976. The Depletion of carbon dioxide from lake water by phytoplankton. *Journal of Ecology* 64(1):79–121. Viewed online at: <https://doi.org/10.2307/2258685>.
- Teh, S. J., A. A. Schultz, W. R. Duarte, S. Acuña, D. M. Barnard, R. D. Baxter, P. A. T. Garcia, and B. G. Hammock. 2020. Histopathological assessment of seven year-classes of Delta Smelt. *Science of the Total Environment*:138333.
- Terzopoulos, D., and A. Witkin. 1988. Physically based models with rigid and deformable components. *IEEE Computer Graphics and Applications* 8(6):41–51. Viewed online at: <https://doi.org/10.1109/38.20317>.
- Tigan, G., W. Mulvaney, L. Ellison, A. Schultz, and T.-C. Hung. 2020. Effects of light and turbidity on feeding, growth, and survival of larval Delta Smelt (*Hypomesus transpacificus*, Actinopterygii, Osmeridae). *Hydrobiologia* 847:2883–2894. Viewed online at: <https://doi.org/10.1007/s10750-020-04280-4>.
- Tobias, V. D., J. L. Conrad, B. Mahardja, and S. Khanna. 2019. Impacts of water hyacinth treatment on water quality in a tidal estuarine environment. *Biological Invasions* 21(12):3479–3490. Viewed online at: <https://doi.org/10.1007/s10530-019-02061-2>.
- Toft, J. D., C. A. Simenstad, J. R. Cordell, and L. F. Grimaldo. 2003. The effects of introduced water hyacinth on habitat structure, invertebrate assemblages, and fish diets. *Estuaries* 26(3):746–758.
- Ustin, S., S. Khanna, J. Bellvert, J. D. Boyer, and K. Shapiro. 2016. Impact of Drought on Submerged Aquatic Vegetation (SAV) and Floating Aquatic Vegetation (FAV) Using AVIRIS-NG Airborne Imagery. Sacramento: California Department of Fish and Wildlife.
- Ustin, S. L., S. Khanna, M. Lay, and K. Shapiro. 2020. Enhancement of Delta Smelt (*Hypomesus transpacificus*) Habitat through Adaptive Management of Invasive Aquatic Weeds in the Sacramento–San Joaquin Delta. Davis, CA: University of California, Davis, Center for Spatial Technologies and Remote Sensing.
- Utermöhl, H. 1958. Methods of collecting plankton for various purposes are discussed. *SIL Communications* 1953–1996 9(1):1–38. Viewed online at: <https://doi.org/10.1080/05384680.1958.11904091>.

- Verspagen, J. M. H., D. B. Van de Waal, J. F. Finke, P. M. Visser, and J. Huisman. 2014. Contrasting effects of rising CO₂ on primary production and ecological stoichiometry at different nutrient levels. *Ecology Letters* 17(8):951–960. Viewed online at: <https://doi.org/10.1111/ele.12298>.
- Visser, P. M., B. W. Ibelings, M. Bormans, and J. Huisman. 2016. Artificial mixing to control cyanobacterial blooms: a review. *Aquatic Ecology* 50(3):423–441. Viewed online at: <https://doi.org/10.1007/s10452-015-9537-0>.
- Vroom, J., M. van der Wegen, R. Martyr-Koller, and L. Lucas. 2017. What determines water temperature dynamics in the San Francisco Bay-Delta system? *Water Resources Research* 53(11):9901–9921.
- Wan, L., X. Chen, Q. Deng, L. Yang, X. Li, J. Zhang, C. Song, Y. Zhou, and X. Cao. 2019. Phosphorus strategy in bloom-forming cyanobacteria (*Dolichospermum* and *Microcystis*) and its role in their succession. *Harmful Algae* 84:46–55. Viewed online at: <https://doi.org/10.1016/j.hal.2019.02.007>.
- WHO (World Health Organization). 2021. WHO Guidelines on Recreational Water Quality. Volume 1: Coastal and Fresh Waters. Geneva, Switzerland.
- Wilde, S. B., J. R. Johansen, H. D. Wilde, P. Jiang, B. Bartelme, and R. S. Haynie. 2014. *Aetokthonos hydrillicola* gen. et sp. nov.: Epiphytic cyanobacteria on invasive aquatic plants implicated in Avian Vacuolar Myelinopathy. *Phytotaxa* 181(5):243–260.
- Wilhelm, S. W., G. S. Bullerjahn, R. M. L. McKay, and M. A. Moran. 2020. The complicated and confusing ecology of *Microcystis* blooms. *mBio* 11(3):e00529-20. Viewed online at: <https://doi.org/10.1128/mBio.00529-20>.
- Wu, Z., J. Shi, and R. Li. 2009. Comparative studies on photosynthesis and phosphate metabolism of *Cylindrospermopsis raciborskii* with *Microcystis aeruginosa* and *Aphanizomenon flos-aquae*. *Harmful Algae* 8(6):910–915. Viewed online at: <https://doi.org/10.1016/j.hal.2009.05.002>.
- Wynne, T., A. Meredith, T. Briggs, W. Litaker, and R. Stumpf. 2018. *Harmful Algal Bloom Forecasting Branch Ocean Color Satellite Imagery Processing Guidelines*. NOAA Technical Memorandum NOS NCCOS 252. Silver Spring, MD: National Oceanic and Atmospheric Administration. 48 pp.
- Zastepa, A., F. R. Pick, and J. M. Blais. 2014. Fate and persistence of particulate and dissolved microcystin-LA from *Microcystis* blooms. *Human and Ecological Risk Assessment: An International Journal* 20(6):1670–1686. Viewed online at: <https://doi.org/10.1080/10807039.2013.854138>.
- Zhang, M., Z. Yang, Y. Yu, and X. Shi. 2020b. Interannual and seasonal shift between *Microcystis* and *Dolichospermum*: A 7-year investigation in Lake Chaohu, China. *Water* 12(1978). Viewed online at: <https://doi.org/10.3390/w12071978>.
- Zhang, Y., F. Ye, E. V. Stanev, and S. Grashorn. 2016. Seamless cross-scale modeling with SCHISM. *Ocean Modelling* 21(3):71–76.

Zhang, Y. J., N. Gerds, E. Ateljevich, and K. Nam. 2020a. Simulating vegetation effects on flows in 3D using an unstructured grid model: model development and validation. *Ocean Dynamics* 70(2):213–230. Viewed online at: <https://doi.org/10.1007/s10236-019-01333-8>.

Appendix A

Additional Statistics Tables

TABLE A-1
TOXIN ANALYSIS COLLECTED IN CLIFTON COURT FOREBAY AND BANKS PUMPING PLANT IN SUMMER 2021

Date	Station	Analyte	Result (ng/mL)
4/26/2021	Clifton Court	Microcystin	ND
4/26/2021	Banks PP	Microcystin	ND
5/10/2021	Banks PP	Microcystin	ND
5/24/2021	Clifton Court	Toxin analysis not recommended	
5/24/2021	Banks PP	Microcystin	ND
6/7/2021	Clifton Court	Toxin analysis not recommended	
6/7/2021	Banks PP	Microcystin	ND
6/21/2021	Banks PP	Microcystin	ND
6/21/2021	Clifton Court	Microcystin	ND
7/12/2021	Banks PP	Microcystin	ND
7/12/2021	Clifton Court	Microcystin	ND
7/26/2021	Banks PP	Microcystin	ND
7/26/2021	Clifton Court	Microcystin	ND
8/9/2021	Clifton Court	Microcystin	ND
8/9/2021	Banks PP	Microcystin	ND
8/9/2021	Banks PP	Cylindrospermopsin	ND
8/9/2021	Banks PP	Saxotoxin	ND
8/9/2021	Banks PP	Anatoxin-a	ND
8/23/2021	Clifton Court	Microcystin	ND
8/23/2021	Banks PP	Microcystin	ND
9/13/2021	Clifton Court	Toxin analysis not recommended	
9/13/2021	Banks PP	Microcystin	ND
9/27/2021	Clifton Court	Toxin analysis not recommended	
9/27/2021	Banks PP	Microcystin	ND

NOTES: ND = no toxin detected; ng/mL = nanograms per milliliter; PP = Pumping Plant

TABLE A-2
PAIRWISE COMPARISONS BETWEEN YEARS FROM AN ORDINAL REGRESSION ON *MICROCYSTIS* VISUAL INDICES
ACROSS THE ENTIRE DELTA AND SUISUN REGIONS

contrast	estimate	SE	z.ratio	p.value
2014–2015	0.4241	0.2050	2.0689	0.4353
2014–2016	-0.3485	0.2064	-1.6885	0.6948
2014–2017	2.4709	0.2424	10.1952	0.0000
2014–2018	0.1448	0.1836	0.7890	0.9937
2014–2019	1.2042	0.1856	6.4881	0.0000
2014–2020	-0.6834	0.1785	-3.8276	0.0033
2014–2021	-0.2383	0.1837	-1.2972	0.9003
2015–2016	-0.7725	0.1959	-3.9430	0.0021
2015–2017	2.0468	0.2321	8.8169	0.0000
2015–2018	-0.2792	0.1711	-1.6323	0.7307
2015–2019	0.7801	0.1724	4.5238	0.0002
2015–2020	-1.1075	0.1669	-6.6362	0.0000
2015–2021	-0.6624	0.1718	-3.8561	0.0029
2016–2017	2.8194	0.2341	12.0410	0.0000
2016–2018	0.4933	0.1683	2.9303	0.0667
2016–2019	1.5527	0.1726	8.9942	0.0000
2016–2020	-0.3350	0.1648	-2.0328	0.4595
2016–2021	0.1101	0.1714	0.6427	0.9983
2017–2018	-2.3261	0.2123	-10.9544	0.0000
2017–2019	-1.2667	0.2131	-5.9429	0.0000
2017–2020	-3.1543	0.2120	-14.8776	0.0000
2017–2021	-2.7092	0.2152	-12.5881	0.0000
2018–2019	1.0594	0.1398	7.5752	0.0000
2018–2020	-0.8283	0.1335	-6.2063	0.0000
2018–2021	-0.3832	0.1407	-2.7228	0.1157
2019–2020	-1.8876	0.1391	-13.5665	0.0000
2019–2021	-1.4425	0.1447	-9.9703	0.0000
2020–2021	0.4451	0.1343	3.3150	0.0206

TABLE A-3
PAIRWISE COMPARISONS OF YEARS AND REGIONS FOR ORDINAL REGRESSION OF VISUAL *MICROCYSTIS* DATA
IN THE AREA IMMEDIATELY SURROUNDING THE EMERGENCY DROUGHT BARRIER

contrast	Estimated marginal mean	SE	t.ratio	p-value	
2014–2015	0.5106	0.2217	2.3037	0.2914	
2014–2016	-0.4390	0.2220	-1.9775	0.4972	
2014–2017	2.9251	0.2649	11.0426	0.0000	***
2014–2018	-0.1532	0.2209	-0.6935	0.9972	
2014–2019	1.7253	0.2342	7.3674	0.0000	***
2014–2020	-0.6544	0.2159	-3.0305	0.0501	
2014–2021	-0.3333	0.2319	-1.4369	0.8402	
2015–2016	-0.9496	0.2125	-4.4687	0.0002	
2015–2017	2.4145	0.2527	9.5531	0.0000	
2015–2018	-0.6638	0.2108	-3.1495	0.0350	
2015–2019	1.2147	0.2212	5.4918	0.0000	
2015–2020	-1.1650	0.2074	-5.6175	0.0000	
2015–2021	-0.8439	0.2235	-3.7750	0.0040	
2016–2017	3.3641	0.2582	13.0307	0.0000	
2016–2018	0.2858	0.2025	1.4113	0.8524	
2016–2019	2.1643	0.2239	9.6652	0.0000	
2016–2020	-0.2154	0.2024	-1.0645	0.9640	
2016–2021	0.1057	0.2224	0.4752	0.9998	
2017–2018	-3.0783	0.2555	-12.0484	0.0000	
2017–2019	-1.1998	0.2544	-4.7158	0.0001	
2017–2020	-3.5795	0.2568	-13.9373	0.0000	
2017–2021	-3.2584	0.2687	-12.1247	0.0000	
2018–2019	1.8785	0.2214	8.4865	0.0000	
2018–2020	-0.5012	0.2021	-2.4800	0.2039	
2018–2021	-0.1801	0.2218	-0.8120	0.9925	
2019–2020	-2.3797	0.2231	-10.6647	0.0000	
2019–2021	-2.0586	0.2380	-8.6508	0.0000	
2020–2021	0.3211	0.2152	1.4920	0.8121	
Sacramento–San Joaquin	-1.7239	0.1470	-11.7235	0.0000	
Sacramento—South Delta	-1.6383	0.1638	-10.0032	0.0000	
San Joaquin—South Delta	0.0856	0.1393	0.6148	0.8120	

TABLE A-4
PAIRWISE COMPARISONS FOR EACH YEAR AND EACH REGION USED IN THE ZERO-INFLATED MODEL ON
TOTAL HARMFUL ALGAE CONCENTRATIONS

contrast	estimate	SE	df	t.ratio	p.value	Coefficient type
2014–2015	1.258	0.401	246	3.132	0.0403	count
2014–2016	-1.032	0.400	246	-2.583	0.1672	count
2014–2017	0.300	0.491	246	0.611	0.9987	count
2014–2018	-0.696	0.410	246	-1.698	0.6885	count
2014–2019	1.653	0.729	246	2.266	0.3165	count
2014–2020	1.533	0.384	246	3.991	0.0022	count
2014–2021	-0.887	0.379	246	-2.339	0.2770	count
2015–2016	-2.290	0.349	246	-6.569	<0.0001	count
2015–2017	-0.958	0.460	246	-2.082	0.4294	count
2015–2018	-1.953	0.363	246	-5.383	<0.0001	count
2015–2019	0.395	0.709	246	0.558	0.9993	count
2015–2020	0.275	0.333	246	0.826	0.9915	count
2015–2021	-2.144	0.323	246	-6.644	<0.0001	count
2016–2017	1.332	0.459	246	2.903	0.0764	count
2016–2018	0.336	0.353	246	0.952	0.9804	count
2016–2019	2.685	0.708	246	3.792	0.0046	count
2016–2020	2.565	0.327	246	7.849	<0.0001	count
2016–2021	0.145	0.310	246	0.469	0.9998	count
2017–2018	-0.996	0.467	246	-2.132	0.3973	count
2017–2019	1.353	0.761	246	1.777	0.6362	count
2017–2020	1.233	0.445	246	2.773	0.1068	count
2017–2021	-1.187	0.442	246	-2.687	0.1316	count
2018–2019	2.349	0.713	246	3.293	0.0248	count
2018–2020	2.228	0.341	246	6.536	<0.0001	count
2018–2021	-0.191	0.325	246	-0.588	0.9990	count
2019–2020	-0.120	0.699	246	-0.172	1.0000	count
2019–2021	-2.540	0.697	246	-3.643	0.0078	count
2020–2021	-2.419	0.298	246	-8.125	<0.0001	count
Sacramento–San Joaquin	-1.928	0.367	246	-5.260	<0.0001	count
Sacramento—South Delta	-1.805	0.347	246	-5.197	<0.0001	count
San Joaquin—South Delta	0.123	0.226	246	0.544	0.8494	count
2014–2015	1.409	0.773	246	1.823	0.6051	zero inflation
2014–2016	0.567	0.659	246	0.860	0.9892	zero inflation
2014–2017	-1.407	0.690	246	-2.038	0.4585	zero inflation
2014–2018	-0.206	0.636	246	-0.324	1.0000	zero inflation
2014–2019	-2.706	0.897	246	-3.017	0.0559	zero inflation

TABLE A-4
PAIRWISE COMPARISONS FOR EACH YEAR AND EACH REGION USED IN THE ZERO-INFLATED MODEL ON
TOTAL HARMFUL ALGAE CONCENTRATIONS

contrast	estimate	SE	df	t.ratio	p.value	Coefficient type
2014–2020	0.448	0.632	246	0.709	0.9967	zero inflation
2014–2021	1.705	0.676	246	2.520	0.1919	zero inflation
2015–2016	-0.843	0.706	246	-1.194	0.9332	zero inflation
2015–2017	-2.816	0.752	246	-3.747	0.0054	zero inflation
2015–2018	-1.616	0.694	246	-2.329	0.2822	zero inflation
2015–2019	-4.115	0.947	246	-4.346	0.0005	zero inflation
2015–2020	-0.962	0.683	246	-1.408	0.8528	zero inflation
2015–2021	0.295	0.707	246	0.417	0.9999	zero inflation
2016–2017	-1.974	0.633	246	-3.120	0.0418	zero inflation
2016–2018	-0.773	0.561	246	-1.378	0.8664	zero inflation
2016–2019	-3.272	0.856	246	-3.822	0.0041	zero inflation
2016–2020	-0.119	0.546	246	-0.218	1.0000	zero inflation
2016–2021	1.138	0.581	246	1.959	0.5121	zero inflation
2017–2018	1.201	0.608	246	1.975	0.5008	zero inflation
2017–2019	-1.299	0.877	246	-1.481	0.8170	zero inflation
2017–2020	1.855	0.605	246	3.067	0.0486	zero inflation
2017–2021	3.112	0.653	246	4.766	0.0001	zero inflation
2018–2019	-2.500	0.836	246	-2.989	0.0606	zero inflation
2018–2020	0.654	0.531	246	1.232	0.9217	zero inflation
2018–2021	1.911	0.576	246	3.316	0.0230	zero inflation
2019–2020	3.153	0.835	246	3.775	0.0049	zero inflation
2019–2021	4.410	0.873	246	5.053	<0.0001	zero inflation
2020–2021	1.257	0.554	246	2.267	0.3162	zero inflation
Sacramento–San Joaquin	1.488	0.474	246	3.139	0.0054	zero inflation
Sacramento–South Delta	2.942	0.478	246	6.159	<0.0001	zero inflation
San Joaquin–South Delta	1.454	0.370	246	3.925	0.0003	zero inflation

TABLE A-5
PERCENT COVERAGE OF WATERWAYS OF TYPES OF AQUATIC VEGETATION IN THE DELTA OVER TIME, AS MEASURED BY HYPERSPECTRAL IMAGERY

Year	SAV	WH	WP	Pen
2004	13.35	1.48	1.75	0.77
2005	12.16	0.90	0.69	0.51
2006	13.19	2.18	1.10	0.53
2008	7.16	0.49	0.99	0.68
2014	14.60	5.70	1.55	0.00
2015	22.53	1.74	1.92	0.15
2019	22.14	0.92	2.94	0.00
2020	19.63	1.45	2.64	0.00

NOTES: pen = water pennywort; WH = water hyacinth; WP = water primrose